

Development of Micellar Draw Solution and Process Optimization of the Forward Osmosis Membrane Bioreactor (FO-MBR)



By

MUHAMMAD SAQIB NAWAZ

Institute of Environmental Sciences & Engineering (IESE)

School of Civil & Environmental Engineering (SCEE)

National University of Sciences & Technology (NUST)

2014

Development of Micellar Draw Solution and Process Optimization of the Forward Osmosis Membrane Bioreactor (FO-MBR)



MUHAMMAD SAQIB NAWAZ

Reg. No. 2010-NUST-Tfr -PhD-ENV-05

**This work is submitted as a PhD thesis in partial fulfillment of the
requirement for the degree of**

(PhD in Environmental Engineering)

Supervisor: Dr. Sher Jamal Khan

Institute of Environmental Sciences & Engineering (IESE)

School of Civil & Environmental Engineering (SCEE)

National University of Sciences & Technology (NUST),

Islamabad, Pakistan

2014

Certificate

Certified that the contents and form of thesis entitled “Development of Micellar Draw Solution and Process Optimization of the Forward Osmosis Membrane Bioreactor (FO-MBR)” submitted by Mr. Muhammad Saqib Nawaz have been found satisfactory for the requirement of the degree.

Supervisor

Dr. Sher Jamal Khan

Associate Professor (IESE-SCEE-NUST)

GEC Members

Professor Dr. Ishtiaq A Qazi

Associate Dean (IESE-SCEE-NUST)

Dr. Zahiruddin Khan

Associate Professor (IESE-SCEE-NUST)



Dr. Nicholas P Hankins

Associate Professor

(Department of Engineering Science, University of Oxford, UK)

Dedication

This work is dedicated to my beloved parents (L) Mr. & Mrs.

Professor Rao Rab Nawaz, their support and encouragement

brought me to this stage today!!!

Acknowledgements

I am thankful to the almighty ALLAH for all his blessings upon me. I appreciate the efforts of my parents and family who really encouraged me to continue for higher education, financed and supported me at every step whenever I needed them. I want to acknowledge all my teachers who taught me throughout my academic career, particularly my PhD supervisor Dr. Sher Jamal Khan who guided and persuaded me during the research phase. I am grateful to my GEC members Professor Dr. Ishtiaq A. Qazi and Dr. Zahiruddin Khan for their kind guidance and support.

I would also like to extend my gratitude to IESE-SCEE-NUST and all the faculty and staff members working here. Gratitude is also due to the faculty and staff at the Department of Engineering Science, University of Oxford for providing me the opportunity to work under the kind supervision of Dr. Nicholas P Hankins. A special thanks to the Higher Education Commission (HEC) of Pakistan and British Council for providing the financial assistance for the collaborative work under the INSPIRE program (Project No. SP-192). Once again thanks to HEC for granting me PhD scholarship under indigenous scholarship program batch IV. I am thankful to Hydration Technology Innovations (HTI) Albany, USA, for providing flat sheet FO membranes for this study. The fundamental guidance in setting up of FO systems and providing hollow fiber FO modules by Dr. Wang Rong and Dr. Chuyang Y Tang from Singapore Membrane Technology Centre (SMTC), Nanyang Technological University (NTU) is highly appreciated.

A special thank to Gabriela Gadelha for all her support in lab work and paper writing. Among the friends and colleagues I will name Tanvir-Ul-Haq Zia, Fozia Parveen, Ghalib Hasnain, Nazeer Abbas, Bilal Aftab, Andrea Chen and Cordelia Rampley who really helped me during my research. At last but not least I will express gratitude to my lovely wife Sara Ali without whose support all of this was not possible.

Muhammad Saqib Nawaz

TABLE OF CONTENTS

<i>Chapter 1</i>	1
INTRODUCTION	1
1.1. BACKGROUND AND PROBLEM STATEMENT	1
1.2. OBJECTIVES	2
1.3. SCOPE.....	2
1.4. SIGNIFICANCE AND NOVELTY.....	3
<i>Chapter 2</i>	4
LITERATURE REVIEW	4
2.1. WASTEWATER TREATMENT AND REUSE	4
2.2. FORWARD OSMOSIS PRINCIPLE AND APPLICATIONS	5
2.3. FO MEMBRANES.....	7
2.4. FO MEMBRANE FOULING AND CONCENTRATION POLARIZATION	9
2.5. DRAW SOLUTIONS IN FO SYSTEMS	13
2.6. MICELLAR SOLUTIONS	19
2.7. REVERSE SOLUTE TRANSPORT IN FO SYSTEMS	23
2.8. FLUX AND MASS TRANSFER OF MICELLAR SOLUTIONS.....	24
2.9. PROCESS OPTIMIZATION OF FO-MBR.....	26
<i>Chapter 3</i>	29
MATERIALS AND METHODS.....	29
3.1. MICELLAR SOLUTION AS DRAW SOLUTION IN FO.....	29
3.1.1. Membranes and Chemicals	29
3.1.2. Experimental Setup and Procedures.....	30
3.1.3. Analytical Methods	34
3.1.4. Reverse Transport of Draw Solutions	35
3.1.5. Recovery/Regeneration of Diluted Micellar Draw Solutions	35
3.1.6. Microbial Toxicity of Micellar Solutions.....	37
3.2. PROCESS OPTIMIZATION OF FO-MBR.....	40

3.2.1.	Optimization of Draw Solution Concentration	40
3.2.2.	Optimization of Membrane Chemical Cleaning	41
3.2.3.	Optimization of Osmotic Backwashing	41
3.2.4.	Optimization of Cross-flow Velocity	42
<i>Chapter 4</i>		44
RESULTS AND DISCUSSION		44
4.1.	MICELLAR DRAW SOLUTION	44
4.1.1.	FO System Flux Using Micellar Draw Solutions.....	44
4.1.2.	Mass Transfer of Micellar Draw Solutions	50
4.1.3.	Reverse Transport of Micelles	51
4.1.4.	Recovery/Regeneration of Diluted Micellar Solution.....	53
4.1.5.	Direct Reuse of Diluted Micellar Solution.....	55
4.1.6.	Toxicity of Inorganic and Micellar Draw Solutions to <i>E.coli</i>	55
4.1.1.	Toxicity of Micellar Solutions to <i>Pseudomonas aeruginosa</i> and mixed activated sludge	68
4.2.	PROCESS OPTIMIZATION OF THE FO-MBR.....	81
4.2.1.	Optimization of Draw Solution Concentration	81
4.2.2.	Membrane Chemical Cleaning Optimization.....	83
4.2.3.	Dynamics of FO Membrane Fouling.....	91
4.2.4.	Osmotic Backwashing Optimization.....	94
4.2.5.	Cross-flow Velocity Optimization for FO-MBR	96
<i>Chapter 5</i>		103
CONCLUSIONS AND RECOMMENDATIONS		103
5.1.	CONCLUSIONS	103
5.1.1.	Development of Micellar Draw Solution	103
5.1.2.	Process Optimization of FO-MBR	104
5.2.	RECOMMENDATIONS	105
REFERENCES		107
ANNEXURES		1211

LIST OF TABLES

Table no.	Caption	Page no.
2-1	Summary of draw solutions used in FO	14
2-2	Summary of studies for FO process optimization	28
3-1	Surfactants used in the study	30
3-2	Chemical Composition of the synthetic wastewater	34
4-1	Mass transport coefficient for different surfactants	51
4-2a	Comparison of reverse solute transport (mg/L) of micellar and NaCl draw solutions	52
4-2b	Comparison of reverse solute transport (mol/L) of micellar and NaCl draw solutions	52
4-3	Regeneration potential of micelles from diluted draw solution	54
4-4	Evaluation of inorganic draw solutes for FO-MBR keeping in view osmotic pressure, specific reverse salt transport and percent growth	64
4-5	Evaluation of surfactants as draw solutes for FO-MBR keeping in view osmotic pressure, specific reverse salt transport and percent growth	67
4-6	Recommendation of surfactants as draw solutes in FO-MBR based on their toxicity to <i>Pseudomonas</i> and mixed sludge	80
4-7	Optimization of draw solution concentration for hollow fiber FO membrane	82
4-8	Chemical cleaning of inorganics fouled hollow fiber FO membrane	84
4-9	EDTA chemical cleaning for micellar fouled FO membranes	89
4-10	Contaminant transfer through hollow fiber FO membrane	93
4-11	Osmotic backwashing in hollow fiber FO-MBR	95
4-12	Effect of cross-flow velocity on flux through hollow fiber FO module	96
4-13	Initial and final EPS during flat sheet FO-MBR four different runs	100
4-14	Effect of cross-flow velocity on sludge particle size during flat sheet FO-MBR four different runs	101

LIST OF FIGURES

Figure no.	Caption	Page no.
2-1	Principle of forward osmosis	6
2-2	Morphology of hollow fiber FO membrane (a) 45 times enlarged and (b) 200 times enlarged cross-section	8
2-3	SEM images of flat sheet FO membrane (a) plan view and (b) cross-section of the active layer	8
2-4	(a) AL-DS configuration illustrating concentrative ICP, (b) AL-FS configuration illustrating dilutive ICP	12
2-5	Micelle and reverse phase micelle formation in the aqueous and non aqueous media	20
2-6	Variation in physical properties of surfactant solution below and above CMC	21
2-7	Surfactant solubility variation with Krafft temperature	22
2-8	Reverse solute transport in asymmetric FO membrane	24
3-1	Schematic of hollow fiber FO setup at University of Oxford	31
3-2	Flat sheet FO setup at University of Oxford	32
3-3	(a) Batch and (b) semi-continuous hollow fiber FO-MBR setup at NUST	33
3-4	Structure of (a) Dimidium bromide and (b) Disulphine blue	37
3-5	Bacterial colony counting on a digital colony counter	40
4-1	ICP effect on the flat sheet FO membrane with 1.0 M TMOAB as draw solution	45
4-2	ECP effect on the flat sheet FO membrane with 0.50 M TEAB as draw solution	45
4-3	Flux with hollow fiber FO membrane using (a) 0.010 M SDS and (b) 0.50 M SDS as draw solution	46
4-4	Flux with hollow fiber FO membrane using (a) 0.50 M TEAB, (b) 0.50 M 1-OSA and (c) 0.50 M MTAB as draw solution	48
4-5	Flux with hollow fiber FO membrane using 0.50 M NaCl as draw solution	49
4-6	Flux with SDS as draw solution and MBR sludge as feed solution using flat sheet FO-MBR setup	49
4-7	Effect of NaCl on <i>E.coli</i> growth	57
4-8	Effect of KCl on <i>E.coli</i> growth	57
4-9	Effect of CaCl ₂ on <i>E.coli</i> growth	58
4-10	Effect of MgCl ₂ on <i>E.coli</i> growth	58
4-11	Effect of NH ₄ HCO ₃ on <i>E.coli</i> growth	59
4-12	Effect of (NH ₄) ₂ SO ₄ on <i>E.coli</i> growth	59

4-13	Effect of Na ₂ SO ₄ on <i>E.coli</i> growth	60
4-14	Effect of K ₂ SO ₄ on <i>E.coli</i> growth	60
4-15	Effect of TMOAB on <i>E.coli</i> growth	65
4-16	Effect of DTAB on <i>E.coli</i> growth	65
4-17	Effect of MTAB on <i>E.coli</i> growth	66
4-18	Effect of SDS on <i>E.coli</i> growth	66
4-19	TOC reduction by (a) <i>Pseudomonas</i> and (b) mixed sludge in presence of TEAB	70
4-20	Growth of (a) <i>Pseudomonas</i> and (b) mixed sludge in presence of TEAB	71
4-21	TOC reduction by (a) <i>Pseudomonas</i> and (b) mixed sludge in presence of TMOAB	72
4-22	Growth of (a) <i>Pseudomonas</i> and (b) mixed sludge in presence of TMOAB	73
4-23	TOC reduction by (a) <i>Pseudomonas</i> and (b) mixed sludge in presence of SDS	76
4-24	Growth of (a) <i>Pseudomonas</i> and (b) mixed sludge in presence of SDS	77
4-25	TOC reduction by (a) <i>Pseudomonas</i> and (b) mixed sludge in presence of 1-OSA	78
4-26	Growth of (a) <i>Pseudomonas</i> and (b) mixed sludge in presence of 1-OSA	79
4-27	Flux with different NaCl concentrations as draw solution using hollow fiber FO membrane	81
4-28	Membrane cleaning with 0.0005 M EDTA and 0.5 g/L NaOH for 1 hr	85
4-29	Membrane cleaning with 0.0005M EDTA and 0.5g/L NaOH for 30 minutes	85
4-30	Hollow fiber membrane cleaning with 0.5 g/L NaOH for 30 minutes	86
4-31	Hollow fiber membrane cleaning with 0.0005M EDTA and 0.25 g/L NaOH for 30 minutes	86
4-32	Hollow fiber membrane cleaning with 0.0005M EDTA and 0.125 g/L NaOH for 30 minutes	87
4-33	Hollow fiber membrane cleaning by reusing the same cleaning solution (0.0005M EDTA and 0.125 g/L NaOH for 30 minutes) for 3 times	87
4-34	Cleaning of TEAB fouled membrane with 0.0005M EDTA and 0.125 g/L NaOH for 30 minutes	88
4-35	Optical microscopic images (200 times enlarged) of flat sheet FO membranes (a) nascent membrane, (b) fouled with SDS, (c) cleaned with EDTA solution after SDS fouling, (d) fouled with TEAB and (e) cleaned with EDTA solution after TEAB fouling	88
4-36	Conductivity of draw solution in flat sheet FO-MBR operation at different cross-flow velocities	99
4-37	Flux generated during flat sheet FO-MBR operation at different cross-flow velocities	99
4-38	AFM image after (a) Run 1 (100 mL/min), (b) Run 2 (300 mL/min), (c) Run 3 (1000 mL/min) and (d) Run 4 (700 mL/min)	102

LIST OF ABBREVIATIONS

AFM	Atomic force microscopy
AL-DS	Active layer facing draw solution
AL-FS	Active layer facing feed solution
CMC	Critical micelle concentration
CP	Concentration polarization
CTA	Cellulose triacetate
DS	Draw solution
<i>E.coli.</i>	Eschericia coli
ECP	External concentration polarization
EDTA	Ethylenediaminetetraacetic
FO-MBR	Forward osmosis membrane bioreactor
HTI	Hydration Technology Innovations
ICP	Internal concentration polarization
IESE	Institute of environmental sciences and engineering
MBR	Membrane bioreactor
MLSS	Mixed liquor suspended solids
NUST	National university of sciences and technology
PSA	Particle size analyzer
SEM	Scanning electron microscope
SMTC	Singapore membrane technology center
TDS	Total dissolved solids

T _k	Krafft temperature
TOC	Total organic carbon
UF	Ultra filtration
ΔP	Hydrostatic pressure difference (atm)
A	Water permeability coefficient (L/m ² h atm)
B	Solute permeability coefficient (L/m ² h; m/s)
C	Solute concentration (mol/m ³)
D _{eff}	Solute diffusion coefficient (m ² /s)
H _o	Proportionality coefficient (m ³ atm/mol; m ³ Pa/mol)
J _s	Solute flux (mol/s m ²)
J _w	Water permeation flux (L/m ² h; m/s)
K	Mass transfer coefficient (L/m ² h; m/s)
R	universal gas constant (m ³ atm/k mol)
S	Membrane structural parameter (m)
	Osmotic pressure difference across the membrane (atm; Pa)
	Membrane porosity
nC	Osmolality
	Tortuosity

ABSTRACT

The wide spread application of forward osmosis (FO) awaits substantial investigation in the development of novel draw solutions. When surfactant monomers aggregate above the critical micelle concentration (CMC) and Krafft temperature (T_k), micelles are formed. Micellar solutions were evaluated as novel draw solutions for FO systems. It was found that the micellar solutions generate stable water fluxes, independent of declining draw solution concentration, around their CMCs. The reverse transport of different micellar solutions was found to be 53-268 times lower as compared to the sodium chloride, at similar molar concentrations. Upto 95 % recovery of micellar solutions with energy efficient methods like ultra filtration (UF) or Krafft temperature swing is another advantage. Microbial toxicity effects of the reverse transported micellar draw solutions were studied using isolated microbial species and mixed activated sludge. Micellar solutions were recommended for use in the forward osmosis membrane bioreactor (FO-MBR) but with concentrations above CMC. Different operational parameters for improving the efficiency of the FO-MBR were also optimized. A draw solution concentration of 2 M was found most suitable since the higher concentrations invited extensive concentration polarization (CP) which caused a net water flux decline. Cross-flow velocity was optimized to circulate the feed solution (sludge) in FO-MBR and the optimized value was 300 mL/min, because greater velocities caused a breakdown of flocs to encourage severe membrane fouling. Micellar fouled FO membranes were found to show 100 % flux recovery after cleaning with Ethylenediaminetetraacetic acid (EDTA) solution. It was discovered that the major transport of organic contaminants and draw solute, across the FO membrane, occurs in the first hour of operation of the FO-MBR. In short, micellar solutions can be considered as a reliable draw solution to the development of FO system.

INTRODUCTION

1.1. BACKGROUND AND PROBLEM STATEMENT

One of the best ways to deal with the ever increasing world fresh water demand is to reuse the treated wastewater for agricultural, horticultural, industrial and non potable domestic applications. There is, however, a strong need that treatment technique must produce good quality reusable water and may be operated with some natural source of energy. Membrane technologies for wastewater treatment are gaining importance compared to other treatment techniques, in terms of efficiency, production rate and physical foot prints.

Forward osmosis (FO) is a recently established membrane based treatment process that can be used as an energy saving substitute to conventional membrane based treatment techniques. The driving force in FO is osmotic pressure difference that is generated when a high concentration draw solution (DS) flows on one side of the membrane against a low concentration feed solution on the other side. Forward osmosis membrane bioreactor (FO-MBR) is a combination of conventional membrane bioreactor (MBR) technology with FO membrane for the separation of sludge particles, organic and inorganic contaminants from the treated water.

The FO technology is still under the development phase and research is needed in some areas to make this technology viable for domestic, agricultural and industrial applications. Investigation

of novel draw solutes for FO systems and optimization of FO-MBR processes are two very critical areas. The literature available on FO, however, focuses more on desalination and the development of new membranes.

This study investigates the potential of novel micellar draw solutions in FO processes. Emphasizing on the optimization of operational parameters, the study also focuses on the potential microbial toxicity to the biomass from the reverse transported draw solute in FO-MBR. In short the study fills up some of the important gaps existing in the literature on FO-MBR and provides fundamental data that serves as a platform for further research in this area.

1.2. OBJECTIVES

Keeping in view the critical areas of the research work as discussed above, the study aimed to achieve the following objectives:

- a) To investigate micellar solutions as a potential draw solute for FO systems.
- b) To optimize the operational parameters of FO-MBR to increase the water flux.
- c) To investigate the potential effect of reverse transported draw solute on the biomass in FO-MBR.

1.3. SCOPE

- a) The study was limited to laboratory scale FO systems at NUST, Pakistan and the University of Oxford, UK.
- b) Synthetic feed solution, simulating domestic wastewater, was used in the FO-MBR.

- c) Micellar solutions of ionic surfactants were studied as novel draw solutions with comparison to sodium chloride.
- d) Microbial toxicity of micellar solutions were studied *using E.coli, Pseudomonas aeruginosa* and mixed sludge while inorganic draw solutions with *E.coli* only.

1.4. SIGNIFICANCE AND NOVELTY

The study enjoys vital significance for the researchers working in the field of FO and particularly FO-MBR. The use of micellar draw solutions in FO has not been reported in the literature. The micellar solutions were found to have certain advantages over the conventional ionic draw solutes, like easy regeneration, less reverse transport and stable water fluxes. These distinctive properties are significant for stable FO-MBR operations. The potential impact of the reverse transported draw solute on the microbial community in FO-MBR has also been studied for the first time in this study. The cross-flow velocity of the activated sludge was optimized in association with the sludge particle size and extra polymeric substances (EPS); such process optimization is difficult to find in the literature.

LITERATURE REVIEW

2.1. WASTEWATER TREATMENT AND REUSE

Pakistan is currently under water stressed conditions with water availability of only 1200 m³/capita/year and is moving towards water scarcity “1000 m³/capita/year”. With improving life style and increasing population (190 million) overall requirement of fresh water has increased considerably. Building of new water reservoirs is politically not favored. Hence, the only option left is to treat the wastewater and reuse it for agricultural, industrial and non potable domestic purposes. Moreover, due to rising land costs in densely populated cities of Pakistan it is not feasible to go for conventional wastewater treatment technologies like conventional activated sludge (CAS) process, which acquire more space and generate average quality non reusable treated water.

The developments in the membrane based water treatment technologies provide a viable solution to meet the challenge of wastewater reuse. In the last two decades, membrane technology has been applied to produce clean water, including wastewater treatment and reuse by MBRs (Williams and Pirbazari, 2007; Alturki et al., 2012). MBR enjoys many advantages like reduced footprint and greater decomposition of organics in the wastewater which results in a high quality product water. Hence, reuse of the MBR treated effluent is technically and economically practicable.

Although MBR is a well established technology for wastewater reclamation, it is currently facing the problem of high operational cost due to the associated high energy demand for operating membranes under suction pressure. This suction pressure also encourages the contaminants deposition onto or inside the membrane surface which contributes towards continuous flux decline and membrane deterioration due to frequent chemical cleaning. As a result, the wide spread commercialization of membrane processes is suppressed. For sustainable operation of membranes the prospective wastewater treatment technologies have to defeat these restrictions. Recently established membrane based technology that has the prospective to become a sustainable substitute is forward osmosis (Cath et al., 2006; Yang et al., 2009).

2.2. FORWARD OSMOSIS PRINCIPLE AND APPLICATIONS

Forward osmosis is an emerging technology that consists of an osmotically driven membrane process (McGinnis and Elimelech, 2008). FO generates a water flow utilizing the osmotic pressure difference which is produced when a semi-permeable membrane separates two solutions of dissimilar concentrations, i.e. an intense draw solution (DS) and a relatively mild feed solution. The hydraulic pressure is not needed in FO so, it is expected to utilize less energy with lower membrane fouling (Mi and Elimelech, 2010a).

It is a well known fact that FO is a lower fouling propensity technique implying lower operational costs (Mi and Elimelech, 2008; Lay et al., 2010). Some studies have discovered the use of FO to treat and reclaim wastewater using FO-MBR (Cartinella et al., 2006; Achilli et al., 2009 a). FO is studied for many applications including desalination (McCutcheon et al., 2006), generating drinking water (Wallace et al., 2008), dewatering the high nutrient sludge (Nguyen et

al., 2013), dewatering orange peel process liquor (Garcia-Castello and McCutcheon, 2011), wastewater reclamation in space (Cath et al., 2005) and many others.

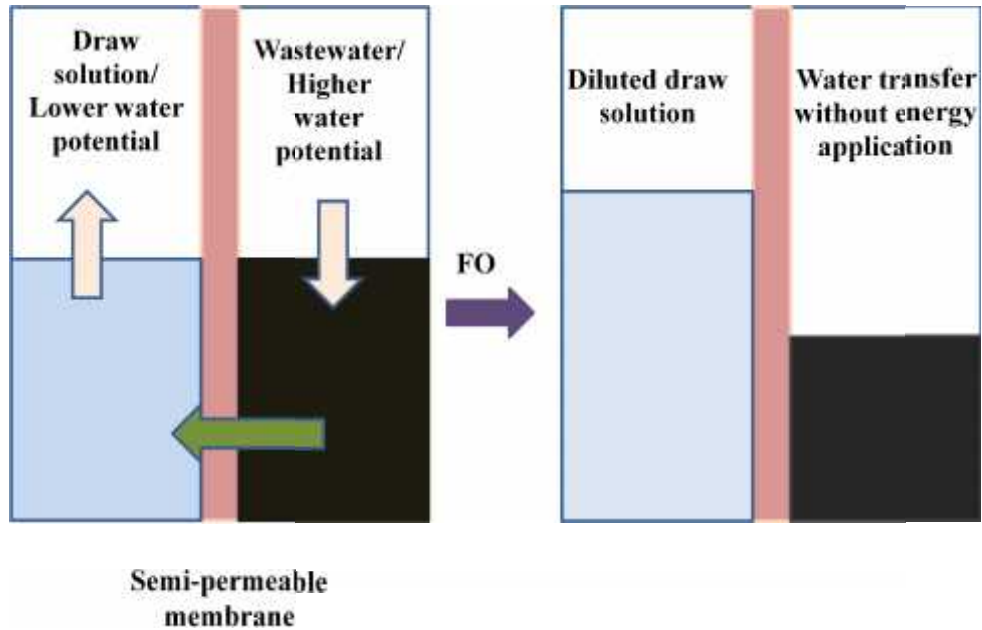


Figure 2-1: Principle of forward osmosis

The basic principle of FO is depicted in the **Figure 2-1**. Wastewater has lower total dissolved solids (TDS)/ higher water potential compared to the draw solution that has higher TDS/ lower water potential. Hence an osmotic gradient is established between two sides of the membrane and water starts flowing naturally from the wastewater towards the draw solution. The movement of the contaminants in the wastewater however is hindered by the FO membrane and only water crosses the membrane to reach the draw solution.

2.3. FO MEMBRANES

An ideal FO membrane should be able to provide better water permeability, high solute rejection, better chemical stability and good mechanical strength. FO uses composite, asymmetric membranes composed of two layers: one is the porous support layer and the other is the dense, active layer (AL). The membrane can be positioned between the feed and the draw solution in two different configurations: active layer facing the draw solution (AL-DS) or active layer facing the feed solution (AL-FS). The first method is more frequent for feed solutions with very low contaminant level such as de-ionized (DI) water or treated wastewater, however, for the highly contaminated feed solutions, AL-FS is the preferred configuration (Nayak and Rastogi, 2010).

The two most commonly used FO membranes as reported by the researchers include i) flat sheet FO membranes made up of cellulose triacetate (CTA) coated on polyester mesh sourced from Hydration Technology Innovations (HTI) and ii) hollow fiber (HF) membranes prepared in house by the Singapore Membrane Technology Center (SMTC), Nanyang Technological University (NTU), Singapore (McCutcheon et al., 2005; Wang et al., 2010a). A large proportion of the research papers and patents on FO belong to the category of designing novel FO membranes with characteristics to enhance the water flux and solute rejection.

The scanning electron microscope (SEM) images of the cross-sections of two most commonly used FO membranes are shown in **Figures 2-2 and 2-3**. Both of these membranes were used in this study. In HF membrane the active layer was coated on the inner side of fibers and outer side was used as the support layer. In flat sheet membranes the active layer was coated on the thick

support layer. A polyester mesh was embedded within the polymeric material for mechanical strength. The membrane thickness was less than 50 μm .

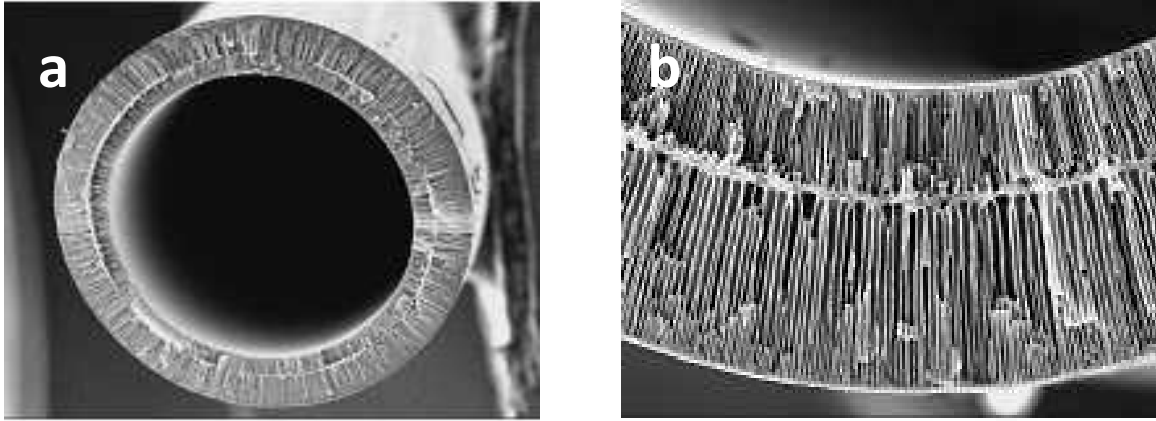


Figure 2-2: Morphology of hollow fiber FO membrane (a) 45 times enlarged and (b) 200 times enlarged cross-section. Source: (Wang et al., 2010a).

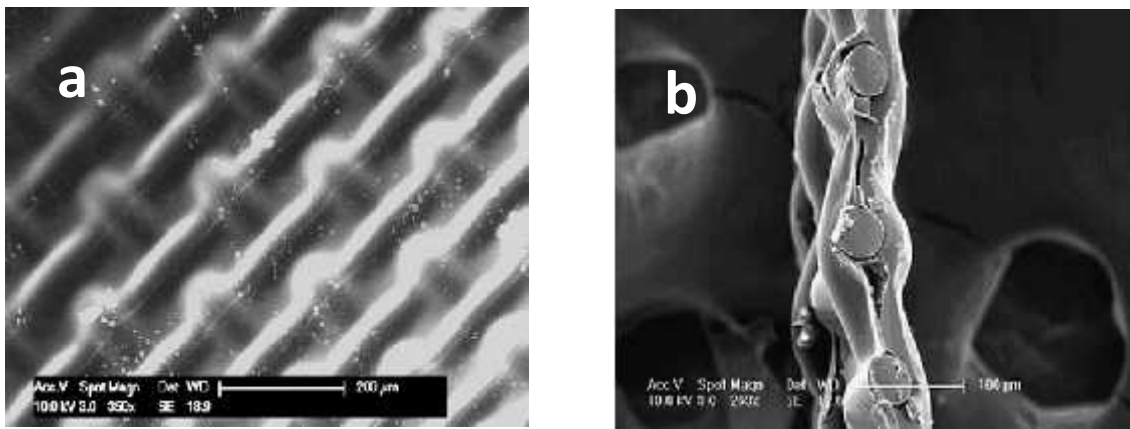


Figure 2-3: SEM images of flat sheet FO membrane (a) plan view and (b) cross-section of the active layer. Source: (McCutcheon et al., 2005).

The water permeability coefficient (A) and the solute permeability coefficient (B) are two very important parameters to assess the quality of a membrane. Ideally “A” should be maximum and “B” must be minimum (zero) for a membrane. These parameters are calculated by testing the

membrane in RO mode. Values of “A” and “B” for the HTI flat sheet FO membranes are 0.81 L/m²h bar (2.2×10^{-12} m/s Pa) and 0.62 L/m²h (1.7×10^{-7} m/s), respectively (Wang et al., 2010). For SMTC hollow fiber FO membrane the “A” and “B” are 2.22 L/m²h bar (5.94×10^{-12} m/s Pa) and 0.2 L/m²h (0.54×10^{-7} m/s), respectively (Chou et al., 2010).

2.4. FO MEMBRANE FOULING AND CONCENTRATION POLARIZATION

Like other membrane based treatment processes, FO also suffers from the permanent trouble of membrane fouling. Fouling occurs when solute particles deposit onto the surface or into the pores of the membrane. Fouling may affect membrane performance by decreasing the water flux, weakening product water quality, and increasing maintenance difficulty (Li and Elimelech, 2004).

There are four different types of fouling: i) organic fouling, caused by macromolecular organic compounds (Bellona et al., 2010); ii) inorganic fouling, caused by crystallization of salts; iii) biofouling, caused due to bacteria deposition and growth of biofilms (Kang et al., 2004; Herzberg et al., 2009); and iv) colloidal fouling, caused by the deposition of colloidal particles (Zhu and Elimelech, 1997; Vrijenhoek et al., 2001). FO membrane fouling has, however, not been studied extensively. A slow flux decline and high flux recovery rate in the FO process was found, as compared to RO, while treating anaerobic digester concentrate. The reason for this was less compaction of the fouling layer due to the absence of applied hydraulic pressure in FO (Holloway et al., 2007). Similarly, fouling in FO-MBR was found to be quite lower than conventional MBR (Achilli et al., 2009 a).

To increase the understanding of the fouling mechanisms in FO, atomic force microscopy (AFM) was used to study the role of membrane–foulant and foulant–foulant interactions, inorganic fouling and scaling of FO membranes (Mi and Elimelech, 2010a, Mi and Elimelech, 2010b). It was discovered that foulant–foulant interactions were crucial in affecting the rate and level of organic fouling. Despite the fact that FO enjoys lower fouling propensity compared to pressure-driven membranes (Achilli et al., 2009b), radical flux loss may occur under certain unfavorable conditions such as extremely high draw solution concentrations (Lay et al., 2010). The reverse transported draw solute to the feed solution may also cause critical impact on FO fouling (Tang et al., 2010).

The main reasons for lower-than-expected flux in FO are linked with numerous membrane-associated transport phenomena like the external concentration polarization (ECP) or internal concentration polarization (ICP). Concentration polarization may occur during FO, on both feed and permeate sides of the membrane. In AL-FS configuration the solutes build up at the active layer, called concentrative ECP. Meanwhile, the draw solution in contact with the permeate side of the membrane is diluted at the permeate–membrane interface through the permeating water, which is termed as dilutive ECP.

Both concentrative and dilutive ECP reduce the effective osmotic pressure difference and consequently the flux. In FO the impact of ECP may be reduced by increasing cross-flow velocity and turbulence at the membrane surface. ECP effect on flux decline is less in FO compared to RO, due to the absence of the applied hydraulic pressure. It is also believed that ECP is not the major cause of flux decline in FO (McCutcheon et al., 2006).

In AL-DS configuration a polarized layer is established inside of the dense active layer as water and solute propagate the porous layer as shown in **Figure 2-4 (a)**. This is called concentrative ICP which takes place within the porous support layer and cannot be reduced by raising the cross-flow velocity. In AL-FS configuration as water permeates through the active layer, the draw solution within the porous substructure becomes diluted. This is called as dilutive ICP, as shown in **Figure 2-4 (b)**.

The flux and ICP in FO may be modeled by combining solution-diffusion theory for the active layer and the diffusion convection transport in the support layer (Lee et al., 1981; McCutcheon and Elimelech, 2006). Such model depicts that ICP is mainly related to the support layer structure and it becomes less effective for membranes with thinner and more porous support layers, due to their reduced mass transfer resistance. Six times flux increment was observed by just removing the fabric layer of a commercial cellulose acetate asymmetric membrane (Loeb et al., 1997). It explains why the commercial flat sheet FO membrane by HTI with a thin support layer ($<50\mu\text{m}$) has a much better flux than conventional RO membranes used in FO processes (Cornelissen et al., 2008; McCutcheon and Elimelech, 2008).

Normally ICP reduces the overall flux but in some cases, it provides a self compensating mechanism that can maintain fairly stable flux under fouling conditions (Tang et al., 2010). It was found that FO fouling is more complicated than RO due to ICP. Flux change in FO may cause a severe change in ICP, due to its exponential dependence on flux. Also in AL-DS configuration fouling in the support layer may substantially enhance ICP by reducing the

porosity of the support layer. So, ICP and membrane fouling in FO complement each other (Mi and Elimelech, 2008).

To reduce ICP the ideal FO membrane should be semi-permeable thin film and without a porous support layer but it will have lower mechanical strength which will limit its practical application. Efforts for the exploration of novel membrane materials and configurations are continuing (Wang et al., 2009; Wang et al., 2010), however, another potential area of research in FO is the identification of novel draw solutions.

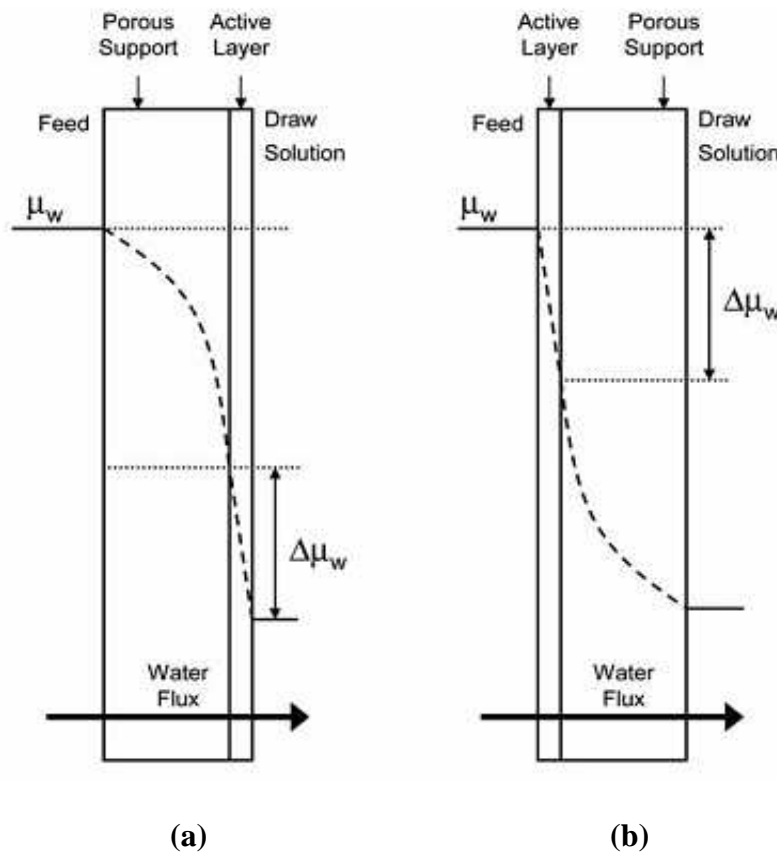


Figure 2-4: (a) AL-DS configuration illustrating concentrative ICP, (b) AL-FS configuration illustrating dilutive ICP. Source: (Cath et al., 2006).

2.5. DRAW SOLUTIONS IN FO SYSTEMS

For the commercial application of the FO, several aspects of the technique require further investigation. One such aspect is the identification of appropriate draw solution which is capable of generating high osmotic pressure with minimum reverse transport and low toxicity to the membrane and the biomass. Such a draw solution should be hydrophilic in nature and easily separable from the diluted draw solution at a low energy input.

According to the Morse equation (2-1) by considering dilute ionic solutions, the osmotic pressure of a solution () can be expressed as follows:

$$\pi = iMRT = i \left(\frac{n}{V} \right) RT \dots\dots\dots (2 - 1)$$

Where “i” is the Van’t Hoff’s factor, “M” is the molarity of the solute which is equal to the ratio of the number of solute moles (n) to the volume of the solution (V), “R” is the gas constant (8.3145 J K⁻¹ mol⁻¹), and “T” is the absolute temperature. The “i” is the ratio between the actual concentration of particles produced when the substance is dissolved, and the concentration of a substance as calculated from its mass. For most non-electrolytes dissolved in water, the Van’t Hoff factor is essentially 1. For most ionic compounds dissolved in water, the Van’t Hoff factor is equal to the number of discrete ions in a formula unit of the substance.

Table 2-1 summarizes the draw solutes used in FO since beginning. It may be observed that the interest of researchers in novel draw solutes discovery was developed in the last decade.

Table 2-1: Summary of draw solutions used in FO

Draw solute (S)	Method of Recovery	Drawbacks	References
Ammonia and carbon dioxide	Heating	Energy intensive	Neff,1964
Organic acids and inorganic salts	Temperature variation or chemical reaction	Complicated procedures, corrosive chemicals involvement	Hough, 1970
Al ₂ SO ₄	Precipitation by doping Ca(OH) ₂	Toxic by-products	Frank,1972
Glucose- Fructose	None	Not pure water	Kravath and Davis, 1975
MgCl ₂	None	Not pure water	Loeb et al., 1997
KNO ₂ & SO ₂	SO ₂ recycled through standard means	Energy intensive, toxic	McGinnis, 2002
NH ₃ & CO ₂ (NH ₄ HCO ₃) or NH ₄ OH-NH ₄ HCO ₃	Moderate heating (60°C)	High reverse draw solute flux insufficient removal of ammonia, toxicity to biomass in FO-MBR	McCutcheon et al., 2005; McGinnis et al., 2007; McCutcheon et al., 2006; Nawaz et al., 2013
Salt, ethanol	Pervaporation-based separations	High reverse draw solute flux and low water flux	McCormick et al., 2008
Magnetic nanoparticles	Recycled by external magnetic field	Agglomeration	Ling et al., 2010; Ge et al., 2011
Stimuli- responsive polymer hydrogels	De-swelling of the polymer hydrogels	Energy intensive, poor water flux	Li et al., 2011a
Hydrophilic nanoparticles	Ultra filtration (UF)	Poor water flux	Ling and Chung, 2011
Fertilizers	None	Only applicable in agriculture	Phuntsho et al., 2011
Fatty acid – polythethylene glycol	Thermal method	Poor water flux	Iyer and Linda, 2011
Sucrose	Nano filtration (NF)	Relatively low water flux	Su et al., 2012
Polyelectrolytes	UF	Relatively high viscosity	Ge et al., 2012
Thermo- sensitive solute (Derivatives of Acyl-TAEA)	Not studied	Poor water flux	Noh et al., 2012

Draw solute (S)	Method of Recovery	Drawbacks	References
Urea, ethylene glycol and glucose	Not studied	Low water flux and high draw solute flux	Yong et al., 2012
Organic salts	RO	Low water flux, energy intensive	Bowden et al., 2012
Polyglycol copolymers	NF	High viscosity, severe ICP	Carmignani, 2012
Hexavalent phosphazene salts	Not studied	Not economical and practical	Stone et al., 2013
Volatile solutes (e.g. SO ₂)	Heating or air stripping	Toxic	McCutcheon et al., 2006
Copper sulfate	Metathesis precipitation reaction	Complex regeneration process	Alnaizy et al., 2013

Source: (Ge et al., 2013)

So, high solubility of the draw solute in solvent will increase the osmotic pressure by increasing the “i” e.g. NaCl has an “i” value of 2 and MgCl₂ has 3. It shows that multivalent ionic solutes are the more favorable for FO applications. There are four main types of compounds that are commercially available as draw solutes for FO. These compounds may be classified according to their physicochemical properties like i) volatile compounds, ii) nutrient compounds, iii) inorganic salts and iv) organic salts or polymers.

With the development of FO technology, its applications were explored for other needs including the production of drinking water. Nutrient compounds were initially studied for short term water supplies in lifeboats, but later on their use was extended for the concentration of food and wines (Herron et al., 1994). Glucose was originally studied as a draw solute for seawater desalination (Kravath and Davis, 1975). Glucose with the product water was used as a drink for emergency purposes and military deployments. So, no draw solute recovery/regeneration step was required. Kessler and Moody (1976) investigated the combination of glucose– fructose as draw solutes and

found better FO performance compared to a pure glucose solution. Then fructose was used alone and it showed that there was no thirst generated in human body after drinking the fructose water that make it more attractive as a draw solute (Stache, 1989).

After 1990s researchers studied the potential of inorganic salts as draw solutes in FO applications. These draw solutes were found to produce large water fluxes and were separable through RO. Many acids like valeric acid, manganic acid and a number of water soluble inorganic salts like calcium, sodium and potassium were used as draw solutes in FO. These salts may be separated from the final treated water through precipitation by changing their solubility with temperature variation or by their reactions with sulfuric acid or carbon dioxide (Hough, 1970).

Some fertilizers were also studied as a potential draw solute. The advantage of using fertilizers was that the diluted draw solution can be right away used for irrigation of crops; hence no regeneration/recovery step was required, which was energetically favorable (Phuntsho et al., 2011). Most of the chemical fertilizers, however, exhibited acidic properties in aqueous solutions which question their use for certain membrane materials like cellulose acetate (CA) or CTA. The membrane structure may be altered by the reaction between the groups present over the membrane surface and cause inconsistent FO performance. Also, some fertilizers dissolve only partially in water and may not have enough osmotic pressure to draw water from saline water feed solution.

A series of draw solutions based on organic salts were proposed for the use in FO-MBR. The advantage of using organic (biodegradable) salts in FO-MBR minimizes the potential toxicity to the microbial community in the feed solution (sludge) from the reverse transported draw solute. These salts were a combination of organic anions and inorganic cations (Na^+ or Mg^{2+}). Organics showed better rejection with RO compared to the inorganic salts, however, the water flux generated through organics salts were comparatively lower than those of their inorganic counterparts under similar operational conditions. Also the use of RO for the regeneration of the draw solute was energy intensive (Bowden et al., 2012).

The hydrophilic magnetic nano particles (MNPs), synthesized by one pot reaction, were used as a draw solution in FO systems. Their regeneration was carried out through an external magnetic field. It was found that the osmotic pressure of MNPs can be increased by improving their surface hydrophilicity or reducing their particle size. It is worth noticing that the reverse transport of MNPs was found negligible compared to the inorganics, due to their large particle sizes. The regeneration of nanoparticles may be done by various methods available like, magnetic field, UF or electric field. The choice of method depends strictly on the particle size and properties (Ling et al., 2010).

It was observed that nanoparticles agglomerate under a high-strength magnetic field and the performance of recycled MNPs was reduced. Even ultra-sonication remained unsuccessful to re-disperse the agglomerated nano particles (Ling et al., 2011a). Thermo-responsive MNPs were synthesized and used as draw solutes in FO. Above a fixed temperature, thermo-responsive

polymer that was coated on the nano particle surface, causes these to agglomerate; these relatively big size agglomerates may be recovered easily through UF (Ling et al., 2011b).

Polyelectrolytes of polyacrylic acid sodium (PAA-Na) salts were also studied as the draw solutes. It was observed that the water flux was good and the reverse solute transport was negligible with these draw solutes. Also, the salt rejection was good during the regeneration of PAA-Na by UF processes. The recycled PAA-Na exhibited consistent performance and indicated no solute aggregation. It was observed, however, that an increase in PAA-Na solution concentration resulted in viscosity enhancement of the draw solution which prevents polyelectrolytes from being practically used as draw solutes at ambient conditions (Ge et al., 2012).

Stimuli-responsive polymer hydrogels, such as Poly-N-isopropyl acrylamide (PNIPAM) were also used as draw solute. These polymer hydrogels are able to extract and release water when stimulated by either temperature or pressure, or by light with the incorporation of light-absorbing carbon particles (Li et al., 2011 b). They can extract water from a feed saline solution in an FO desalination process and then undergo a reversible volume change when exposed to environmental stimulus. The reported performance of all hydrogels as draw solutes remained poor at room temperature. In short, the search for an ideal draw solute that can maintain fairly stable flux with minimum reverse transport and energy efficient regeneration continues, serving as an innovation for this study that examines the potential of surfactant based micellar solutions as a novel draw solute in FO systems.

2.6. MICELLAR SOLUTIONS

Surfactants are a blend of organic and amphiphilic molecules, which present both structural units: hydrophilic groups (polar group, the head) and hydrophobic groups (long chain hydrocarbon, the tail) (Myers, 2005). Surfactants are classified according to the presence of formally charged groups in the hydrophilic head e.g. i) anionic, ii) cationic, iii) nonionic and iv) zwitterionic; where the head carries both negative and positive charges.

Micelles arise spontaneously in the solution as a result of the reversible colloidal aggregation of surfactants monomers at concentrations above the critical micelle concentration (CMC). The monomers are amphiphilic, with hydrophobic tails and hydrophilic heads, so that above the CMC it becomes energetically beneficial for the monomers to aggregate and minimize the free energy of the system. Their hydrophobic tails are protected from the water in the core of the micellar structure and their hydrophilic heads remain in contact with the polar water. It is interesting that in non aqueous or semi aqueous solvents the reverse phase micellar formation takes place as described in **Figure 2-5**.

Micellar systems have found wide application in industries as diverse as petroleum, food, chemicals and biotechnology (Schramm et al., 2003). Micelles are normally spherical in shape but, other forms like ellipsoids, cylindrical, and bilayers are also possible. The shape and size of a micelle is totally dependent on the molecular geometry of monomers and solution conditions like concentration, temperature, pH and ionic strength.

Micellar masses comprising of 50-100 agglomerated monomers normally varies from a few hundred up to several thousand g/mol. It is worth knowing that the transition between micelles

and monomers exist over a wide concentration range. Above a certain temperature, the solubility of a surfactant increases dramatically, due to the phase boundary between saturated, micellar solution and hydrated crystalline surfactant in the concentration region above the CMC (Offen and Turley, 1983). This temperature is known as the Krafft temperature (T_k), below which there is no value of CMC, which means no micelle formation can take place and only monomers exist. Micelle-monomer equilibrium in aqueous solution plays an important role in generating a constant osmotic pressure, independent of concentration above the CMC (Us'yarov, 2004; Xiao and Li, 2008). Due to an increase in the formation of micelles, the rise in the osmotic pressure is decelerated, as a result of the interactions between the solution components.

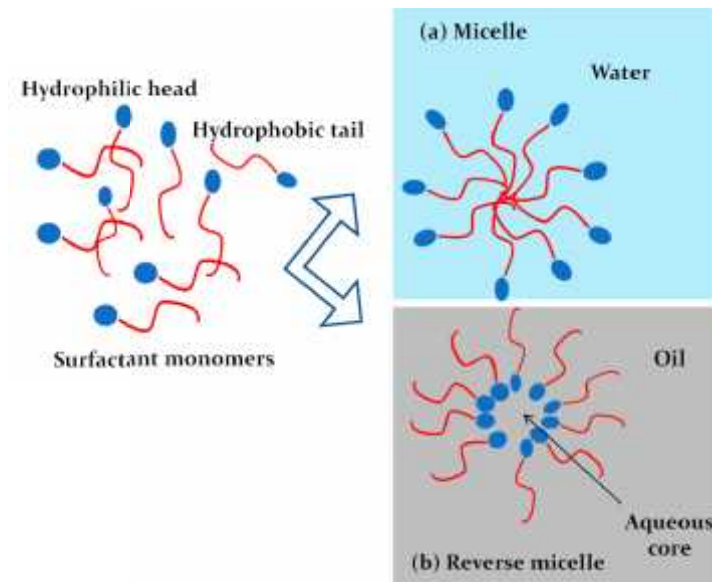


Figure 2-5: Micelle and reverse phase micelle formation in the aqueous and non aqueous media

Figure 2-6 describes the physical properties of surfactant solutions below and above the CMC. It may be noted that with micelle formation the properties of the solution change abruptly. Taking the property of osmotic pressure in view it may be seen that below the CMC, surfactant

monomers behave like an ordinary solution, for which the osmotic pressure increases with the concentration, but above CMC the phase equilibrium constrains them to maintain a fairly constant osmotic pressure. This unique micellar property of generating constant osmotic pressure above CMC can be useful in the stable operation of the FO systems, particularly FO-MBR, as we may achieve a fairly consistent flux even with declining draw solution concentration.

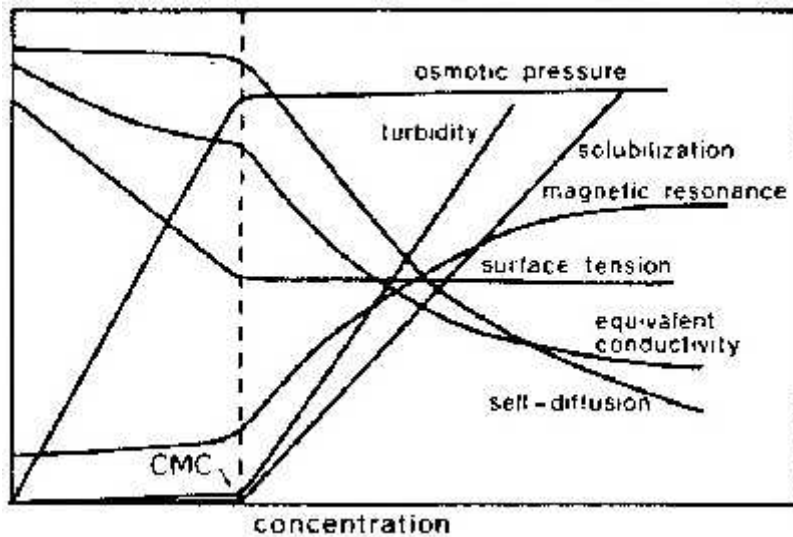


Figure 2-6: Variation in physical properties of surfactant solution below and above CMC.
Source: (Schramm et al., 2003)

Figure 2-7 shows that the solubility of surfactant depicts an abrupt increase above the Krafft point. However, below the T_k the solubility of the surfactant is too low for micellization so, only monomers are present in the solution. Above T_k a relatively large quantity of surfactant may be dispersed in micelles and the overall solubility elevates. Non-ionic surfactants do not show a T_k because their solubility varies inversely with temperature and they may start to lose their properties above a transition temperature which is termed as the “cloud point”. Addition of the ionic surfactants may increase the cloud points of their non-ionic counterparts, but this depends mainly on the composition of the mixed micelle.

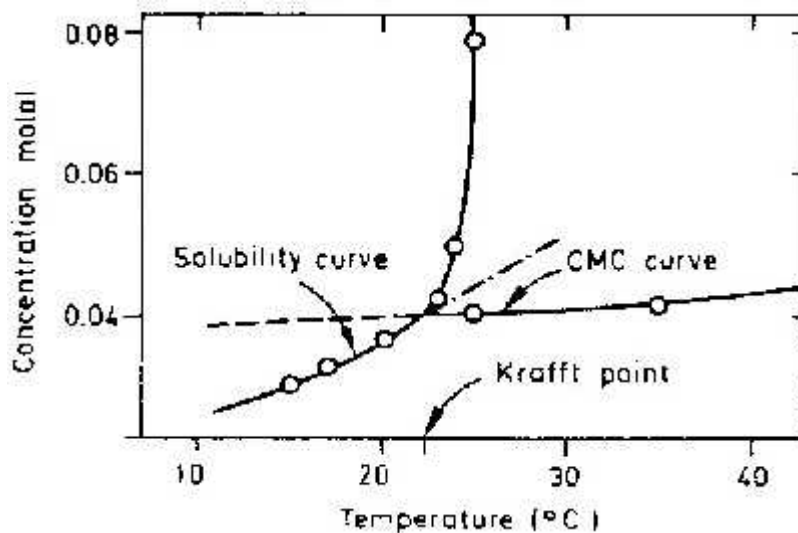


Figure 2-7: Surfactant solubility variation with Krafft temperature. Source: (Schramm et al., 2003)

It is interesting to note that the micellar solution, if brought below the T_k , will cause the surfactant monomers to crystallize. These crystals are of big size and may be separated from the water by simple gravity filtration through paper filters; this facilitates their energy efficient removal from the diluted draw solution. It is important to know that with increase in the solubility of the surfactants the CMC increases and the T_k decreases. So, the T_k swing method is effective only for the regeneration of surfactants with low CMC and for surfactants with higher CMC values the T_k could be so low that it may become energetically unfavorable to cool the diluted draw solution to that temperature.

Micelles can form a layer over the membrane surface by the adsorption of their hydrophobic organic tails on the hydrophobic organic membrane. This layer initially increases the flux due to the hydrophilic heads oriented towards the water, but, then the adsorbed micelle cake layer gets thicker and causes a net flux decline (Naim et al., 2012).

2.7. REVERSE SOLUTE TRANSPORT IN FO SYSTEMS

One area of FO that has earned minimum attention of researchers is the reverse transport of draw solute to the feed solution (Hancock and Cath, 2009). The phenomenon of reverse transport of draw solutes is inevitable in the current stage of FO technology. The reverse salt transport is mainly determined by membrane selectivity (Xiao et al., 2011; Phillip et al., 2010).

Ideally a semi permeable membrane must stop all draw solute particles from reverse transport, but practically a small amount of draw solute passes the membrane and moves into the feed side. It may affect FO in a number of ways; i) if draw solute is toxic for bacterial species present in the bioreactor it can affect the FO-MBR process and treatment efficiency, ii) if draw solute is harmful to the aquatic environment then the treatment of the feed solution concentrate would be required, iii) if the reverse transported draw solute is entrapped by the fouling layer, it may enhance the osmotic pressure on the feed side and cause a flux decline. So, a detailed understanding of the reverse solute transport is crucial for the development of the FO technology (William et al., 2010; Boo et al., 2010).

It was discovered that the reverse solute transport varies directly with the draw solution concentration and inversely to the size of hydrated ions in draw solution (Achilli et al., 2010). In order to avoid the reverse solute transport, multivalent ions with lower diffusivity are preferred in a draw solution. Mathematical models predicting the reverse solute transport are also developed by various researchers (William et al., 2010; Yong et al., 2012) but there is no data available on the potential microbial toxicity of the reverse transported draw solute on the biomass in FO-MBR. **Figure 2-8** describes the reverse solute transport in an asymmetric FO

membrane. The specific reverse solute transport has become an important draw solute selection parameter along with the osmotic pressure it generates and its energy efficient recovery.

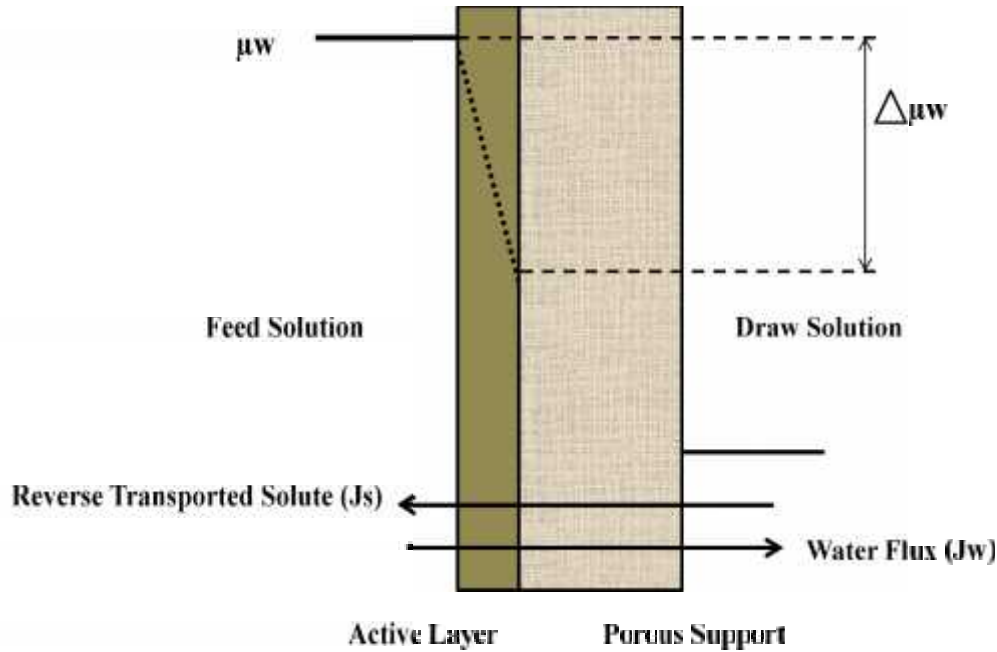


Figure 2-8: Reverse solute transport in asymmetric FO membrane

2.8. FLUX AND MASS TRANSFER OF MICELLAR SOLUTIONS

Suppose the AL-DS configuration with controlled ECP i.e. zero, then the concentration of the bulk draw solution ($C_{D,b}$) will be equal to the concentration of draw solution at membrane interface (C_{draw}). In such situation the water flux will be:

$$J_w = A(\Delta\pi_{eff} - P) = A(\pi_{draw} - \pi_{support} - P) \dots \dots \dots (2 - 2)$$

Where “A” is the water permeability coefficient of the membrane, “ π ” is the osmotic pressure difference across the active layer, and “P” is the hydrostatic pressure difference across the active layer.

Assuming that the osmotic pressure of the draw solution is proportional to its concentration (C_{draw}) and no hydraulic pressure ($\Delta P = 0$) is applied, then equation 2-2 becomes:

$$J_w = AH_o(C_{draw} - C_{support}) \dots \dots \dots (2 - 3)$$

Here, “ H_o ” is the proportionality coefficient relating solute concentration to osmotic pressure, and “ $C_{support}$ ” is the concentration of the feed solution at the support-membrane interface. An ideal membrane would only allow water to flow through it, however, draw solute reverse transport may also occur which may be calculated by the equation 2-4:

$$J_s = -B(C_{draw} - C_{support}) \dots \dots \dots (2 - 4)$$

Where “B” is the solute permeability coefficient and positive flux is from feed to draw solution. In the porous support of the FO membrane, the solute flow consists of two parts: (i) Diffusive, due to reverse transport of draw solute and (ii) Convective, due to the bulk flow of water through the membrane. Therefore, at steady-state, the solute flux by convection-diffusion is given by:

$$J_w C(x) - D_{eff} \nabla C - J_s = 0 \dots \dots \dots (2 - 5)$$

Where “C” is the solute concentration as a function of the distance x (distance from membrane-draw solution interface in the porous support layer) and “D” is the solute diffusion coefficient.

Merging equations 2-4 and 2-5 in a single equation:

$$B(C_{draw} - C_{support}) + J_w C - D_{eff} \nabla C = 0 \dots \dots \dots (2 - 6)$$

Where, $D_{\text{eff}} = \epsilon D$ is the effective diffusion coefficient and “ ϵ ” is the porosity of the support layer. Applying boundary conditions to equation 2-6, as $C(x = 0) = C_{\text{feed}}$ and $C(x = l_{\text{eff}}) = C_{\text{support}}$.

Where “ l_{eff} ” is the effective thickness of the membrane support as given by $l_{\text{eff}} = l \cdot \tau$. Here, “ l ” is the actual thickness of the membrane support and “ τ ” is the tortuosity of the membrane. The mass transfer coefficient (K) within the porous support layer is defined as (Tang et al., 2010).

$$K = \frac{\epsilon D}{l \tau} \dots \dots \dots (2 - 7)$$

Therefore, inserting equation 2-3 in 2-6:

$$J_w = K \ln \left[\frac{A H_o C_{\text{draw}} - J_w + B}{A H_o C_{\text{feed}} + B} \right] \dots \dots \dots (2 - 8)$$

Similarly, for AL-FS configuration, the water and solute flux on the dense layer are as follows:

$$J_w = K \ln \left[\frac{A H_o C_{\text{draw}} + B}{A H_o C_{\text{feed}} + J_w + B} \right] \dots \dots \dots (2 - 9)$$

$$J_s = -B(C_{\text{support}} - C_{\text{feed}}) \dots \dots \dots (2 - 10)$$

For the equations 2-4 and 2-10, for simplicity, it is assumed that same solution is flowing on both sides of the FO membrane.

2.9. PROCESS OPTIMIZATION OF FO-MBR

Several attempts were made to optimize the process parameters of the FO systems. The effect of membrane configuration on resultant flux through FO was thoroughly studied under the conditions of no fouling, with inorganic fouling and organic fouling (Mi and Elimelech,

2010a). Isoflux point is that point where both AL-DS and AL-FS configurations produce same flux in FO under similar operating conditions. It was discovered that with drastic membrane fouling, the isoflux point arrives relatively early and AL-FS orientation generated a more stable flux. Comparatively less overall membrane fouling and better fouling removal after physico-chemical cleaning was observed in AL-FS configuration (Zhao et al., 2011).

It was proved that due to the high ICP in AL-FS configuration the inorganic contaminant rejection was greater compared to the AL-DS configuration (Jin et al., 2012). Effects of draw solution temperature on separation performance, scaling and cleaning were thoroughly studied and it was evaluated that higher temperature generates greater starting fluxes, greater water throughput but, it causes harmful effects on scaling and membrane cleaning (Zhao and Zou, 2011).

It has been shown that membrane properties can play a crucial role in fouling trend. Membrane fouling may be reduced through aeration and osmotic backwashing. The osmotic backwashing may be applied in-situ for fouling mitigation and it is a practicable method (Lay et al., 2012). The effect of critical flux and ICP on the flux decline trend through the FO membrane was studied (Tang et al., 2010). The flux showed a starting gradual decline and then it stabilized after four days operation of the FO-MBR. Due to the buildup of salinity in the bioreactor, however, the efficiency of biodegradation was deteriorated significantly in FO-MBR. It was found that organics with high molecular weight were not found in the effluent of FO-MBR, compared to the organics with low molecular weights (< 266 g/mol). It was possibly due to the physical entrapment of the high molecular weight organics by the FO membrane.

The FO-MBR showed stable flux with continuously increasing salinity in the feed solution over the reactor operation period of 73 days (Lay et al., 2011). However, the decline in the membrane performance was very little and the fouling was minimal with significantly lower reverse transport of the draw solute than expected. It may be due to the formation of a gel-like layer on the membrane surface, which hindered the reverse solute transport from the draw solution into the bioreactor (Lay et al., 2011). Weekly osmotic backwashing in FO-MBR was found to be effective to restore 90 % of the initial water flux. FO-MBR was found extremely effective for the removal of the TOC and NH₄-N which suggests its compatibility with downstream RO systems as compared to the MBR-RO systems (Achilli et al., 2009a). Based on all the information gathered through the literature, the present study on the investigation of micellar draw solutions and process optimization of the FO-MBR was initiated.

Table 2-2: Summary of studies for FO process optimization

Study	Inferences	References
Effect of membrane configuration on flux in FO-MBR	Isoflux point arrives early in AL-FS configuration than AL-DS	Mi and Elimelech, 2010a
Fouling and its mitigation in FO	Less fouling and better fouling removal in AL-FS configuration	Zhao et al., 2011
Effect of ICP on inorganic contaminant removal in FO	High ICP in AL-FS caused high salt rejection	Jin et al., 2012
Effect of draw solution temperature on FO performance	High temperature helps high initial flux but harmful effects on membrane cleaning and scaling	Zhao and Zou, 2011
Fouling mitigation by aeration and osmotic backwashing	Methods were successful for fouling mitigation	Lay et al., 2012
Effect of ICP on flux decline in FO-MBR	Salinity buildup in the bioreactor stabilizes the flux	Tang et al., 2010
TOC and NH ₄ -N removal in FO-MBR	Highly effective	Achilli et al., 2009a

MATERIALS AND METHODS

3.1. MICELLAR SOLUTION AS DRAW SOLUTION IN FO

3.1.1. Membranes and Chemicals

Two types of FO membranes were used in this study. The first one was a flat sheet membrane made up of CTA with an embedded polyester mesh for support; Provided by HTI. The use of such flat sheet membranes in FO applications has already been reported (Lee et al., 2010). The membrane was used in a transparent FO module sourced from SMTC, NTU, Singapore. The effective area of the membrane was 47.25 cm² (10.30 cm x 4.58 cm). The second membrane used was a hollow fiber membrane molded in a module with two inlets and two outlets, prepared in house at SMTC. The membrane is constructed with an ultra-thin polyamide-based RO-like skin layer (300–600 nm) on inner surface of a porous hollow fiber substrate. The effective outer skin area of the hollow fibers was 174 cm². Detailed characterization of the membrane has already been reported (Wang et al., 2010).

All the chemicals and the bacterial growth media used in this study were of laboratory grade; purchased from the Sigma Aldrich or Fischer Scientific. The chemicals were used without any purification or alteration in their structure, unless mentioned. All solutions were prepared in de-ionized (DI) water. The main surfactants with their names, type, chemical formulae, molecular weight, CMC and abbreviations, frequently used in this study, are listed in the **Table 3-1**.

Table 3-1: Surfactants used in the study

Surfactant name and Chemical formula	Type	CMC (mol/L)	Mol. Wt. (g/mol)	Abbreviation used
Sodium dodecyl sulfate: [C ₁₂ H ₂₅ OSO ₃ Na]	Anionic	0.008	288.3	SDS
Tetraethyl ammonium bromide: [(C ₂ H ₅) ₄ NBr] or [C ₈ H ₂₀ NBr]	Cationic	0.16	210.1	TEAB
1-Octane sulfonic acid sodium salt: [C ₈ H ₁₇ SO ₃ Na]	Anionic	0.16	216.2	1-OSA
Trimethyloctylammonium bromide: [(CH ₃) ₃ N (C ₈ H ₁₇) Br] or [C ₁₁ H ₂₆ NBr]	Cationic	0.14	252.3	TMOAB
Meristyltrimethyl ammonium bromide [C ₁₄ H ₂₉ N(CH ₃) ₃ Br] or [C ₁₇ H ₃₈ NBr]	Cationic	0.0045	336	MTAB
Dodecyl trimethyl ammonium bromide [C ₁₂ H ₂₅ N (CH ₃) ₃ Br] or [C ₁₅ H ₃₄ NBr]	Cationic	0.015	308	DTAB

3.1.2. Experimental Setup and Procedures

Since a part of the experimental work of this study was performed at University of Oxford, UK and the other part at NUST, Pakistan, so, the laboratory scale FO setup were installed at both the universities. The micellar solution related work was performed at University of Oxford while the FO-MBR related experiments were conducted at NUST. Two batch FO setups; one with flat sheet and the other with hollow fiber membrane module, were installed at University of Oxford. The two setups were identical except the type of membrane module used. The schematic diagram of the hollow fiber FO setup is shown in the **Figure 3-1**.

The setup consisted of two poly-acrylic tanks serving as feed solution and draw solution reservoirs. A conductivity meter (YSI Hydrodata, UK) was installed in the feed solution tank to

monitor the change in conductivity with time. Meter can also measure total dissolved solids (TDS) concentration. Two variable speed gear pumps (R-73011-08, Cole Parmer, USA) were operated to continuously circulate the feed and draw solutions. The water flux was measured by measuring the change in mass of draw solution with time. Flow meters were also installed to cross check the feed and draw solutions cross-flow velocities.

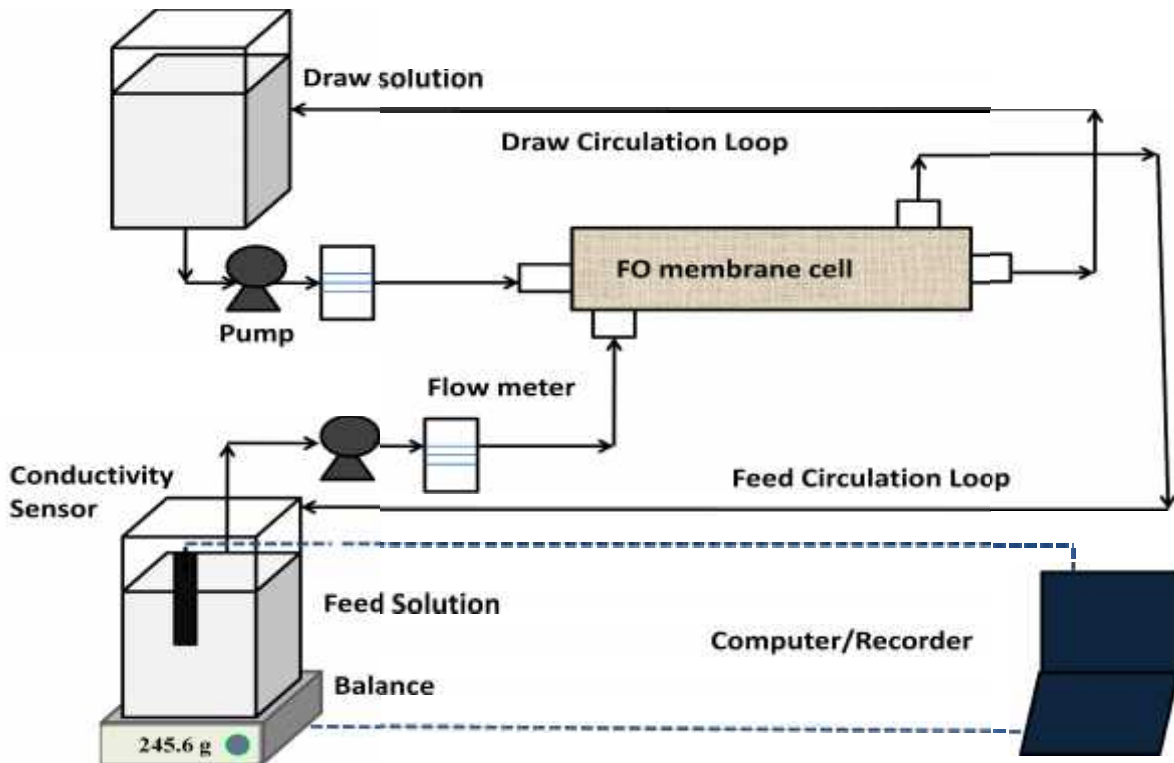


Figure 3-1: Schematic of hollow fiber FO setup at University of Oxford

The reverse solute transport was measured with the difference in the initial and final TDS of the feed solution. For measuring the specific reverse solute transport, solute flux/water flux (J_s/J_w), the experiments were conducted until the transfer of 1 L of feed water into the draw solution. Sodium chloride (NaCl) is the most commonly used draw solution in FO so; it was selected for

the comparison with micellar draw solutions in terms of flux, reverse transport and microbial toxicity. The experimental setup for the flat sheet FO module is shown in the **Figure 3-2**.

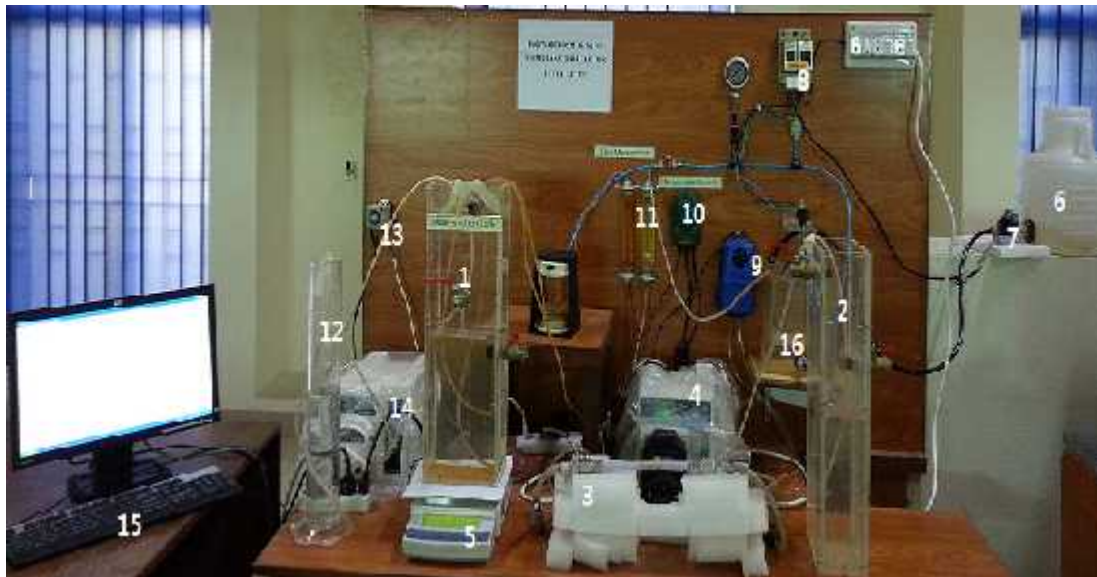


Figure 3-2: Flat sheet FO setup at University of Oxford

Figure 3-3 (a, b) shows the batch and semi-continuous experimental setup for FO-MBR at NUST. The batch setup was identical in configuration to the one installed at University of Oxford, however, the semi-continuous setup included an additional peristaltic pump controlled with a timer to inject the concentrated draw solution at specific time intervals. This maintained a fairly constant conductivity of the diluted draw solution and ultimately a constant osmotic pressure. For the FO-MBR experiments a synthetic wastewater (feed solution) control tank was used in combination with a solenoid valve, relay unit, feed solution control tank and a water level sensor. As the level of feed solution drops due to its transfer to the draw solution, same volume of fresh feed solution was automatically added in the feed solution tank to bring it back to the starting volume.



(a)



- | |
|---|
| <p>1. Draw solution tank 2. Feed solution tank 3. Hollow fiber module 4. Feed solution dosing pump 5. Digital balance 6. Synthetic wastewater reservoir 7. Solenoid valve 8. Relay unit 9. Aeration pump 10. Temperature control heater 11. Flow meters 12. Concentrated draw solution reservoir 13. Timer 14. Draw solution dosing 15. Data recorder 16. Feed control tank</p> |
|---|

(b)

Figure 3-3: (a) Batch and (b) semi-continuous hollow fiber FO-MBR setup at NUST

Characteristics of the synthetic domestic wastewater used in FO-MBR are summarized in **Table 3-2**. The mentioned quantities of different chemicals were added to make a synthetic COD of

500 mg/L and the COD: N: P ratio of 100: 10: 2 to maintain an adequate level of nutrients in the wastewater for microbial growth.

Table 3-2: Chemical composition of the synthetic wastewater

Chemicals	Formula	Quantity (mg/L)
Glucose	$C_6H_{12}O_6 \cdot H_2O$	514
Ammonium Chloride	NH_4Cl	190
Potassium di-Hydrogen Phosphate	KH_2PO_4	55.6
Calcium Chloride	$CaCl_2$	5.7
Magnesium Sulphate	$MgSO_4 \cdot 7H_2O$	5.7
Ferric Chloride	$FeCl_3$	1.5
Manganese Chloride	$MnCl_2 \cdot 4H_2O$	1
pH buffer	$NaHCO_3$	142.8

3.1.3. Analytical Methods

Osmotic pressure of the draw solutions was measured using an Osmometer (Micro-osmometer 13/13DR Roebing, Germany). The instrument measures the osmolality based on the freezing point depression of the solution. Distilled water, which has zero osmotic pressure, was used for calibration. The osmolality of the solution was converted to osmotic pressure using the Mores equation (equation 2-1).

Sludge particle size distribution was analyzed through a particle size analyzer which is based on the laser scattering principle (LA-920 Horiba, Japan). The results were reported in percentage of particle size volume. Total organic carbon (TOC) and total nitrogen (TN) were analyzed by high temperature combustion method using a TOC/TN analyzer (Analytic Jena Multi N/C 3100, Germany). The AFM images of the fouled membranes were taken with a high resolution

scanning probe microscope (JSPM-5200, USA). The optical microscopic images of the membranes were taken from the XXX microscope.

EPS were also measured in the sludge samples. Soluble EPS was separated from the total EPS through sludge centrifugation at 5000 rpm for 15 minutes and then analyzing the supernatant. Bound EPS was separated by the cation exchange resin method (Frølund et al., 1996). The carbohydrate and protein portions of both types of EPS were measured through phenol–sulfuric acid method (Dubois et al., 1956) and the Lowry method (Lowry et al., 1951). The COD was measured by closed reflux titrimetric method “5220 C” (APHA, 2005).

3.1.4. Reverse Transport of Draw Solutions

For measuring the reverse transport of inorganic salts and the surfactants, the AL-DS configuration of hollow fiber module was used. All experiments were conducted at room temperature around 22 ± 1 °C. The experiments were conducted until the transfer of 1 L water from feed to draw side, to calculate specific reverse transport (J_s/J_w). The feed solution was DI water and analytical grade salts were mixed in DI water to make different draw solution concentrations.

3.1.5. Recovery/Regeneration of Diluted Micellar Draw Solutions

Two methods were used for the regeneration/recovery of micelles from the diluted draw solution. The Krafft temperature method involves bringing the solution temperature below the T_k which converts micelles into less soluble monomeric crystals. After crystallization, the monomers were recovered with paper filtration through filter papers (Whatman Grade 1, Sigma Aldrich, UK)

under gravity filtration. The concentration of surfactant in the filtrate gives the amount of surfactants passed through the membrane and by subtracting this value from the original concentration, the recovered value was calculated.

UF was also applied as a regeneration method. The UF membranes of 10,000 Dalton molecular weight cut off (MWCO) (Millipore, USA) were used in the experiments. In each experiment 40 mL of the diluted draw solution were filtered at 2 bar trans membrane pressure (TMP); produced by the inert nitrogen gas. Filtration was carried out until 10 mL was left in the cell or 30 mL was received as the filtrate. For this, the UF membrane was installed in a dead end filtration stirred cell setup (8050 Amicon, USA). Stirring was maintained at 600 rpm (10 Hz) to keep the solution mixed during filtration.

The residual surfactants in the product water after filtration was assessed by two-phase titration. For anionic surfactants 0.004 M Hyamine [$C_{27}H_{42}ClNO_2$] was used as titrant, dimidium bromide-disulphine blue as indicator and chloroform as the second phase. The end point was a color change from pink to blue in the chloroform phase. The sample volume was kept at 5 mL and the ratio of sample to the chloroform was maintained at 2.7:1. **Figure 3-4** shows the structure of dimidium bromide and disulphine blue.

Since chloroform is denser than water, two separate layers were formed in the solution. The Dimidium portion from the indicator makes a complex with the anionic surfactant; which gets soluble in the chloroform phase and develops a pink color in it. As Hyamine is added as a titrant, it displaces the Dimidium from the complex back to the aqueous phase and the chloroform turns

back to transparent in color. Once all the dimidium is replaced, the excess Hyamine forms a salt with the disulphine blue portion of the indicator and develops a blue color in the chloroform phase. For cationic surfactants, the end point is from blue to pink in the chloroform phase and some anionic surfactant like SDS can be used as the titrant. The concentration of the surfactant residue in the permeate sample is calculated as follows.

$$C_{\text{surfactant}} = (0.004 \times V_{\text{hyamine}}) / \text{Volume of sample} \dots\dots (3-1)$$

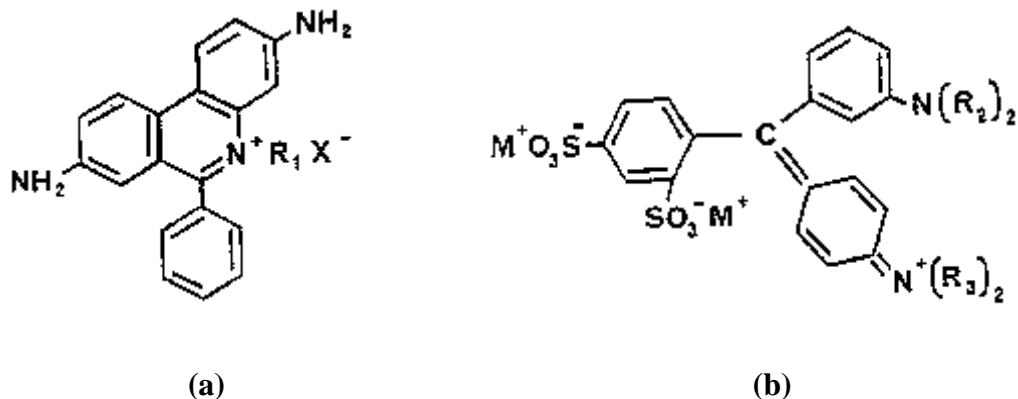


Figure 3-4: Structure of (a) Dimidium bromide and (b) Disulphine blue

3.1.6. Microbial Toxicity of Micellar Solutions

Microbial toxicity was evaluated using two individual microbial species of *E.coli* and *Pseudomonas aeruginosa* and also with mixed activated sludge. Mono culture of *E.coli* was obtained from National Collection of Industrial Bacteria (NCIB) 8879, UK and mono culture of *Pseudomonas aeruginosa* was isolated from the mixed sludge of a lab scale MBR at NUST. The mixed activated sludge was also sourced from the same MBR. Initially the toxicity testing was done on *E.coli* with eight most commonly used inorganic draw solutes and four ionic surfactants,

and then the toxicity testing was done on *Pseudomonas aeruginosa* and mixed activated sludge in more detail using four surfactants. The methodology for mixed activated sludge and *Pseudomonas aeruginosa* toxicity testing was identical; however, there was a slight difference in the methodology for *E.coli*, which is discussed below.

For *E.coli* toxicity eight inorganics; sodium chloride [NaCl], calcium chloride [CaCl₂], potassium chloride [KCl], magnesium chloride [MgCl₂], potassium sulfate [K₂SO₄], magnesium sulfate [MgSO₄], sodium sulfate [Na₂SO₄], ammonium sulfate [(NH₄)₂SO₄] and four surfactants; TMOAB, DTAB, MTAB, SDS were tested. Five different concentrations of 0.1, 0.05, 0.025, 0.010 and 0.005 M were prepared for all twelve draw solutions. These eight inorganic draw solutions are supposed to be the most commonly used draw solutions in FO (Achilli et al., 2010). The four surfactants were chosen on the basis of their type and the ability to generate high water flux. The concentration range was selected based on practically possible reverse transportable draw concentrations in FO-MBR.

The concentration range (0.005–0.1 M) was kept same for surfactants and inorganics to make the comparison more effective. The *E.coli* culture, which was grown over night on nutrient broth, (9 mL) was allowed to react with the solution (1 mL) for 14-16 hours in a shaking incubator at 30 °C and 60 rpm (1 Hz). This time was selected in accordance with the life cycle curve of *E.coli* which shows maximum growth around this time before going into the lag phase. After sixteen hours the samples were immediately transferred on the already prepared and dried nutrient agar plates. These plates were allowed to incubate again for 14-16 hrs at 30 °C and then the colony counting was done on a digital counter (SC6 Plus, UK). **Figure 3-5** shows the colony counting

process. The colony counts of different solutions were compared with the control to see the effect of various draw solutions on net bacterial growth.

For testing the toxicity of micellar solutions to the *Pseudomonas* and mixed activated sludge, the solutions of 0.005, 0.01 and 0.05 M concentration with 10 mL volume, were prepared for the four different surfactants TEAB, SDS, TMOAB and 1-OSA. The first batch of experiments was conducted with *Pseudomonas aeruginosa*, which is believed as one of the leading species in the MBR sludge.

Four flasks were prepared, each with a total volume of 250 mL of the *Pseudomonas aeruginosa* culture grown on the nutrient broth. To each flask was added 0.005 M solution (10 mL) of one of the four surfactants. The four flasks were placed on a mechanical shaker at 60 rpm (1 Hz) for 24 hrs to acclimatize the bacterial specie with the surfactant solution. From one of the above mentioned flasks, e.g. TEAB flask, the acclimatized culture was added into three different flasks (36 mL in each) and 4 mL of 0.005, 0.01 and 0.05 M solutions of TEAB were added in the three flasks, respectively. The ratio of 4 mL surfactant solution/36 mL of bacteria (1:9) was similar to the one used for *E.coli* i.e. 1 mL of solution/9 mL of bacteria. Another flask was prepared as a control with 4 mL of DI water, instead of TEAB solution.

In the same manner samples were prepared for all four surfactants, so a total of twelve flasks were prepared. All the flasks were placed on the mechanical shaker at 60 rpm (1 Hz) for 48 hrs. Samples were taken from all flasks at 0, 24 and 48 hrs and TOC measurement and bacterial counting was done on each sample. For bacterial counting the samples were spread on the already prepared and dried nutrient agar plates which were then placed in the incubator over

night and next day the counting was performed. In the next batch of experiments, similar methodology was adopted with all other surfactants. In the next series of experiments, mixed activated sludge replaced *Pseudomonas aeruginosa*, however, rest of the methodology remained same as above.



Figure 3-5: Bacterial colony counting on a digital colony counter

3.2. PROCESS OPTIMIZATION OF FO-MBR

Several processes that are considered extremely critical in increasing the net flux through FO-MBR were optimized as follows.

3.2.1. Optimization of Draw Solution Concentration

Experiments were conducted for 8 hrs each on hollow fiber FO setup with 1-6 M NaCl (0.5 L) as the draw solution and DI water (1 L) as feed solution. The AL-DS configuration was adopted with 150 mL/min cross-flow velocity.

3.2.2. Optimization of Membrane Chemical Cleaning

EDTA is a well known hexa-dentate chelating agent and is famous for its capability to remove metal ions from solutions by forming insoluble complexes with them. SDS is an anionic surfactant and contains Na⁺ as cation. EDTA can remove the Na⁺ from SDS to break and detach it from the membrane surface. Hence EDTA cleaning was optimized for both flat sheet and hollow fiber membranes. All experiments were conducted using 0.15 M SDS/TEAB (150 mL) as draw solution and DI water as feed solution with AL-DS configuration. All experiments were conducted at the 150 mL/min cross-flow velocity on hollow fiber and 300 mL/min on flat sheet FO modules to minimize ECP.

After every experiment EDTA cleaning was done for different time and concentrations, to optimize it. Fresh 0.15 M SDS solution (150 mL) was used as draw solution for each next experiment. Initially the experiments were done on both flat sheet and hollow fiber membranes, but then due to lower flux difference (immeasurable) between cleaned and fouled flat sheet membranes, they were not studied further. Since the CMC of SDS is 0.008 M which is 18.7 times less than the starting concentration for all experiments (0.15 M), so, ideally the flux should remain constant during the experiment with the constant dilution of the draw solution. Also, as there is no other foulant in the system except SDS so, any drop in flux may only be attributed to the membrane fouling by SDS.

3.2.3. Optimization of Osmotic Backwashing

Osmotic backwashing was performed on hollow fiber FO-MBR batch setup by replacing draw solution from 2 M NaCl to DI water; however, the feed solution remained same i.e. mixed

activated sludge with MLSS concentration of 6000 mg/L. Before changing the draw solution to DI water the module and piping were flushed with DI water for 2 minutes. This was done to avoid contamination of the DI water with NaCl solution present in the piping or module. The normal operation of the FO system was termed as filtrate and reverse operation as backwash. All experiments were of total 8 hrs comprising of 7 hrs filtration and 1 hr backwash. Experiments were conducted in batch mode and after each experiment the membrane was chemically cleaned.

3.2.4. Optimization of Cross-flow Velocity

Two types of experiments were conducted to optimize the cross-flow velocity. For hollow fiber FO module the velocity was varied between 50, 100 and 150 mL/min for both draw and feed solutions. Feed solution was DI water and 0.5 L of 1 M sodium chloride was used as the draw solution. Experiments were conducted with AL-DS configuration in batch mode.

For flat sheet FO-MBR, four different cross-flow velocities i.e. 100, 300, 700 and 1000 mL/min were studied in semi-continuous experiments. The draw solution concentration was 2 M NaCl and volume was 1 L for all experiments. The concentration of concentrated draw solution was 5 M NaCl and membrane orientation was AL-DS for all experiments. Feed solution was activated sludge with a mixed liquor suspended solids (MLSS) concentration of 6000 mg/L and a volume of 2.5 L. All experiments were carried out in a batch mode for 48 hours.

For nullifying the effect of declining draw solution concentration on the net flux, experiments were conducted in the semi-continuous mode by constantly adding the concentrated draw solution. The starting MLSS concentration was maintained at 6000 mg/L because it is within the

recommended concentration range for MBR and also used in previous reported studies for FO-MBR (Achilli et al., 2009 a). The final flux was calculated by excluding the volume of concentrated draw solution added.

RESULTS AND DISCUSSION

4.1. MICELLAR DRAW SOLUTION

4.1.1. FO System Flux Using Micellar Draw Solutions

Membrane orientation and hydrodynamics perform a key role in FO process. The effect of flat sheet membrane orientation and the direction of cross flow velocity on resultant water flux using 1 M TMOAB as draw solution is shown in **Figure 4-1**. The AL-DS configuration produced higher flux but the flux presents a much accentuated decline. The AL-FS configuration generated lower water flux due to higher ICP, however, this phenomenon resulted in a milder decline of the flux, which represents a more stable process. Such severe ICP in AL-FS configuration is reported in the literature (Tang et al., 2010). The effect of flow direction on the water flux can also be observed in Figure 4-1.

It was believed that the maximum amount of heat transfer will occur with countercurrent cross-flow configuration because this will maintain a slowly declining concentration gradient i.e. less osmotic pressure difference inside the membrane. This little osmotic pressure gradient was supposed to produce relatively stable flux than co-current configuration (Loeb and Bloch, 1973). Micellar solutions demonstrated similar flux trends for both countercurrent and co-current cross-flow velocities in AL-DS configuration. Since the DI water was used as the feed solution so, in AL-DS configuration there was no effect of cross-flow velocity direction on resultant flux as

there was no accumulation of any contaminants in the support layer. In AL-FS configuration, however, the porous support layer was facing the micellar solution and so the counter current cross-flow velocity caused a little osmotic pressure gradient and ultimately a lower but stable flux compared to the co-current flow.

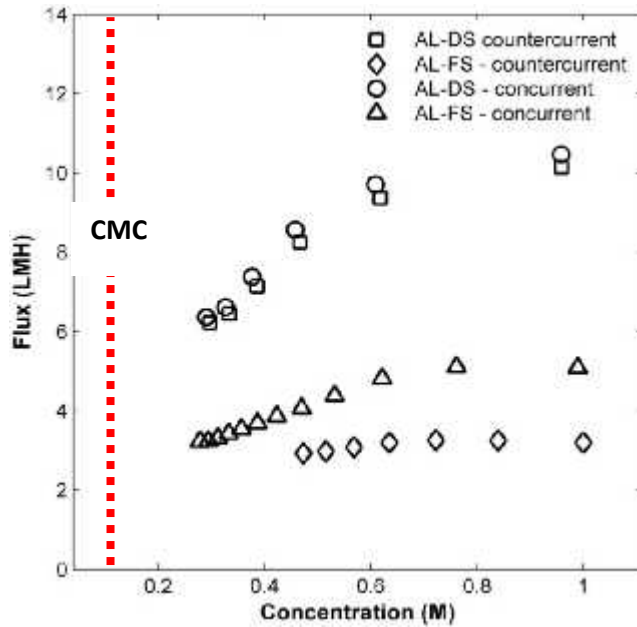


Figure 4-1: ICP effect on the flat sheet FO membrane with 1.0 M TMOAB as draw solution

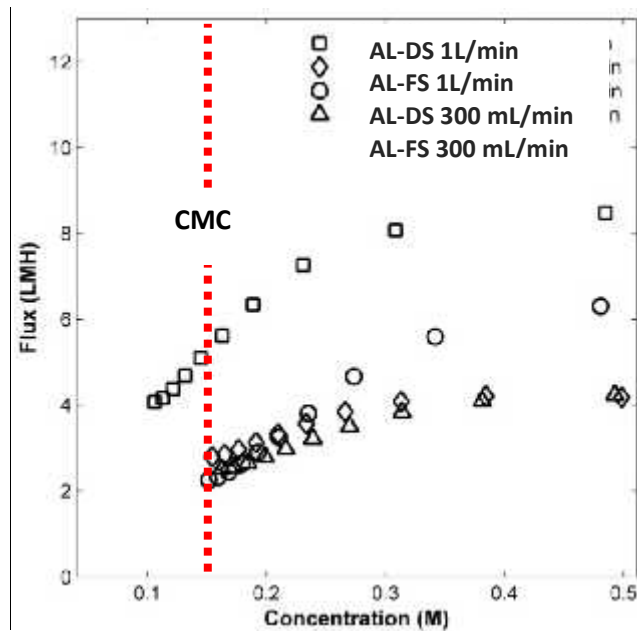


Figure 4-2: ECP effect on the flat sheet FO membrane with 0.50 M TEAB as draw solution

Figure 4-2 demonstrates that the ECP on a flat sheet membrane may be mitigated by increasing the cross-flow velocity of the micellar draw solution. There was 1.5 times increase in flux with 3.3 times increase in the cross-flow velocity from 300 to 1000 mL/min in AL-DS configuration. However, AL-FS flux was not much affected since in this configuration the ICP dominates. So, the effect of cross-flow velocity is more on ECP rather than on ICP. The flux produced with TMOAB and TEAB are comparable to the fluxes generated through fertilizer based draw solutions (Phuntsho et al., 2011) and are better than the fluxes generated by water soluble sodium and lithium phosphazine salts and copper sulfate (Stone et al., 2013; Alnaizy et al., 2013) at similar concentrations.

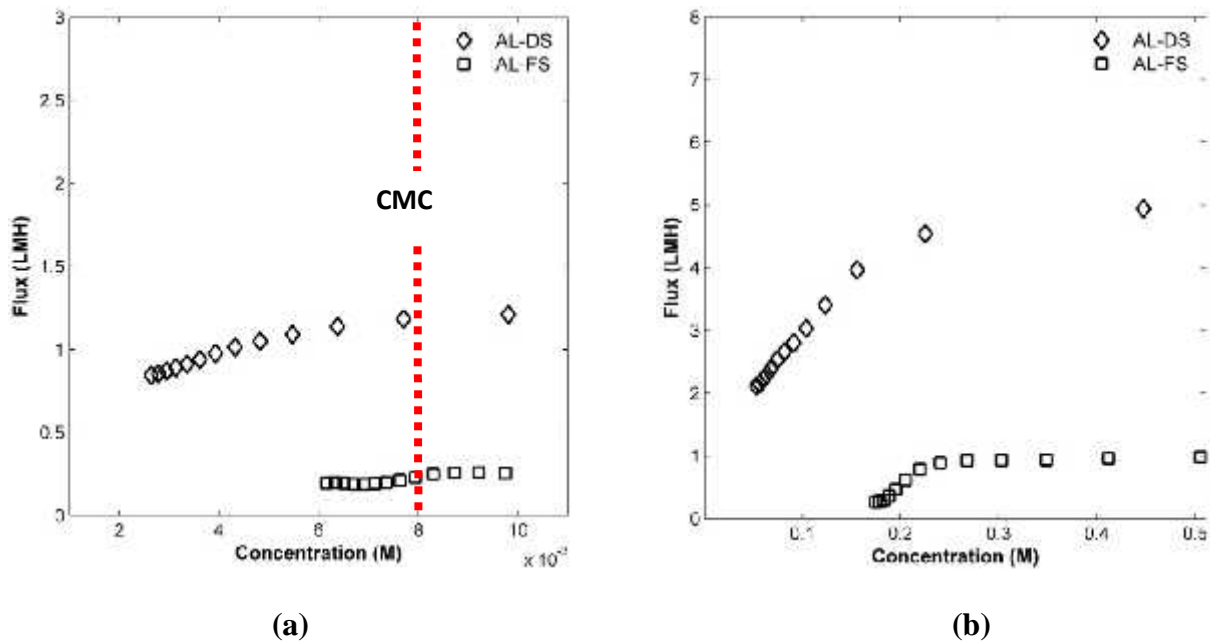


Figure 4-3: Flux with hollow fiber FO membrane using (a) 0.010 M SDS and (b) 0.50 M SDS as draw solution

Figure 4-3 shows the potential use of SDS as draw solute at two different concentrations. Comparing **Figures 4-3a** and **4-3b** it may be noticed that a 50 times decrease in SDS

concentration caused only 4 times decrease in the resultant flux in both AL-DS and AL-FS configurations. This is due to the fact that micellar solutions depict a constant osmotic pressure above the CMC and resultantly they must depict a constant water flux until the concentration of the diluted draw solution is above the CMC. As shown in **Figure 4-3a**, a constant flux was achieved till the concentration of the draw solution was above CMC (0.008 mol/L) and then the flux gradually declined like the flux generated by inorganic draw solutes. It was discovered that the property of constant flux is observable only at the concentrations slightly above the CMC and at higher concentrations micellar solutions start behaving like inorganic draw solutions.

Figure 4-4 demonstrates the effect on the net flux with micellar solutions of low and high CMCs as draw solution. Wherever the membrane orientation is not mentioned it must be taken as AL-DS configuration. It is worth mentioning that, smaller the size of the surfactant chain greater is the CMC, and vice versa. With about 35 times higher CMC the TEAB produced around 18 times higher flux than the MTAB at similar concentrations. Similarly, with about 35 times higher CMC the 1-OSA depicted 14 times higher flux than MTAB. So, an optional choice of surfactant can be made based on the specific FO application and desired water flux.

Comparing the flux of TEAB and 1-OSA (**Figure 4-4**) with NaCl (**Figure 4-5**) it may be observed that although initially NaCl depicted much higher flux, almost double, than both the surfactants, it declined abruptly with declining draw solution concentration. However, the micellar solutions demonstrated a much stable flux with declining draw solution concentration and near 0.20 M concentration the fluxes of both TEAB and 1-OSA were higher than NaCl.

Hence it is proved that micellar draw solutions are a better choice than NaCl for stable FO operations.

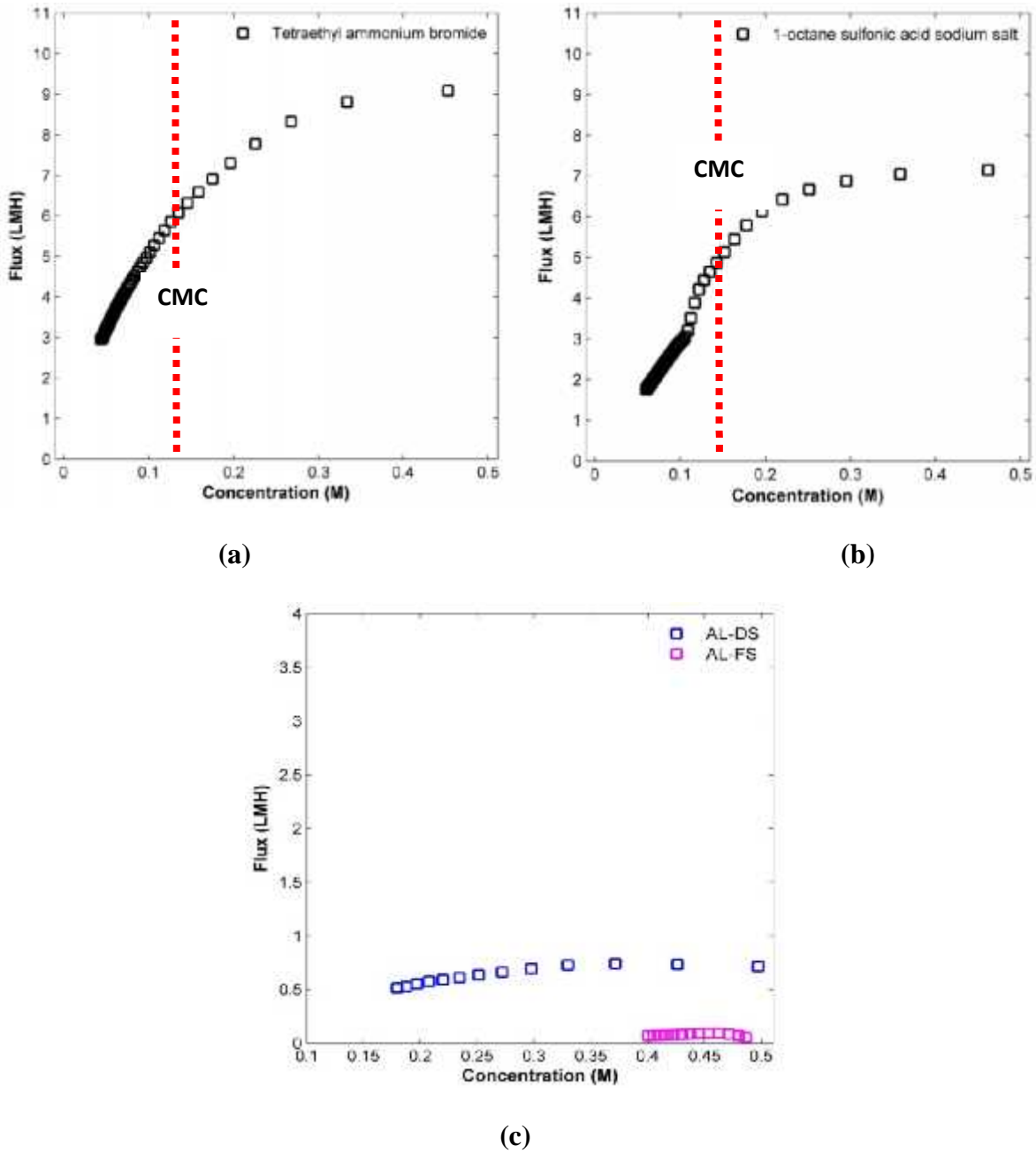


Figure 4-4: Flux with hollow fiber FO membrane using (a) 0.50 M TEAB, (b) 0.50 M 1-OA and (c) 0.50 M MTAB as draw solution

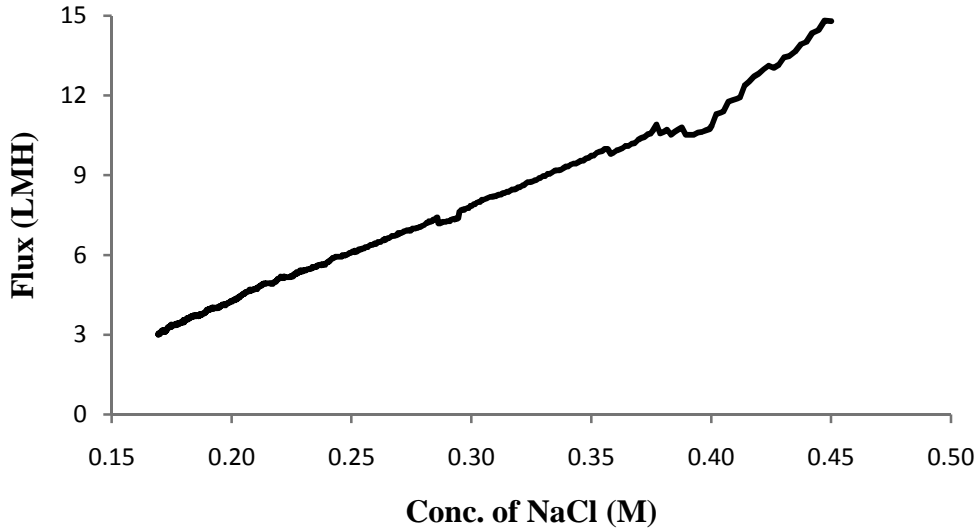


Figure 4-5: Flux with hollow fiber FO membrane using 0.50 M NaCl as draw solution

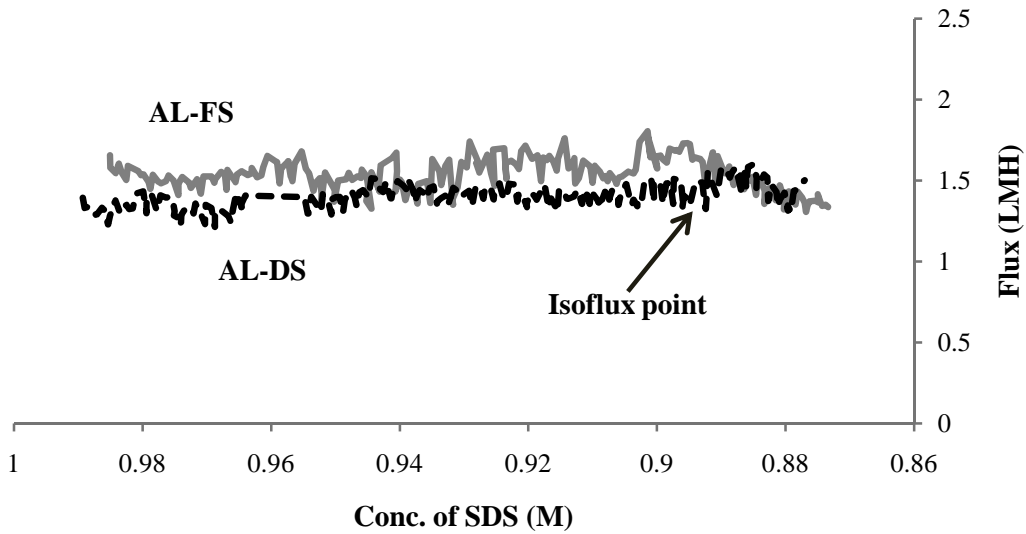


Figure 4-6: Flux with SDS as draw solution and MBR sludge as feed solution using flat sheet FO-MBR setup

Flux generated by 1 M SDS (0.5 L) as draw solution with MLSS concentration of 6000 mg/L as the feed solution is shown in **Figure 4-6**. The batch experiment demonstrated a fairly constant flux around 1.5 Liters/m²/hr (LMH) with declining SDS concentration. Also the AL-FS

configuration (less ICP) demonstrated a bit higher flux compared to the AL-DS (more ICP), but eventually the isoflux point was reached around 0.89 M SDS concentration. This proves the effective use of surfactants as draw solution for stable FO-MBR operation.

4.1.2. Mass Transfer of Micellar Draw Solutions

The structural parameter (S) of the membranes was calculated by characterizing the morphology and structure of the membrane by both SEM and AFM. The values of “S” were 5.75×10^{-4} m for HTI flat sheet FO membrane and 5.95×10^{-4} for hollow fiber FO membrane. The mass transport coefficient of micellar solutions was determined by fitting the reverse transport data in least squares method. The value determined for sodium chloride across the flat sheet membrane was 3.3×10^{-6} m/s in agreement to within 10 % of values for this parameter reported in the literature (Chou et al, 2010; Tang et al., 2010). **Table 4-1** summarizes “K” for different surfactants, different membranes and for different membrane configurations.

The diffusion coefficients in general were on the order of 1 to 5×10^{-6} m/s, with the exception of SDS and MTAB where (except for SDS in AL-DS mode) they are an order or two of magnitude lower. In the former case, these values are of the same order of magnitude as that for sodium chloride. Since the diffusion coefficient generally scales as the inverse square root of molecular weight, one might expect the value for surfactant monomers to be consistently 2 or 3 times smaller than that for NaCl. The agreement can thus be considered reasonable. In the latter two cases of SDS and MTAB only, one is operating at concentrations many times the CMC so that the presence of micelles dominate. As micelles are many times (~100) larger than the individual monomers, the transport within the porous support layer is much slower. In

this case, the small magnitude of the diffusion coefficients as compared with sodium chloride is consistent with the reverse transport results in **Table 4-2a**.

Table 4-1: Mass transport coefficient for different surfactants

Surfactant	Type	Configuration	Mass transport coefficient (K) (10^{-6} m/s)
SDS	Flat sheet	AL-DS	0.3823
	Hollow fiber	AL-DS	1.276
		AL-FS	0.3075
TEAB	Flat sheet	AL-DS	3.4075
		AL-FS	5.4475
	Hollow fiber	AL-DS	2.2413
1-OSA	Hollow fiber	AL-DS	1.658
TMOAB	Flat-sheet	AL-DS	3.872
		AL-FS	2.978
MTAB	Hollow fiber	AL-DS	0.156
		AL-FS	0.0154

4.1.3. Reverse Transport of Micelles

Reverse solute transport of micellar draw solutions was compared to NaCl under similar concentrations. For NaCl it increased proportionally with increasing draw solution concentration from 0.01 to 1 M, while for micellar solutions the values were much lower and the trend was much less pronounced. This may be explained by the fact that under micellar conditions the molecular weight may reach up to 14,400 - 28,800 g/mol, which prevents its leakage on the feed

side. The relatively high micellar reverse transport at smallest concentration (0.01 M) can be attributed to the dominating presence of the monomers in the solution near the CMC.

Table 4-2a: Comparison of reverse solute transport (mg/L) of micellar and NaCl draw solutions

D.S. Conc. (M)	Actual Reverse Transport (mg/L) and reverse transport ratio (NaCl/surfactant)					
	NaCl	SDS	TEAB	TMOAB	1-OSA	MTAB
0.01	0.10	0.028 (3.5)	0.025 (4)	0.033 (3)	0.006 (16)	0.038 (2.6)
0.05	0.70	0.014 (50)	0.008 (87.5)	0.022 (32)	0.0075 (93)	0.014 (50)
0.5	2.67	0.074 (36)	0.011 (242)	0.06 (44)	0.030 (89)	0.0475 (56)
1	3.22	0.012 (268)	0.067 (54)	0.057 (56)	0.062 (53)	0.032 (100)
CMC (mol/L)	N/A	0.008	0.16	0.14	0.16	0.0045

Table 4-2b: Comparison of reverse solute transport (mol/L) of micellar and NaCl draw solutions

D.S. Conc. (M)	Actual Reverse Transport (mol/L) and reverse transport ratio (NaCl/surfactant)					
	NaCl	SDS	TEAB	TMOAB	1-OSA	MTAB
0.01	1.7×10^{-6}	9.7×10^{-8} (17.5)	1.19×10^{-7} (14.2)	1.30×10^{-7} (13)	2.7×10^{-8} (62)	1.13×10^{-7} (15)
0.05	1.19×10^{-5}	4.86×10^{-8} (244)	3.8×10^{-8} (313)	8.7×10^{-8} (136)	3.4×10^{-8} (350)	4.1×10^{-8} (286)
0.5	4.5×10^{-5}	2.56×10^{-7} (175)	5.23×10^{-8} (860)	2.38×10^{-7} (189)	1.38×10^{-7} (326)	1.41×10^{-7} (319)
1	5.5×10^{-5}	4.16×10^{-8} (1322)	3.19×10^{-7} (172)	2.2×10^{-7} (250)	2.8×10^{-7} (196)	9.5×10^{-8} (578)
CMC (mol/L)	N/A	0.008	0.16	0.14	0.16	0.0045

Table 4-2a depicts the actual reverse transported concentrations in mg/L and **4-2b** shows the same concentrations in mol/L. It is interesting to note that the surfactants with lower CMC (large

chain size) depicted less reverse transport, compared to the surfactants with higher CMCs (small chain size), probably due to more steric hindrance experienced by the large chains. This shows that although the low CMC surfactants are not good in generating high flux, but they show minimum reverse transport. The minimal reverse solute transport compared to inorganics is an added advantage of micellar solutions, because it may cause membrane fouling and contamination of the feed stream as well as the biomass in FO-MBR and disturb the overall process. Again, there is an optional choice available as per the requirement of the specific FO process. Also, it is recommended to use micellar solutions always above the CMC to minimize the reverse transport.

4.1.4. Recovery/Regeneration of Diluted Micellar Solution

The regeneration potential of micelles from diluted draw solution was also investigated. **Table 4-3** summarizes the results of the regeneration experiments. Krafft temperature results are not discussed for those surfactants which did not exhibit crystal formation at or below 5 °C or for which the Krafft temperature is not specifically mentioned in the literature. It is worth noticing that the treated concentration for the UF was found to be independent of the influent concentration and the CMC limits the removal efficiency roughly for most of the surfactants. The treated concentrations around or below the CMC describe that monomers can pass through the UF membrane; for their removal nano filtration may be applied.

TEAB demonstrated much better removal at starting concentration (0.15 M) below its CMC which encourages its use even at the lower concentrations. It is also observable that SDS regeneration through both methods depends mainly on the influent concentration therefore, it is

recommended to add concentrated draw solution to the SDS diluted draw solution as it reaches 0.15 M concentration. Unlike other surfactants, MTAB demonstrated a behavior of increasing treated concentration with increasing draw solution concentration. This shows that the MTAB can only be used as a draw solution at low concentrations i.e. where low fluxes are required. It may also be inferred that the surfactants with long straight carbon chain (micellar tail) prefer Krafft crystallization compared to the surfactants with short chain.

The regeneration of diluted micellar draw solution was easier and energy efficient than the regeneration of other draw solutions like NH_4HCO_3 , Sucrose, Organic salts and Copper sulfate (McCutcheon et al., 2005; Su et al., 2012; Bowden et al., 2012; Alnaizy et al., 2013).

Table 4-3: Regeneration potential of micelles from diluted draw solution

Surfactant	CMC (mol/L)	Regeneration Method	Feed conc. (M)	Effluent conc. (M)	Recovery Efficiency (%)
TEAB	0.16	UF	0.15	0.0075	95
		UF	0.24	0.008	96.6
		UF	0.5	0.0032	99.3
SDS	0.008	UF	0.012	0.008	33.3
		UF	0.15	0.008	94.6
		Krafft point	0.075	0.043	42.4
		Krafft point	0.15	0.009	93.7
1-OSA	0.16	UF	0.15	0.029	80.6
		UF	0.25	0.026	89.6

TMOAB	0.14	UF	0.15	0.114	23.5
		UF	0.0045	0.0002	95.5
		UF	0.15	0.011	92.5
MTAB	0.0045	UF	0.50	0.051	89.7
		Krafft	0.075	0.0048	93.6
		Krafft	0.15	0.024	84

4.1.5. Direct Reuse of Diluted Micellar Solution

Although the micelles can be regenerated or separated easily from the diluted draw solution, as discussed above, but the diluted draw solution can also be used directly for a number of domestic, agricultural and industrial applications. As a detergent, the washing of clothes, cars and floors is a useful application at the household level. The concentration of textile dyes from the dyeing wastewater through micellar draw solution and the use of that diluted draw solution in fabric washing or mercerizing process could be an interesting and economical industrial application. Surfactants are also used in the manufacturing of pesticides, water based paints, quality lubricants and defoamers. The surfactants are proven to be good in the remediation of sites contaminated with non aqueous phase liquids (NAPLs) and as foamer solutions for enhanced oil recovery. Such direct reuse of different diluted draw solutions are also reported in the literature (Kravath and Davis, 1975; Phuntsho et al., 2011; Wallace et al., 2008).

4.1.6. Toxicity of Inorganic and Micellar Draw Solutions to *E.coli*

Figures 4-7 to 4-14 describe the growth of *E.coli* in presence of different concentrations of eight most commonly used inorganic draw solutes. Average values of triplicate growth measurements

with standard deviation bars are shown in all the figures. For consistency the units are kept constant in all the graphs. The average growth and the percent growth of *E.coli* to the control are shown. **Figure 4-7** shows the trend of *E.coli* growth after reaction with NaCl, minimum growth was 60 % and maximum was 90 % to the control. The second degree polynomial trend line on the graph suggests that the overall trend was increasing *E.coli* concentration with increase in salt concentration. **Figure 4-8** depicts a similar increasing growth trend after reaction of *E.coli* with KCl. Similar increasing growth trends while reacting different concentrations (0, 0.5, 1.0, 1.5% w/v) of NaCl and KCl with *E.coli* were observed (Abdulkarim et al., 2009). **Figure 4-9** shows that calcium chloride was very effective for *E.coli* growth. The trend was increasing from 75 to 120 % of control. This growth supportive trend of calcium is the reason for its use as one of the micro-nutrients for the biomass growth in the bioreactors. Thus it may be used safely as a draw solution.

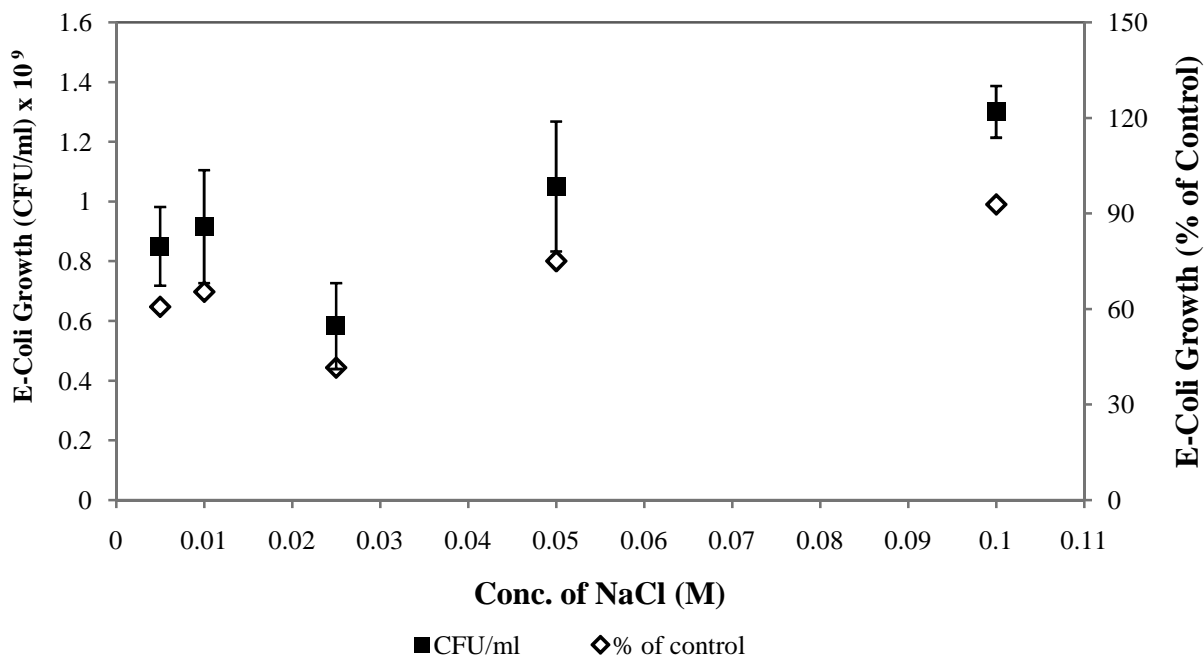


Figure 4-7: Effect of NaCl on *E.coli* growth

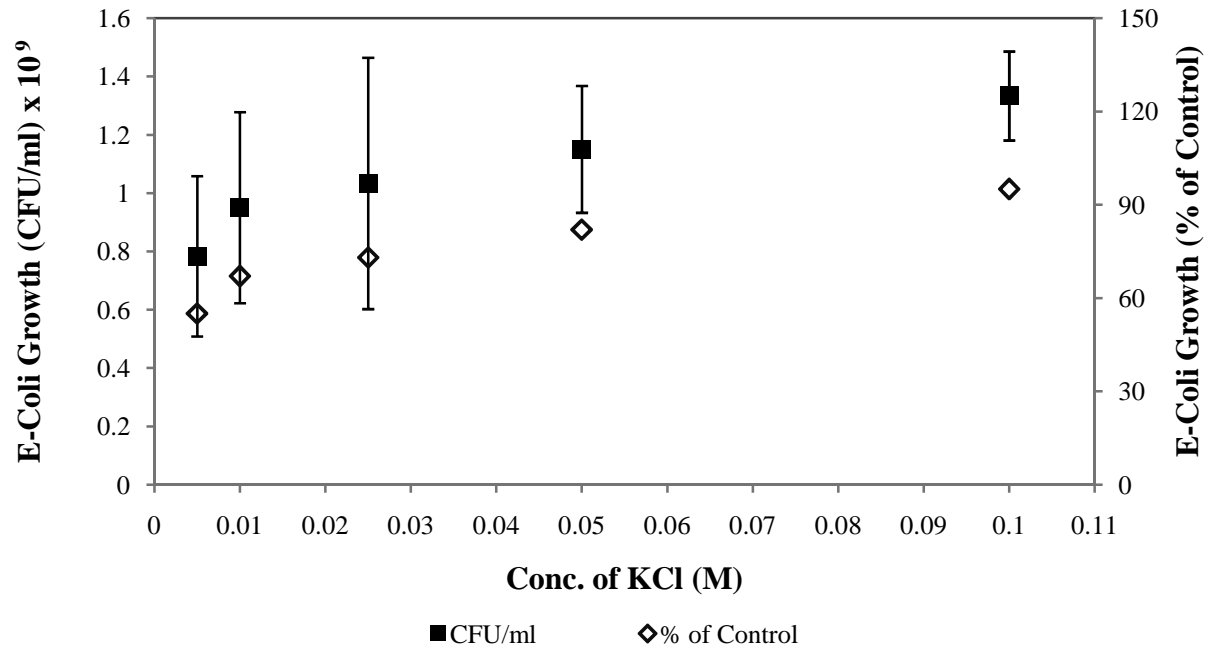


Figure 4-8: Effect of KCl on *E. coli* growth

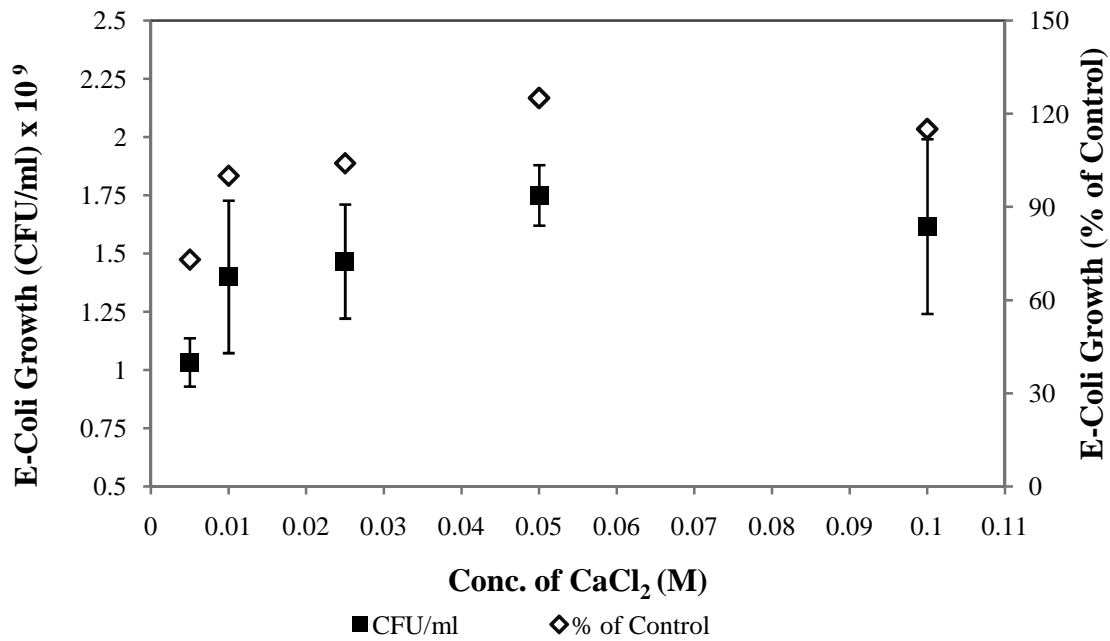


Figure 4-9: Effect of CaCl₂ on *E. coli* growth

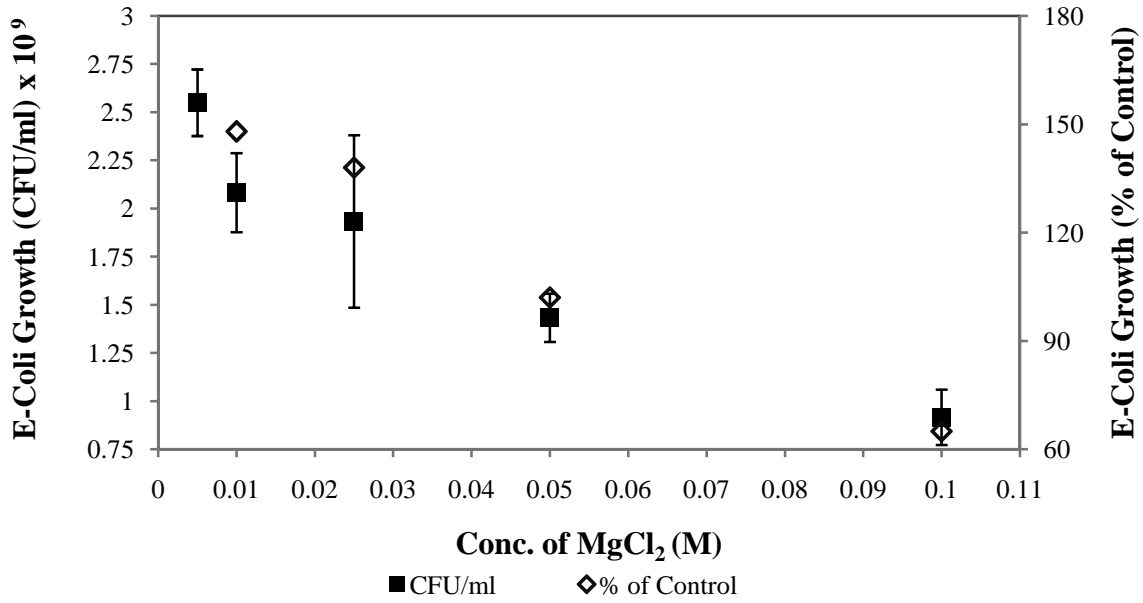


Figure 4-10: Effect of MgCl₂ on *E. coli* growth

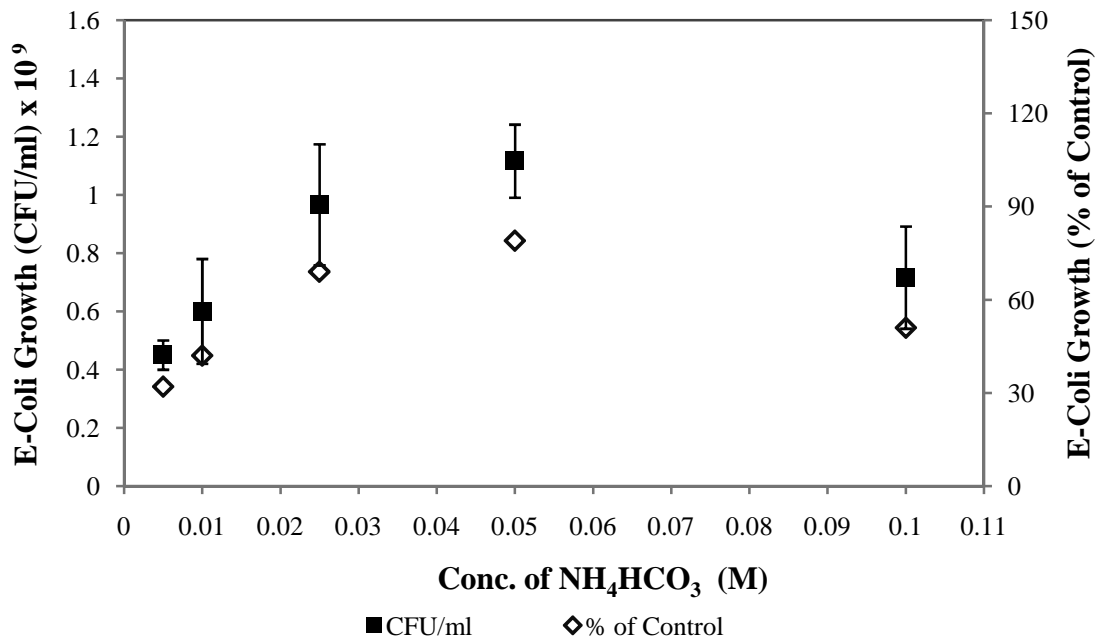


Figure 4-11: Effect of NH₄HCO₃ on *E. coli* growth

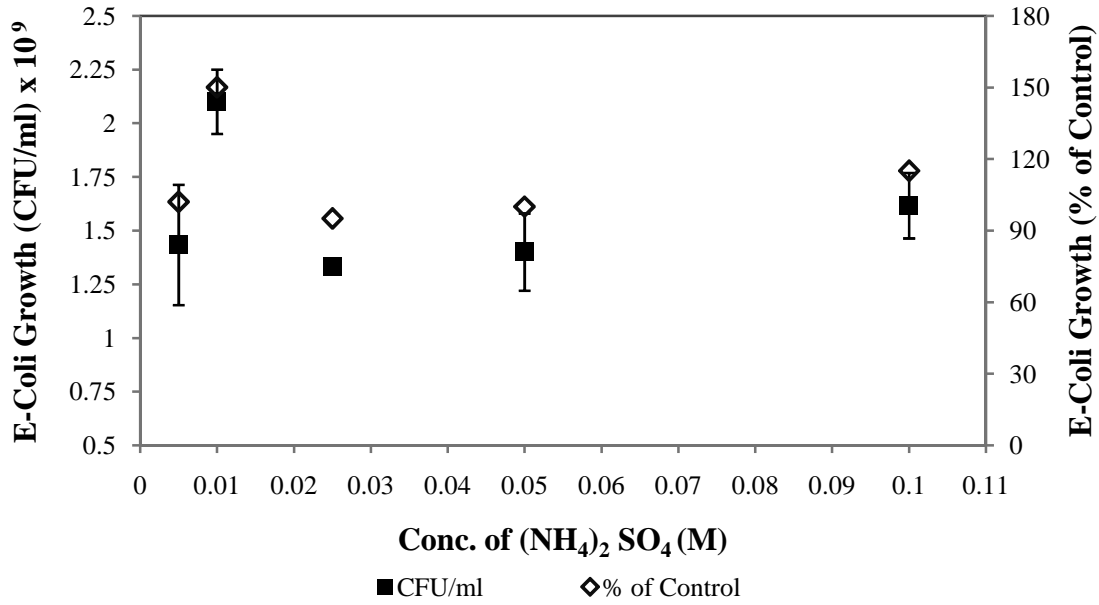


Figure 4-12: Effect of $(\text{NH}_4)_2 \text{SO}_4$ on *E. coli* growth

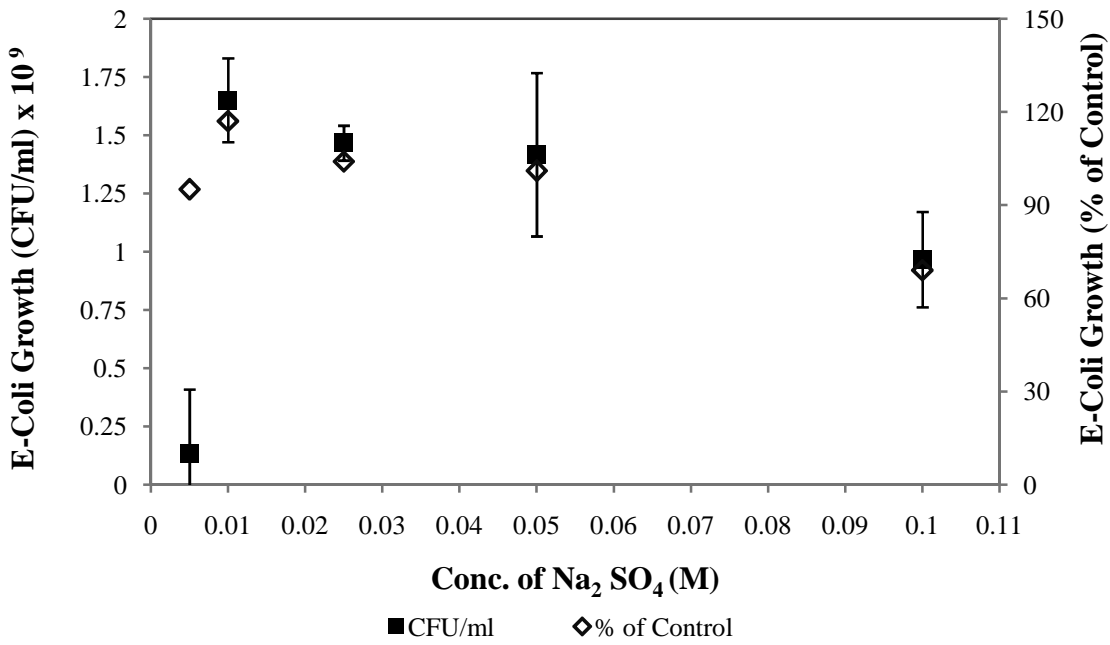


Figure 4-13: Effect of $\text{Na}_2 \text{SO}_4$ on *E. coli* growth

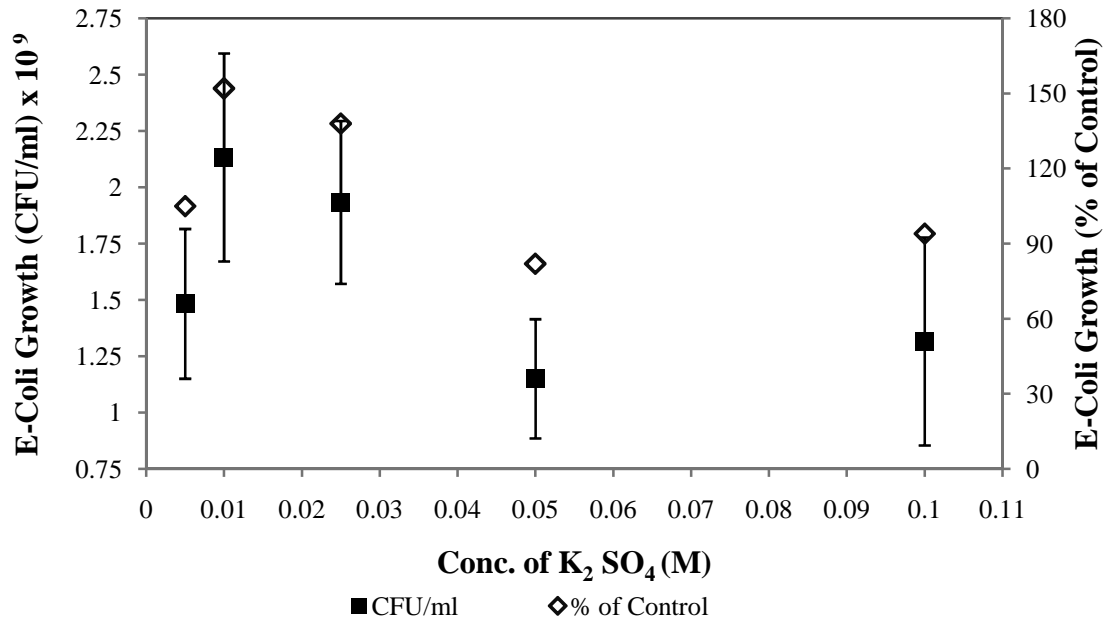


Figure 4-14: Effect of K₂ SO₄ on *E.coli* growth

Figure 4-10 illustrates a different trend of *E.coli* inhibition with increasing magnesium chloride concentration. There was a threefold reduction in percent growth of *E.coli* from 182 to 65 % while changing MgCl₂ concentration from 0.005 to 0.1 M. This may be attributed to the high osmotic pressure generated across the semi permeable cell membrane of *E.coli* with increasing magnesium concentration in the surrounding solution, which caused a net movement of water from inside to outside of the cell and consequently resulted in cell dehydration and growth inhibition. From the results of **Figures 4-7** to **4-10** it may be observed that it is the metal cation and not the chloride anion which affects *E.coli* growth in the system, since chloride is common anion in all four draw solutes used. It may also be seen that bivalent alkaline metals were more supportive for *E.coli* growth as compared to monovalent alkali metals, however, very high concentration of bivalent metals may inhibit growth.

Figure 4-11 explains that ammonium bicarbonate was extremely toxic for *E.coli* growth. The percent growth never exceeded 80 % at any concentration with the lowest value of 30 % at 0.005 M concentration. Ammonium sulfate was found to be very good for *E.coli* growth at all concentrations as shown in **Figure 4-12**. The trend was almost consistent and percent growth was found always above 100 % of the control. Comparing results of **Figure 4-11** and **4-12** it may be observed that it was bicarbonate but not the ammonium ion, which was toxic for *E.coli* growth; since ammonium ion was common in both compounds. Ammonium bicarbonate is an unstable salt and temperature of about 36 °C can convert it into carbon dioxide, water and ammonia. The role of CO₂ for microbial growth is highly dependent upon the conditions in the bioreactor. Under aerobic conditions it is growth supportive and in anaerobic conditions it is inhibitory.

Effect of different CO₂ concentrations on the growth of *E.coli* was studied and it was discovered that 0.0013 M was the optimum concentration, but there was not a linear relationship between CO₂ concentration and *E.coli* growth (Lacoursiere et al., 1986). Similar non linear relationship between CO₂ and *E.coli* growth were found in this study, where under experimental conditions (anoxic) the bicarbonate restricted the *E.coli* growth to maximum 80 % of the control. In FO-MBR where the MLSS concentration is high (6-10 g/L), some anoxic zones within the system can form, where bicarbonate can show its deteriorating effect. So ammonium bicarbonate can only be used with high aeration intensity in the FO-MBR.

Figure 4-13 also supports the positive role of sulfate in *E.coli* growth where the percent growth remained above 100% for most of the concentrations and showed slight decline at 0.1 M concentration of sodium sulfate where it remained 70 %. The trend depicted by potassium sulfate

in **Figure 4-14** was similar to the trend shown by sodium sulfate. Again the sulfate showed growth promoting behavior for *E.coli* and maintained it above 90 % of the control for all the concentrations. Actually numbers of enzymes are present for the metabolism of sulfate inside *E.coli*. These enzymes produce adenosylmethionine in various cell processes which ultimately changes to adenosine diphosphate (ADP) and finally to adenosine triphosphate (ATP), which acts as the main energy source (Sekowska et al., 2000). This energy causes the growth and sustenance of *E.coli* cells. The results from this study are in accordance with the above findings where draw solutes containing sulfates demonstrated a positive effect for *E.coli* growth. Hence any draw solute containing sulfate may be used in FO-MBR.

The above discussed results are summarized in the **Table 4-4** which evaluated the suitability of eight inorganic draw solutes for the use in FO-MBR by adding the cumulative effect of three important factors. The first factor was osmotic pressure, because it directly gave an idea about the water flux that can be achieved using that particular draw solution. Second factor was the specific reverse transport (J_s/J_w), which demonstrated that how much draw solute back diffused when 1 L of water was extracted. The third and most important factor was the effect of reverse transported draw solute on *E.coli* growth.

It is reported that surfactants can deteriorate the biological treatment process at high concentrations (Shcherbakova et al., 1999). It was found that surfactants can affect the respiration rate and enzyme activity of degrading bacteria. Also, it was observed that the volatile suspended solids concentration in the activated sludge decreased, with increasing the exposure time to the surfactants (Proksova et al., 1999). Surfactants can also affect the morphological

characteristics of flocs and minimize settling characteristics of sludge and its separation from treated water (Ewa and Marcin, 2006; Ewa and Marcin, 2007).

Figures 4-15 to 4-18 demonstrated that surfactants were generally toxic to *E.coli*, except SDS which depicted some growth at 0.005 M concentration. Most of the surfactants showed almost 0 % growths at all the concentrations but their concentrations under experimental conditions were below their CMCs which support their existence as monomer. Hence, the use of surfactants in FO-MBR is only recommended with their concentration above CMC, to avoid their reverse transport. The suitability of surfactants for use in FO-MBR is presented in **Table 4-5**.

Table 4-4: Evaluation of inorganic draw solutes for FO-MBR keeping in view osmotic pressure, specific reverse salt transport and percent growth

Ionic Draw Solute	Mol. Wt (g/mol)	Osmotic Pressure at 1M conc. (bar)	(Js/Jw) (g/L)	% Growth of Control at min Conc.	% Growth of Control at max Conc.	Growth Trend	Use in FO-MBR
NaCl	55.5	48	0.75	61	93	Increasing	Recommended
KCl	74.5	41	1.14	55	95	Increasing	Recommended
CaCl₂	110	63	0.82	73	115	Increasing then decreasing	Recommended
MgCl₂	94	56	0.58	182	65	Decreasing	Recommended
NH₄HCO₃	79	36	2.01	32	51	Increasing then decreasing	Not Recommended
(NH₄)₂SO₄	132	66	0.36	102	115	Fluctuating	Highly Recommended
Na₂SO₄	142	64	0.33	95	69	Increasing then decreasing	Recommended
K₂SO₄	174	56	0.40	105	94	Fluctuating	Recommended

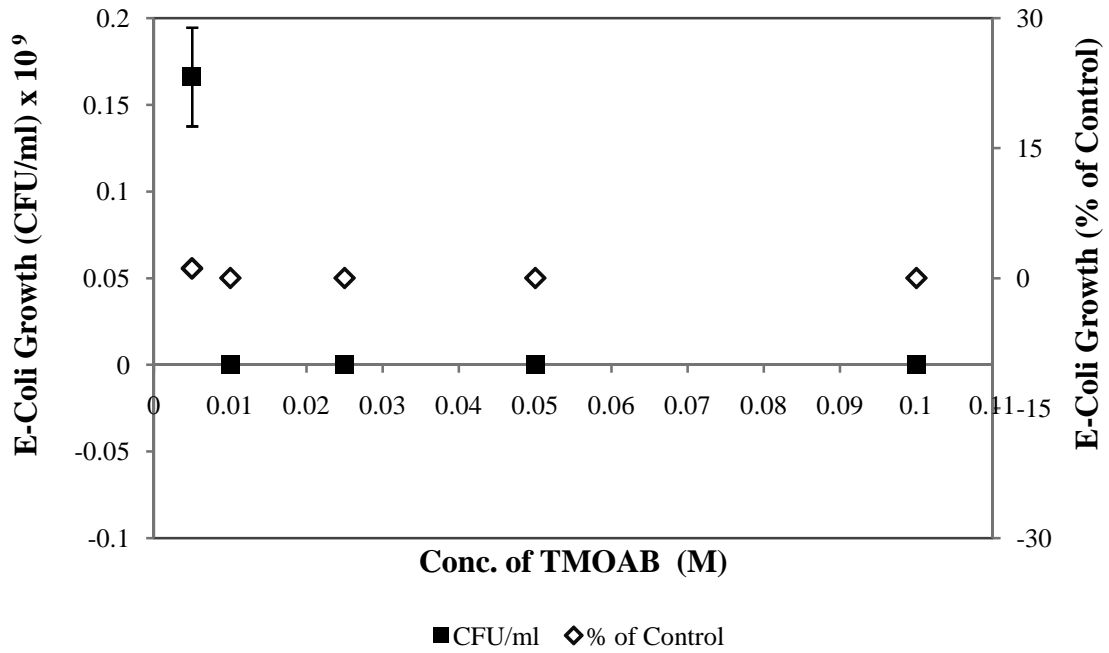


Figure 4-15: Effect of TMOAB on *E.coli* growth

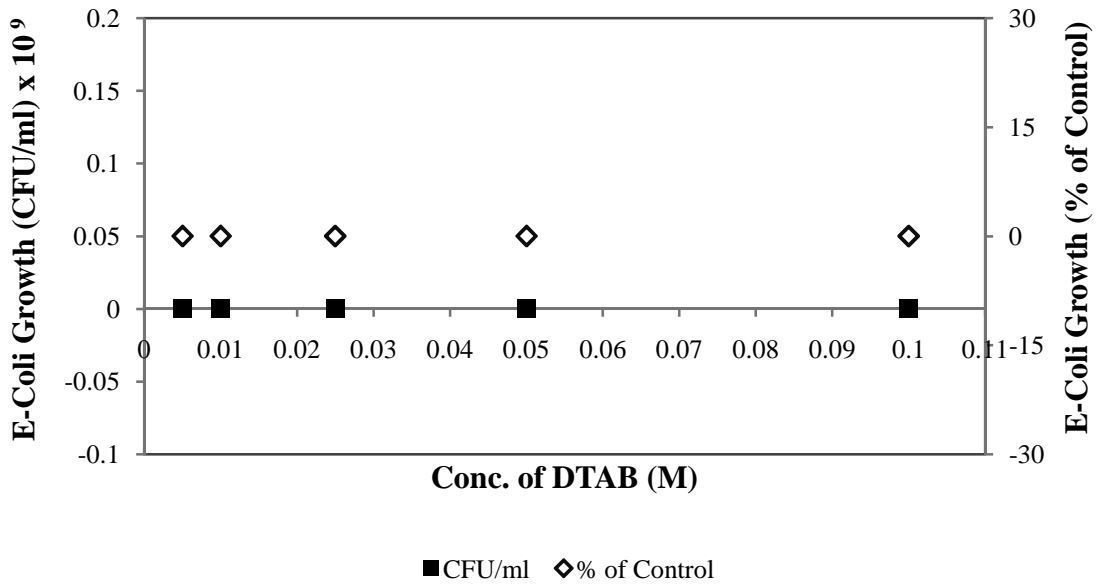


Figure 4-16: Effect of DTAB on *E.coli* growth

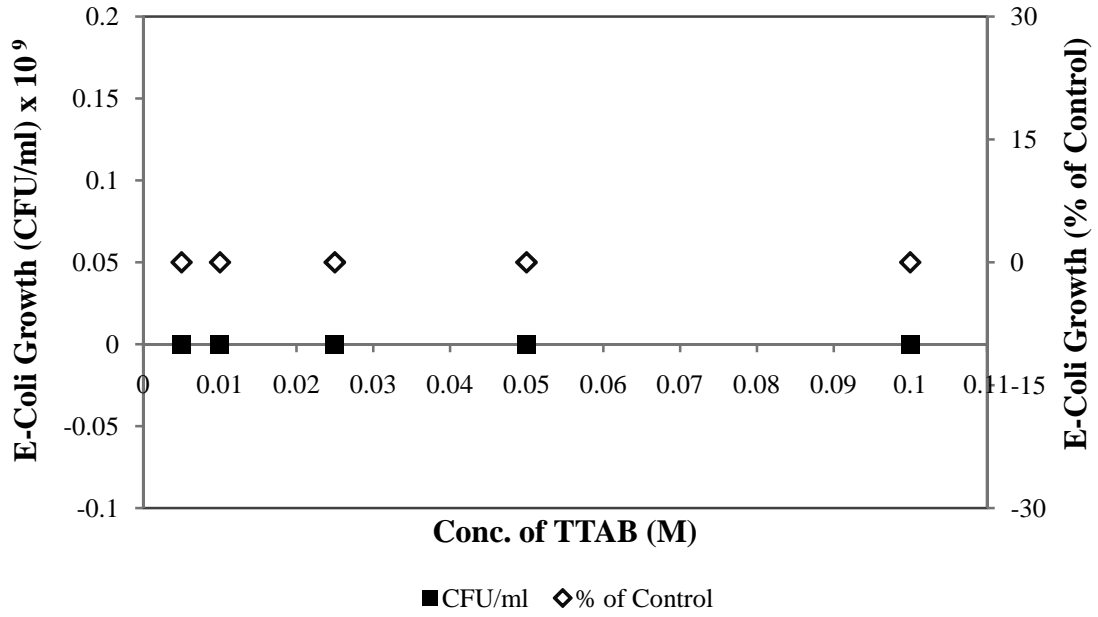


Figure 4-17: Effect of MTAB on *E. coli* growth

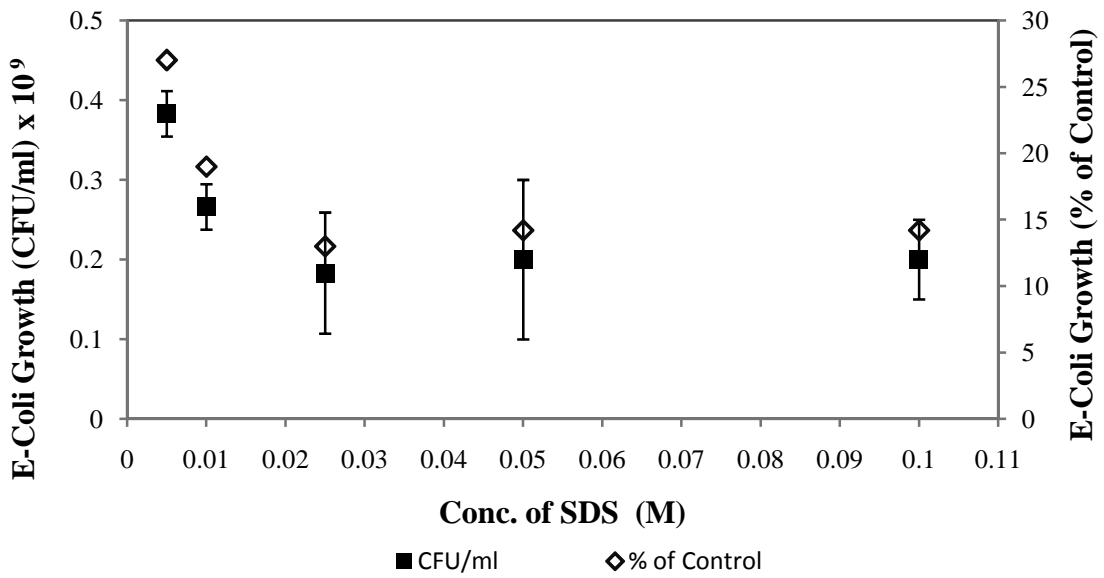


Figure 4-18: Effect of SDS on *E. coli* growth

Table 4-5: Evaluation of surfactants as draw solutes for FO-MBR keeping in view osmotic pressure, specific reverse salt transport and percent growth

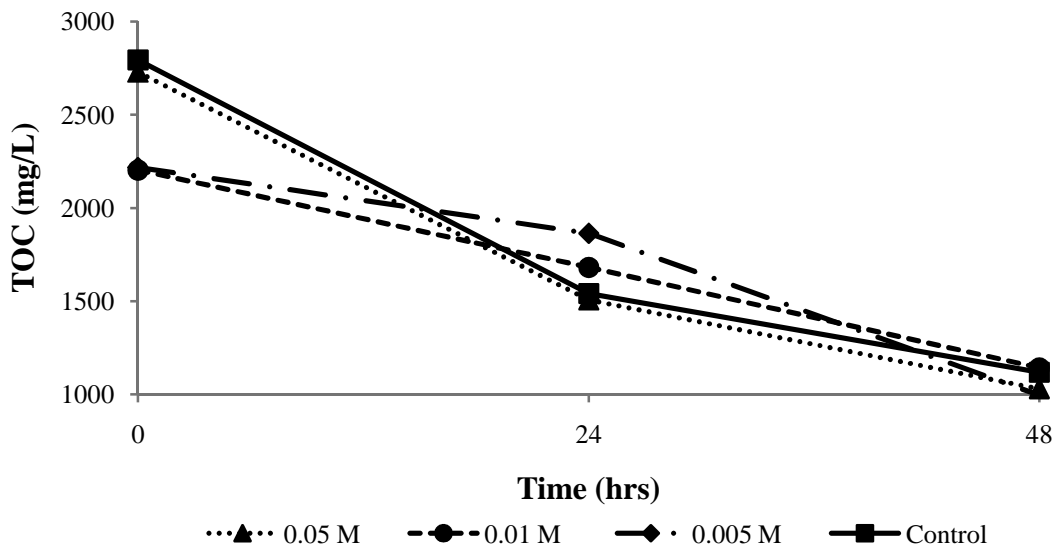
Surfactant	J_s/J_w (g/l)	Osmotic Pressure at 1M conc. (bar)	CMC (mol/L)	% Growth at min Conc.	% Growth at max Conc.	Morphology under Experimental Concentration	Use in FO-MBR
TMOAB	0.06	27.2	0.140	1.1	0	Monomeric	Recommended
DTAB	0.043	1.2	0.015	0	0	Monomeric/Micelles	Not Recommended
MTAB	0.040	1.5	0.0045	0	0	Monomeric/Micelles	Not Recommended
SDS	0.003	0.35	0.008	27	14	Monomeric/Micelles	Recommended

Comparing **Tables 4-4** and **4-5** it is clear that surfactants exhibit 100-150 times less specific reverse transport as compared to sodium chloride. This study recommends surfactants by giving equal weightage to the flux they generate, specific reverse transport and on the biodegradation by the *E.coli*. **Figure 4-18** represents that, as some portion of surfactants changed into the micelles form (in SDS), the growth of *E.coli* was observed. These facts support the potential use of surfactants as a draw solution. Since both DTAB and MTAB have very little osmotic pressure and also they did not supported the *E.coli* growth; they were not recommended and were not included in detailed toxicity studies in the following section. However, the SDS and TEAB were selected for detailed toxicity studies.

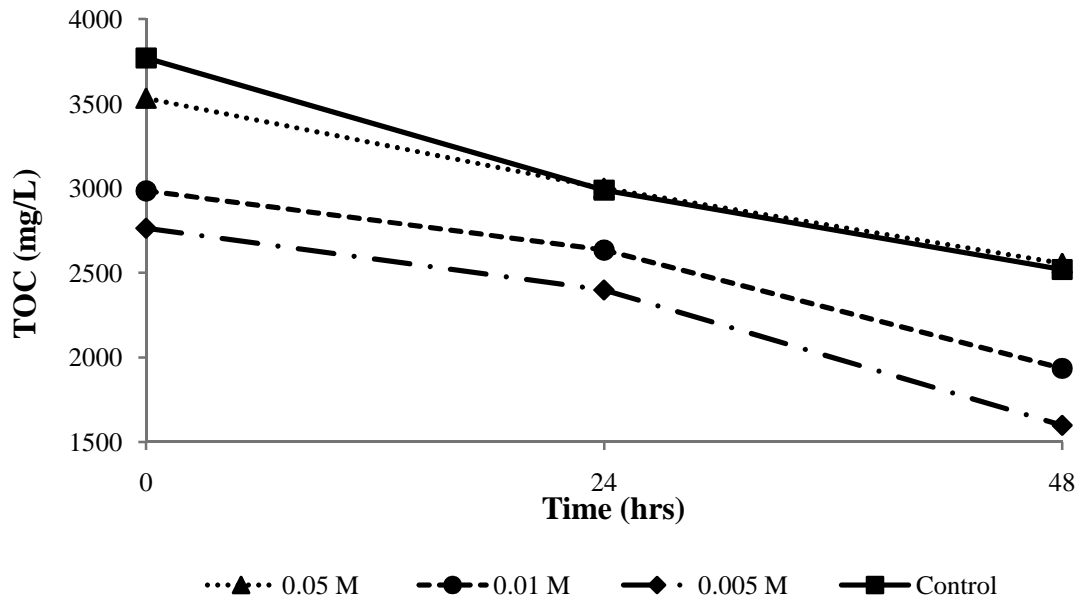
4.1.1. Toxicity of Micellar Solutions to *Pseudomonas aeruginosa* and mixed activated sludge

Figure 4-19 a shows the TOC biodegradation by *Pseudomonas aeruginosa* in presence of different concentrations of TEAB. Nutrient agar and TEAB were the only two substrates available in the system for *Pseudomonas* to consume. The difference in TOC values at 0 hr may be attributed to the presence of different amount of TEAB in the system. Like the control, TOC declined under all three concentrations which showed that TEAB did not resist *Pseudomonas* to consume the available food in the system. Moreover, the rapid decline of TOC in presence of higher concentration of TEAB (0.05 M) depicts that TEAB was not only non toxic to *Pseudomonas*, but it also catalyzed the TOC reduction. This may also be confirmed by looking at the **Figure 4-20 a**, which shows *Pseudomonas* percent growth in presence of TEAB, normalized with the growth over control (DI water).

It is interesting that the *Pseudomonas* grew faster in presence of higher concentration (0.05 M) compared to the lower concentrations in the first 24 hrs. However, ascending growth curves over the smaller concentrations and a flattened growth curve over higher concentration (0.05 M) were observed between 24th to 48th hr. It confirms that TEAB was readily biodegradable with *Pseudomonas* and that is why initially the specific growth rate and substrate utilization rate were quicker in presence of the high available concentration of TEAB, and then with the declining substrate concentration the growth rate also declined. At the end of 48 hrs the final TOC was around 1000 mg/L for all three TEAB concentrations, however, there was a significant difference in total number of bacterial colonies in the system. TEAB is a quaternary ammonium compounds. Results of this study are supported by results in the other studies; where other quaternary ammonium compounds were decomposed by *Pseudomonas* isolated from sewage and activated sludge (Dean-Raymond and Alexander, 1977; Takenaka et al., 2007).

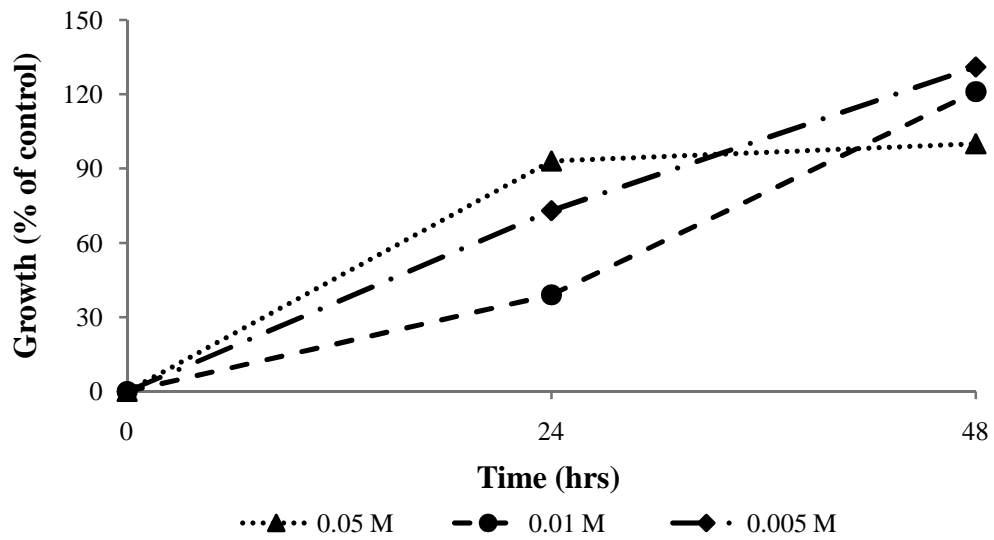


(a)



(b)

Figure 4-19: TOC reduction by (a) *Pseudomonas* and (b) mixed sludge in presence of TEAB



(a)

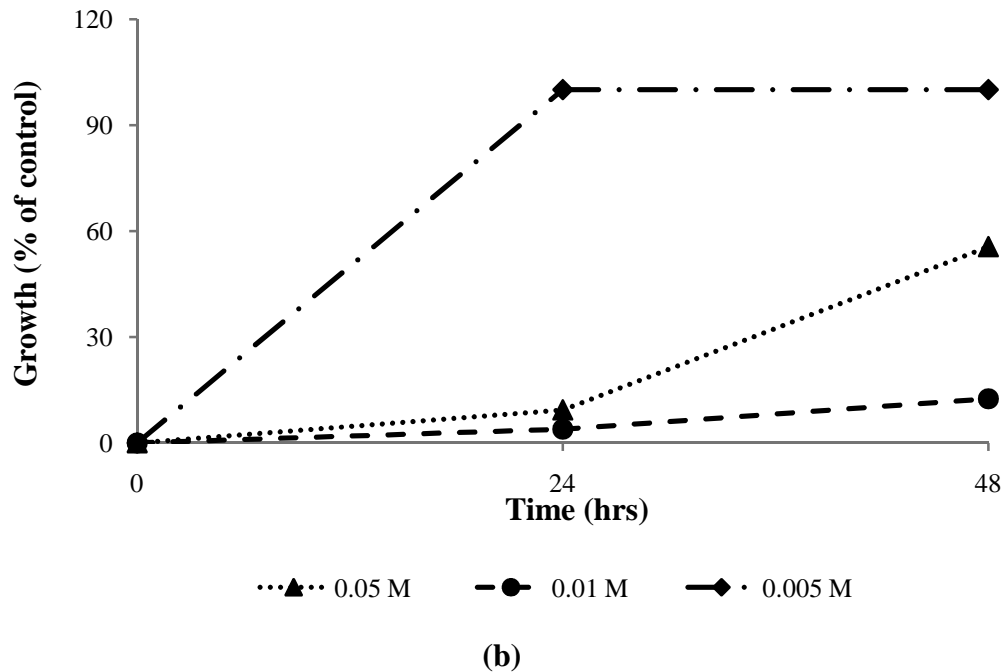


Figure 4-20: Growth of (a) *Pseudomonas* and (b) mixed sludge in presence of TEAB

Comparing **Figures 4-19 a** and **b** it may be noticed that TOC degradation proceeded more smoothly with the mixed sludge compared to the single *Pseudomonas* specie but the trend was reversed, to *Pseudomonas*, as the lowest concentration (0.005 M) showed highest degradation. The TOC removal was equal or more than the control under all three concentrations but the overall removal with mixed sludge was remarkably less than *Pseudomonas* removal. It happened because the mixed sludge also contains those species which cannot biodegrade TEAB. Supporting the TOC degradation results, the mixed sludge growth was maximum (100 %) at the lowest concentration as shown in **Figure 4-20 b**. Simultaneously looking at **Figures 4-19 b** and **4-20 b**, it may be concluded that the growth depends mainly on the TOC removal by the mixed sludge.

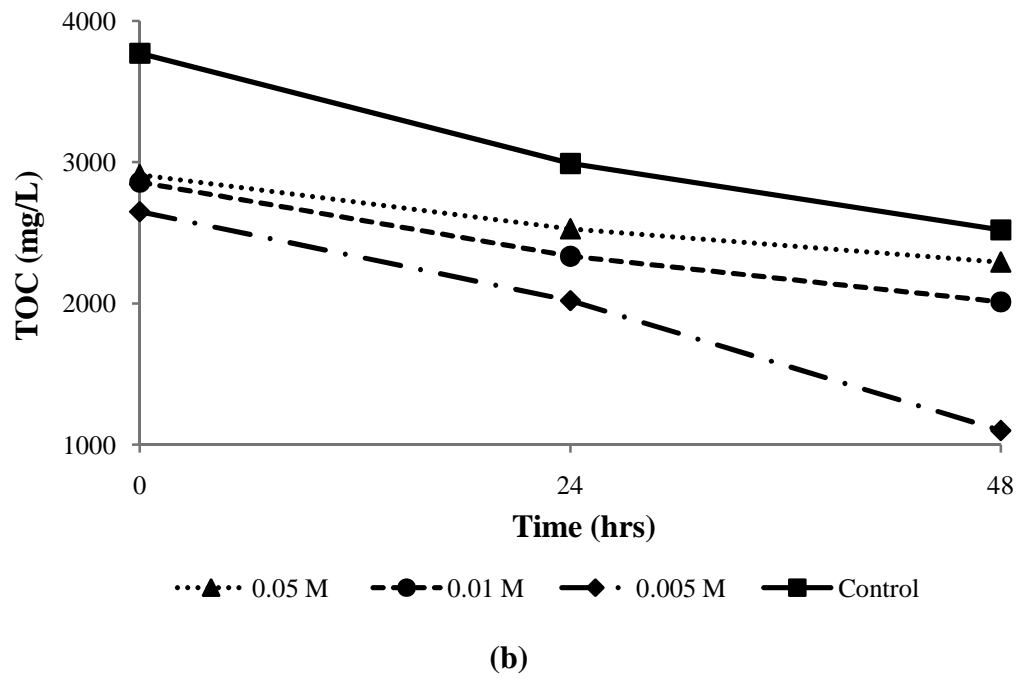
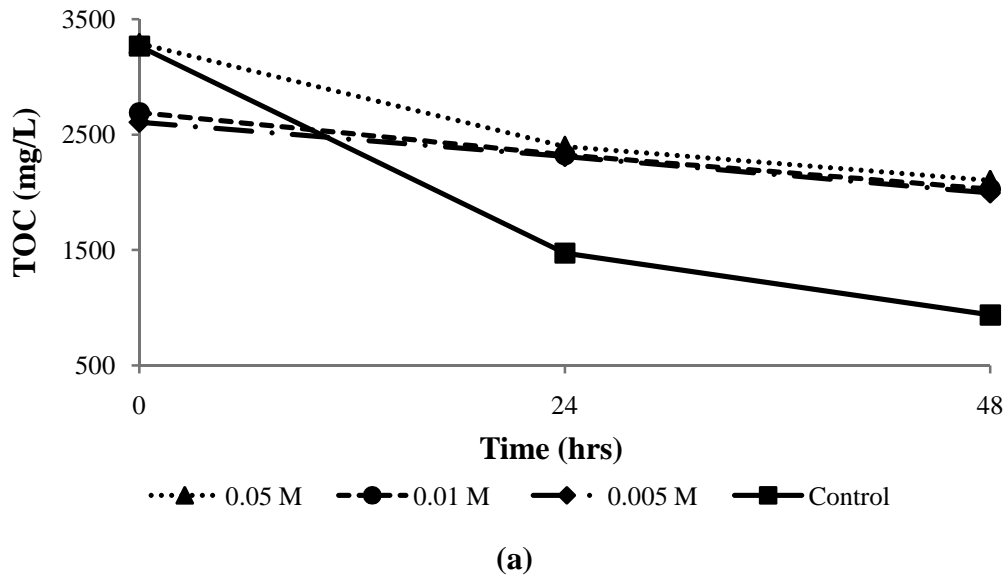


Figure 4-21: TOC reduction by (a) *Pseudomonas* and (b) mixed sludge in presence of TMOAB

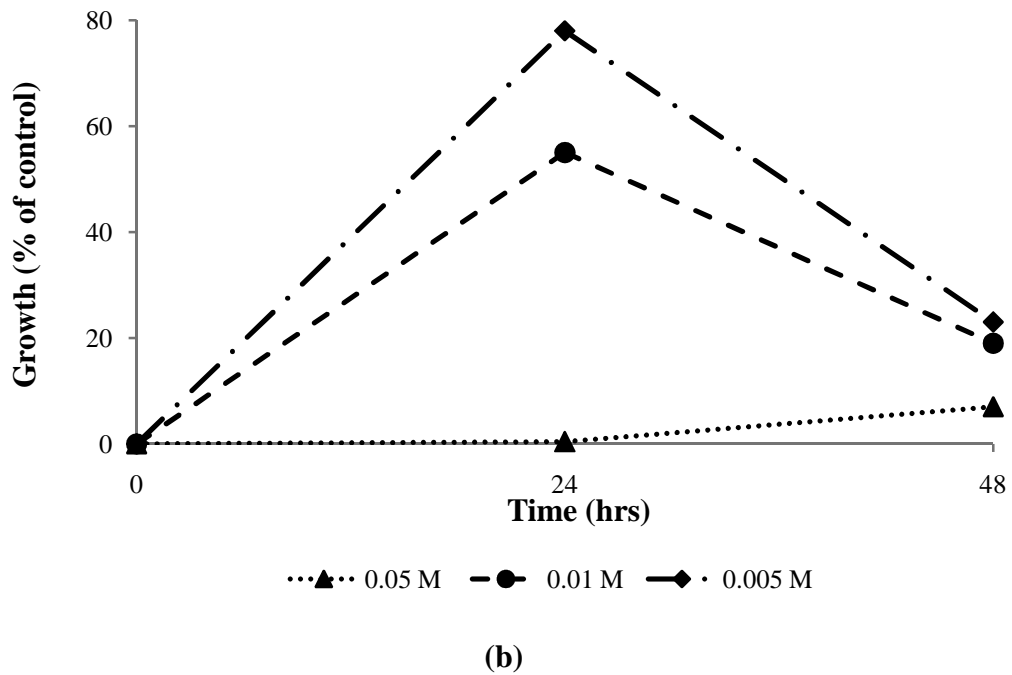
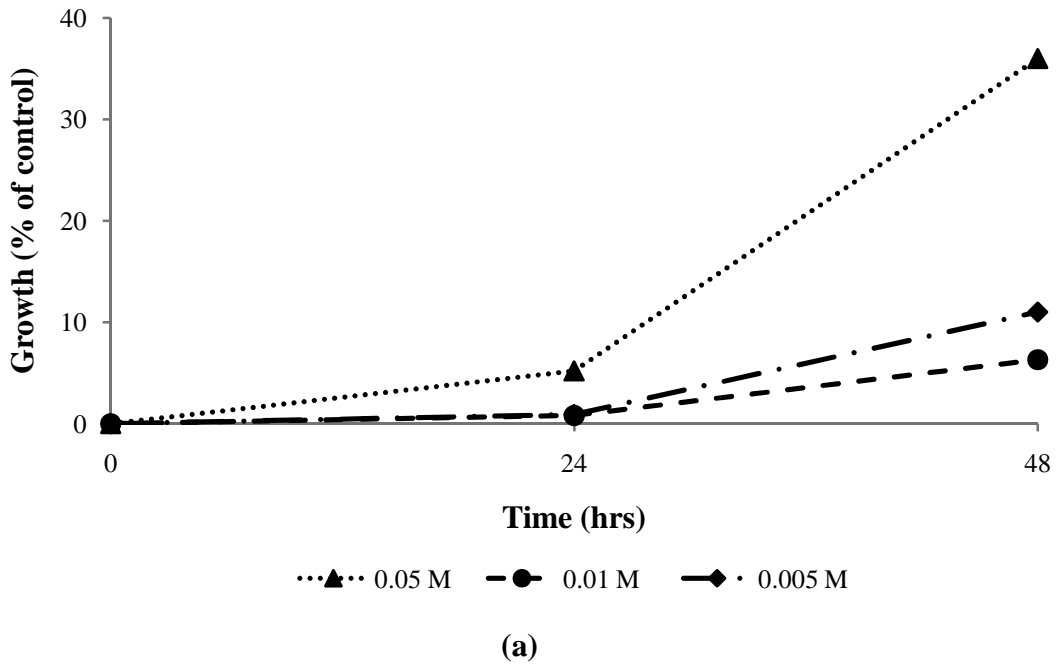


Figure 4-22: Growth of (a) *Pseudomonas* and (b) mixed sludge in presence of TMOAB

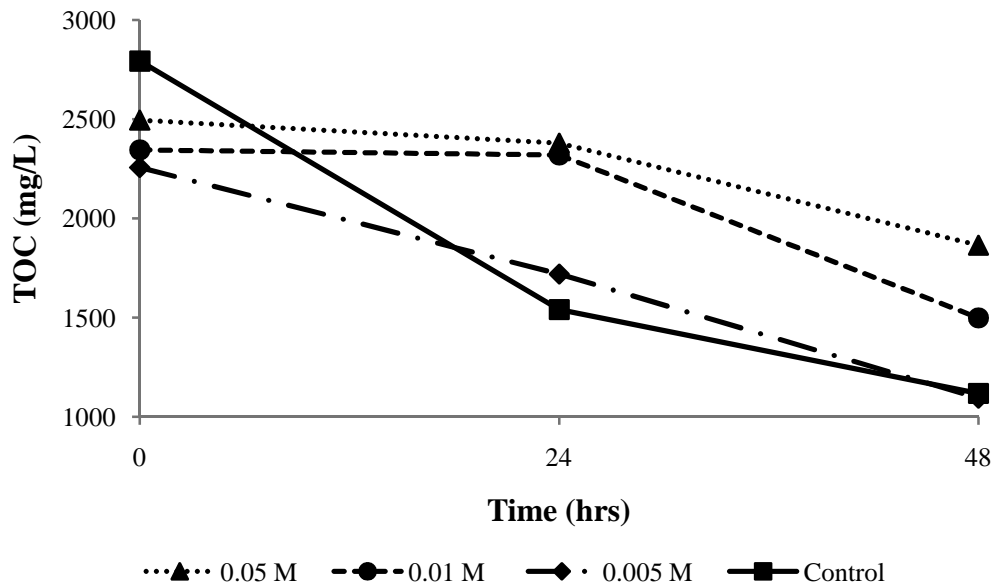
Figure 4-21 a described the toxic nature of TMOAB for the *Pseudomonas* as the decline in TOC was very low in 48 hrs, compared to the control, at all three concentrations. The inhibitory nature

of TMOAB may also be confirmed from the **Figure 4-22 a**, where the *Pseudomonas* growth in presence of TMOAB was significantly lower than the control. With highest TOC removal (1100 mg/L) the 0.05 M concentration depicted highest growth (38 %) of *Pseudomonas*. After 24 hrs the *Pseudomonas* showed some growth at smaller concentrations as well, which shows that with continuous FO-MBR operation the *Pseudomonas* may get acclimatized with TMOAB.

Figures 4-21 b and **4-22 b** demonstrate slightly better degradation of TMOAB with mixed sludge compared to the *Pseudomonas*. But the toxic nature of TMOAB is evident from the percent growth which never exceeded 80 % to the control even for the lowest concentration of 0.005 M. Again there is a direct relationship between TOC removal and growth of sludge. Better removal of TMOAB with mixed sludge compared to the *Pseudomonas* may be attributed to the presence of different microbial species in the mixed sludge.

Figure 4-23 a depicted the slightly toxic nature of SDS to the TOC degradation by *Pseudomonas* at higher concentrations. **Figure 4-24 a** shows that after being imposed by the initial inhibitory effects of SDS at 0.05 and 0.01 M concentrations, the *Pseudomonas* was acclimatized and it depicted good growth between 24th to 48th hr. However, the degradation proceeded smoothly in presence of 0.005 M SDS concentration. **Figures 4-23 b** and **4-24 b** demonstrate slightly smoother but over all lesser substrate degradation by mixed sludge compared to the *Pseudomonas*. The TOC degradation trend by mixed sludge was however similar to the *Pseudomonas* trend as in presence of smaller SDS concentration the degradation was rapid. The toxic nature of SDS for mixed sludge can be observed from the percent growth which never exceeded even 10 % of the control, however, for *Pseudomonas* the growth curves touched 100 %

mark. Hence, for dealing with SDS as draw solution either *Pseudomonas* mono culture FO-MBR may be used or conditions may be maintained in the FO-MBR to promote *Pseudomonas* growth. SDS is a widely used surfactant at household and industrial applications so its successful biodegradation is reported through different microbial species like *Pseudomonas* and *Bacillus cereus* (Abboud et al., 2007; Singh et al., 1998).



(a)

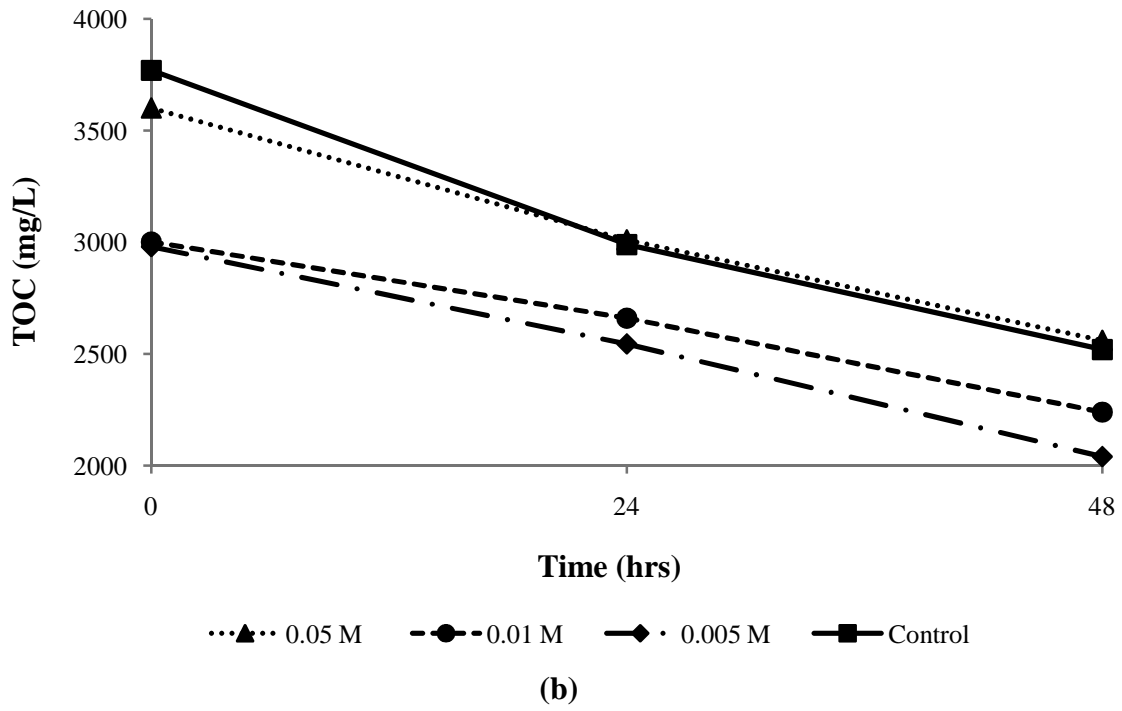
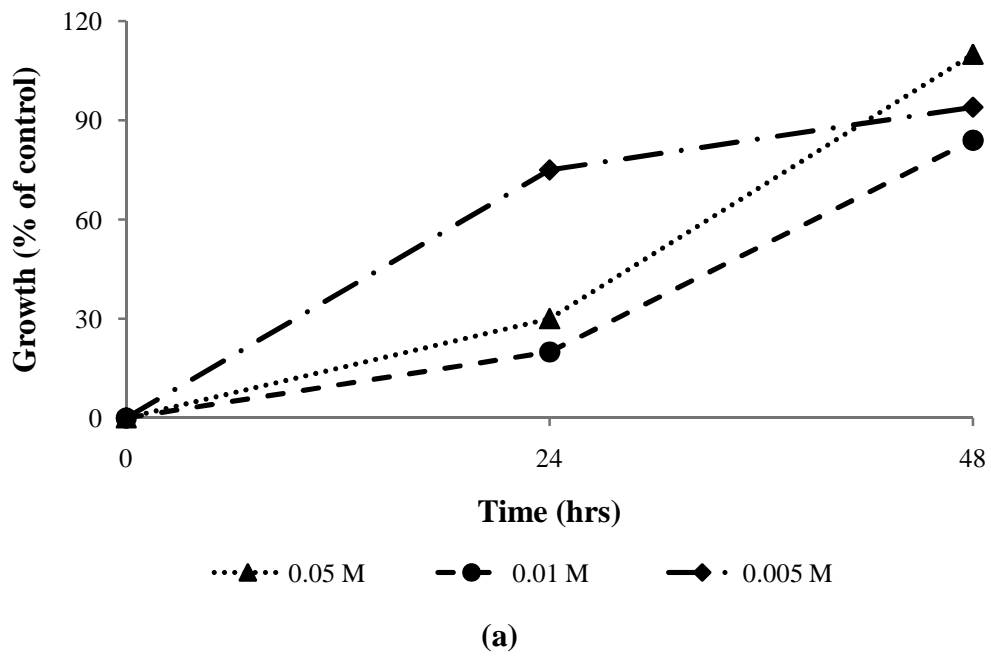
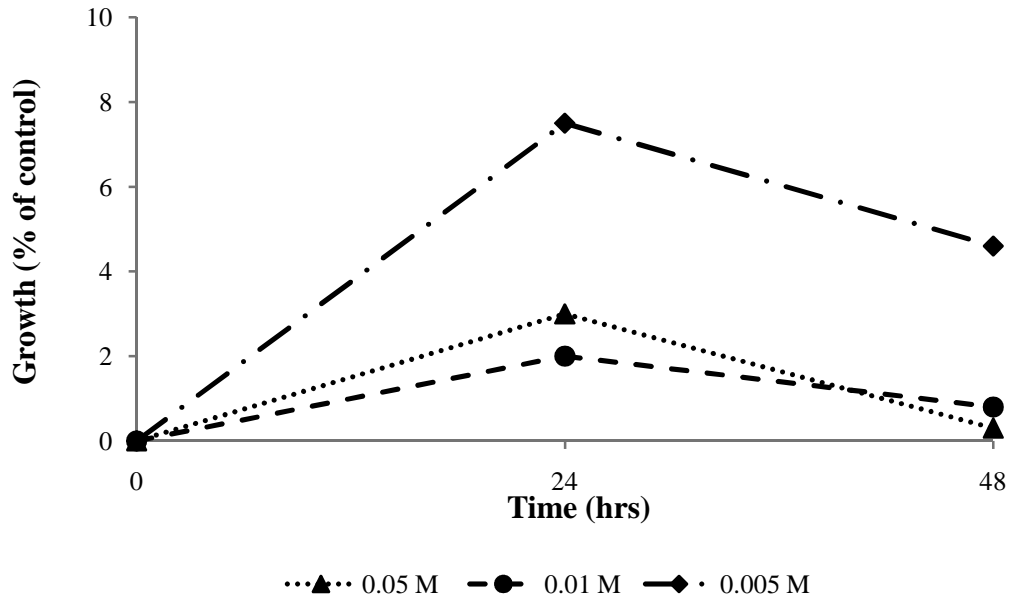


Figure 4-23: TOC reduction by (a) *Pseudomonas* and (b) mixed sludge in presence of SDS

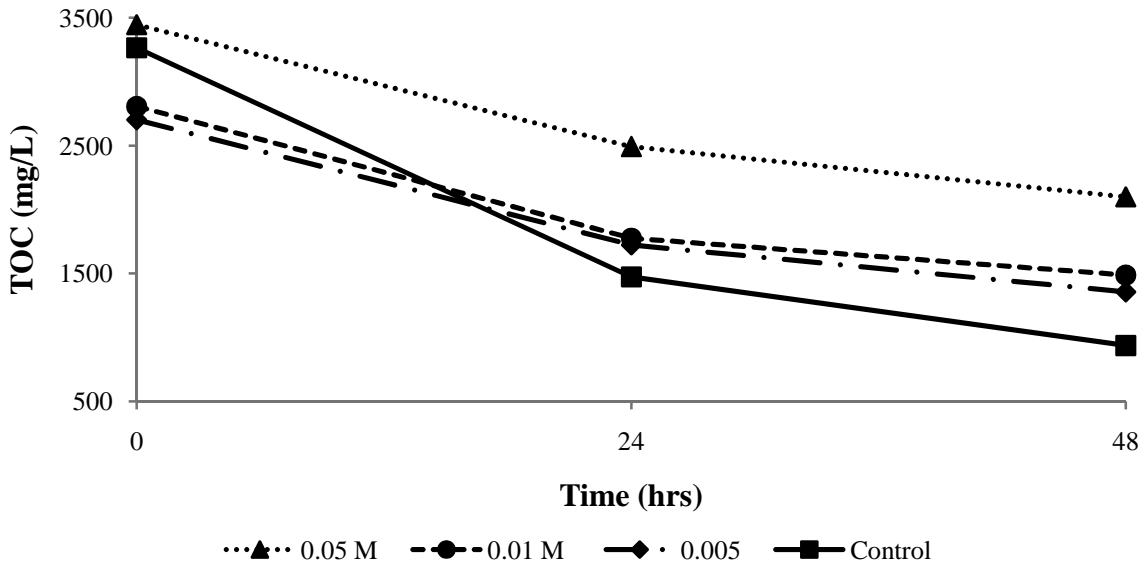




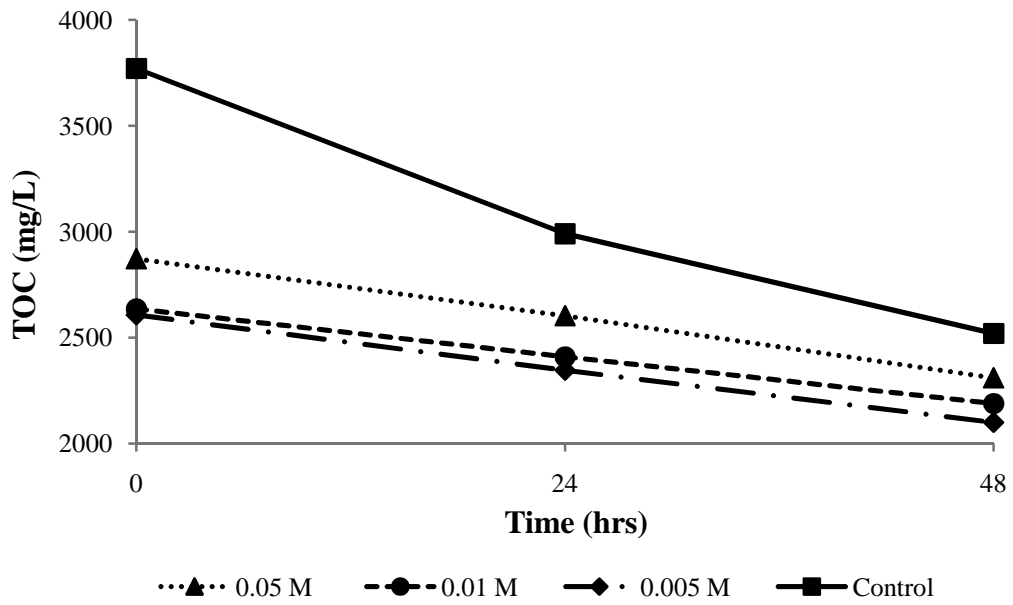
(b)

Figure 4-24: Growth of (a) *Pseudomonas* and (b) mixed sludge in presence of SDS

Figures 4-25 a and **4-26 a** depict the toxic nature of 1-OSA for *pseudomonas* as the TOC degradation was always less than the control, in presence of all three concentrations, and the growth was below 10 % for two higher concentrations (0.05 and 0.01 M). However, the mixed sludge was able to degrade TOC and grow in presence of 1-OSA as shown in **Figures 4-25 b** and **4-26 b**.

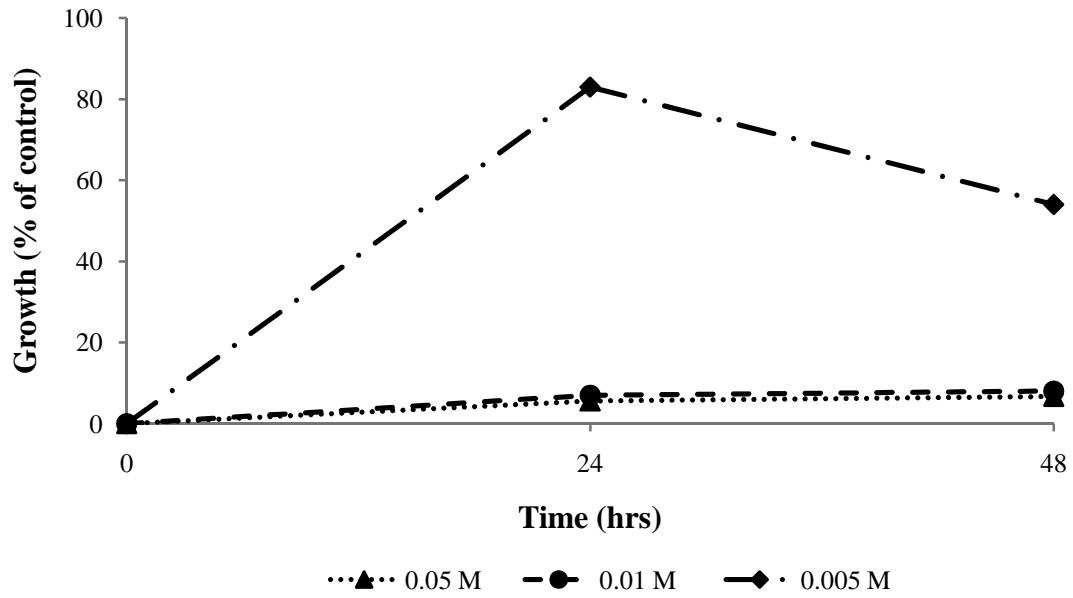


(a)

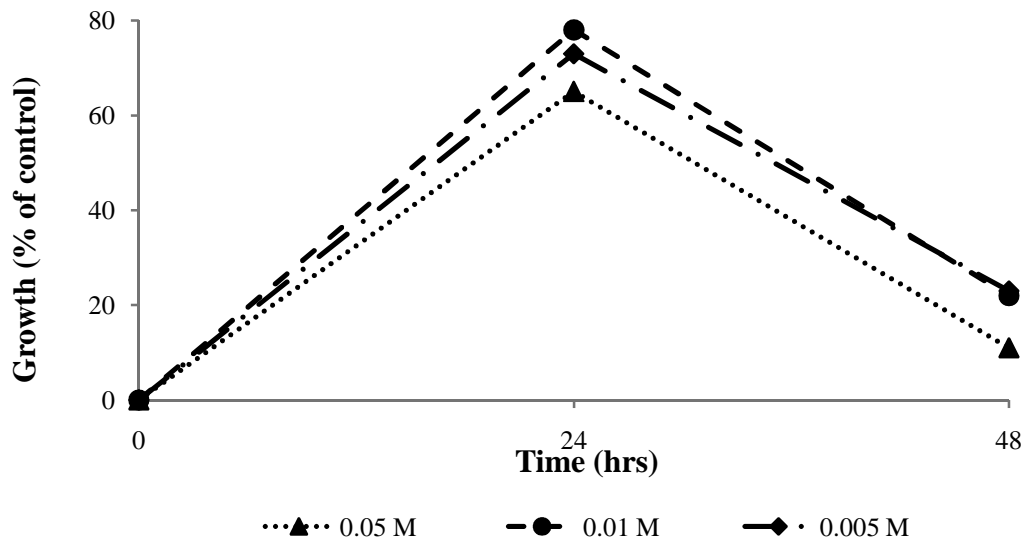


(b)

Figure 4-25: TOC reduction by (a) *Pseudomonas* and (b) mixed sludge in presence of 1-OSA



(a)



(b)

Figure 4-26: Growth of (a) *Pseudomonas* and (b) mixed sludge in presence of 1-OSA

Table 4-6 summarizes the results from the **Figures 4-19** to **4-26** and evaluates which out of the four surfactants may be used in FO-MBR purely on the basis of biodegradability potential/toxicity of the surfactants and not on any other criteria.

Table 4-6: Recommendation of surfactants as draw solutes in FO-MBR based on their toxicity to *Pseudomonas* and mixed sludge

Surfactant	Growth of mixed sludge at min conc. after 48 hours (%)	Growth of mixed sludge at max conc. after 48 hours (%)	Growth of <i>Pseudomonas</i> at min conc. after 48 hours (%)	Growth of <i>Pseudomonas</i> at max conc. after 48 hours (%)	Use in FO-MBR
TEAB	100	55.5	131	100	Highly Recommended
TMOAB	23	7	11	36	Not Recommended
SDS	4.6	0.3	94	110	Recommended for <i>Pseudomonas</i>
1-OSA	23	11	54	6.7	Not Recommended

4.2. PROCESS OPTIMIZATION OF THE FO-MBR

4.2.1. Optimization of Draw Solution Concentration

Figure 4-27 demonstrates the flux profiling with different concentrations of NaCl under similar operational conditions. The detailed methodology for these experiments is already described in section 3.2.1. Since the experiments were performed with DI water as feed solution, and AL-DS configuration, so there cannot be any concentrative ECP and concentrative ICP and major flux decline may only be due to dilutive ECP and dilutive ICP. The increase in flux with draw solution concentration was not directly proportional and it declined with increasing concentration. Such non linear relationship between flux and draw solution concentration in FO, is reported in the literature (Tang et al., 2010).

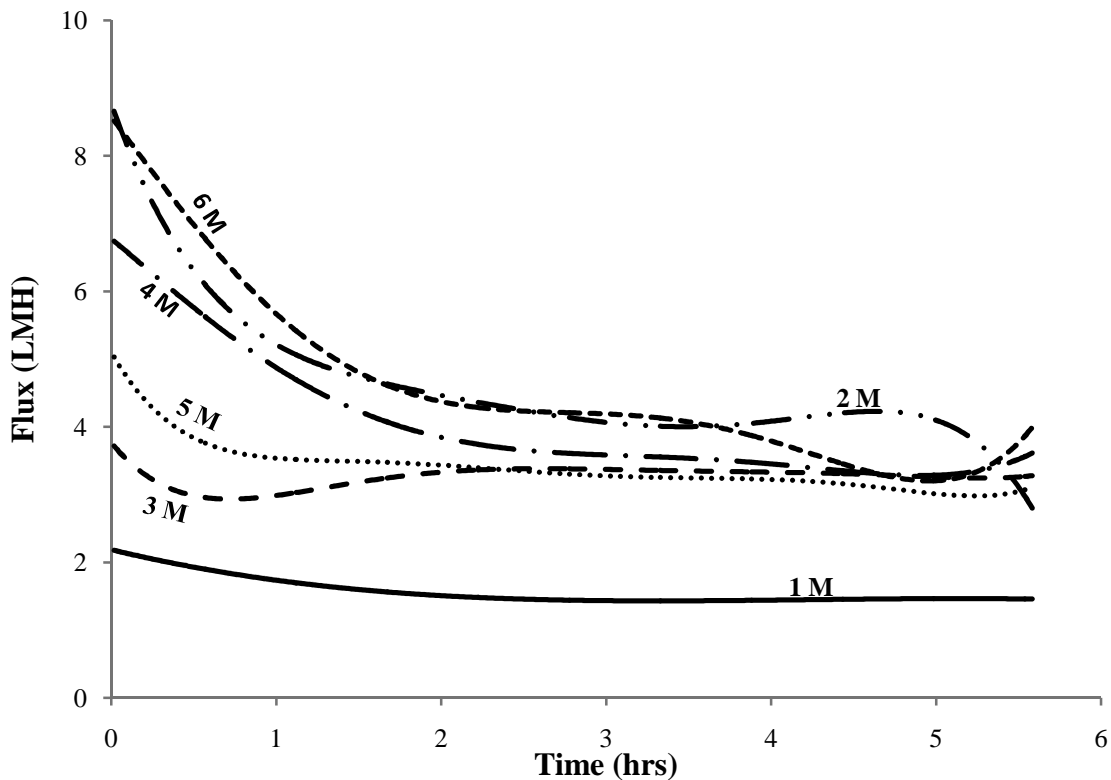


Figure 4-27: Flux with different NaCl concentrations as draw solution using hollow fiber FO membrane

Table 4-7: Optimization of draw solution concentration for hollow fiber FO membrane

Exp. no.	Draw solution volume (L)	Draw solution conc. (M)	Cross-flow velocity (mL/min)	Average flux in 8 hrs (LMH)	Drop in conductivity of DS in 8 hrs (mS/cm)	Drop in conductivity of DS in 8 hrs (%)	Increase in conductivity of Feed Solution in 8 hrs (μ S/cm)	Increase in conductivity of Feed Solution in 8 hrs (%)
1	0.5	1	150	1.57	20	41	498	44
2	0.5	2	150	4.04	77	50	576	2100
3	0.5	3	150	4.59	270	75	1205	1338
4	0.5	4	150	4.63	348	73	967	4835
5	0.5	5	150	3.39	426	71	889	1778
6	0.5	6	150	3.26	Over range	N/A	859	7500

Table 4-7 shows that the average water flux increased with DS concentrations till 2 M, and then it stayed constant up to 4 M followed by a decline from 4 to 6 M. Since the increase in the net flux from 2 to 4 M is not significant, so 2 M concentration may be regarded as the optimum for hollow fiber FO membrane. Actually with increasing osmotic pressure difference the mass transfer of the draw solute molecules also increased and caused a drop in the difference of osmotic pressure between feed and draw solution which ultimately reduced the flux. Although not a direct relationship, but it may be observed that the percent increase in the conductivity of the feed solution is proportional to the draw solution concentration. Since the feed water was DI water which had zero conductivity, any increase was only due to the reverse transport of draw solute. Therefore, it is recommended to use draw solution concentration at maximum of 2 M to avoid reverse transport and net flux decline.

4.2.2. Membrane Chemical Cleaning Optimization

Membrane chemical cleaning was optimized by trial and error method. Various concentrations of cleaning solutions and cleaning intervals were studied for attaining maximum flux recovery. **Table 4-8** summarizes the membrane cleaning protocol for hollow fiber FO membrane, fouled with inorganics, with flux recovery in each step. The flux recovery was tested with 2 M NaCl as draw solution and DI water as feed. A similar acid cleaning protocol with submerged hollow fiber FO module; taking 50 hrs cleaning and attaining 97 % flux recovery is reported (Zhang et al., 2012). In the protocol developed in this study, the cumulative cleaning time is only 5 hrs and flux recovery is 93 % for externally connected hollow fiber module. So, this protocol is much improved than the previous one in terms of robustness and cost. There is, however, a need to achieve 100 % flux recovery by further research in this area.

Table 4-8: Chemical cleaning of inorganics fouled hollow fiber FO membrane

Step no.	Method	Cumulative time (hrs)	Cumulative flux recovery (%)
1	Flushing DI water on both sides of membrane	1	13
2	Flushing 0.75 M (30 g/100 mL) NaOH on both sides of membrane	3	
3	Flushing DI water on both sides of membrane	3.5	70
4	Flushing 0.2 M HNO ₃ on both sides of membrane	4.5	93
5	Flushing DI water on both sides of membrane	5	

Since the study is concerned mainly with micellar solutions efforts were made to establish a chemical cleaning protocol for the FO membranes fouled with micelles. A series of experiments, as shown in **Figures 4-28** to **4-34**, were performed to systematically investigate the cleaning protocol. The methodology of cleaning micellar fouled FO membranes with EDTA has already been discussed in section 3.2.2. EDTA alone was found completely insoluble in water and its partial solubility was possible only within high pH range (9-13). Sodium hydroxide (NaOH) was used to increase the pH of the solution. The amount of EDTA (0.5 mM) was chosen based on literature (Li and Elimelech, 2004) and since this is already a very small concentration, so it was not further optimized. The results of the experiments with discussion and inferences are summarized in **Table 4-9**. For ensuring the reproducibility of results, the experiments were repeated more than once.

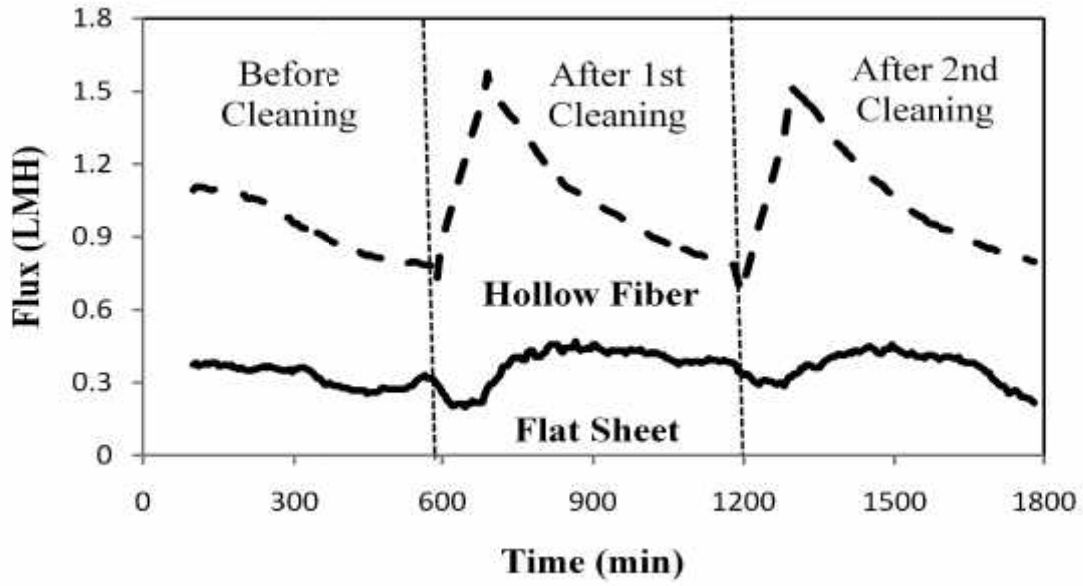


Figure 4-28: Membrane cleaning with 0.0005 M EDTA and 0.5 g/L NaOH for 1 hr

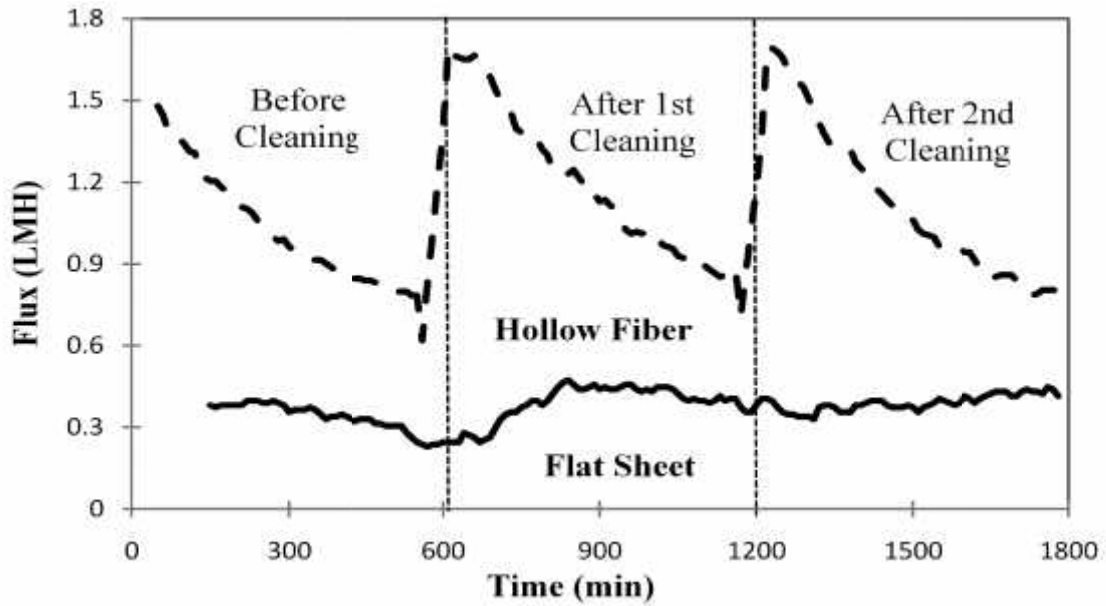


Figure 4-29: Membrane cleaning with 0.0005M EDTA and 0.5g/L NaOH for 30 minutes

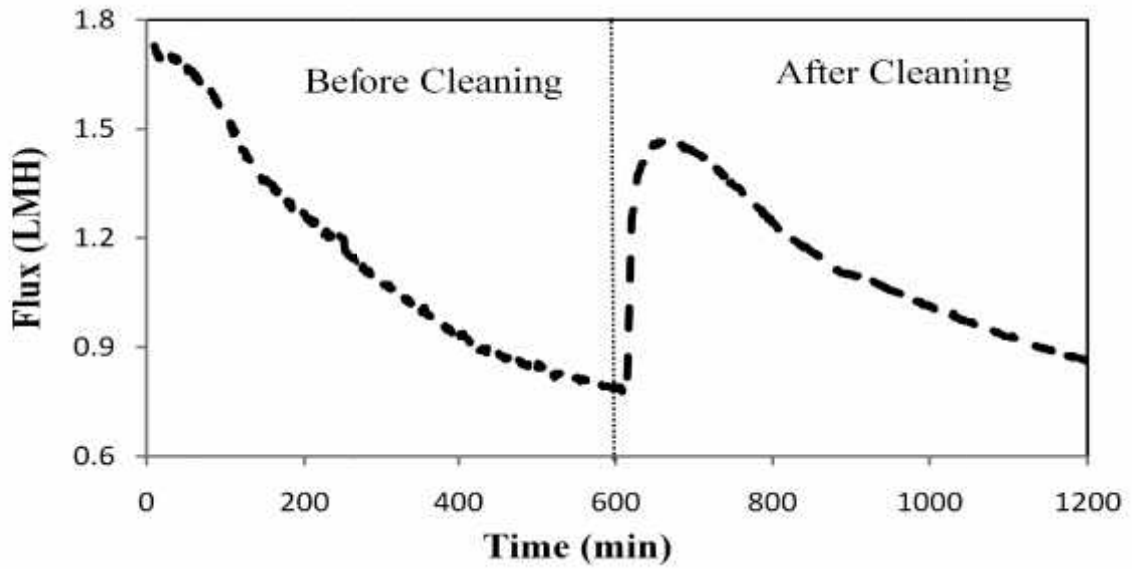


Figure 4-30: Hollow fiber membrane cleaning with 0.5 g/L NaOH for 30 minutes

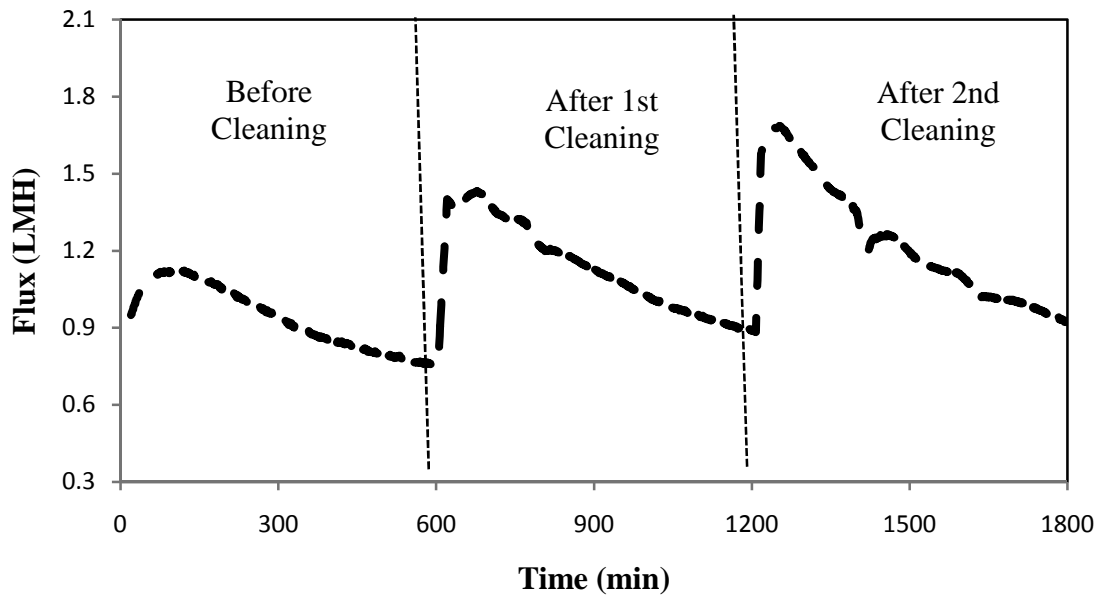


Figure 4-31: Hollow fiber membrane cleaning with 0.0005M EDTA and 0.25 g/L NaOH for 30 minutes

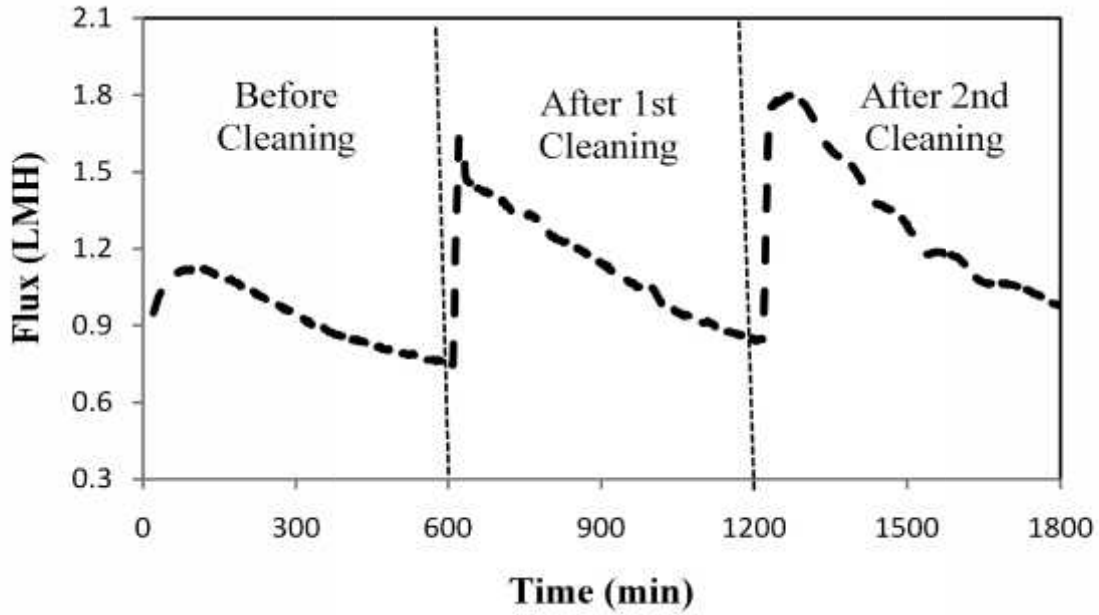


Figure 4-32: Hollow fiber membrane cleaning with 0.0005M EDTA and 0.125 g/L NaOH for 30 minutes

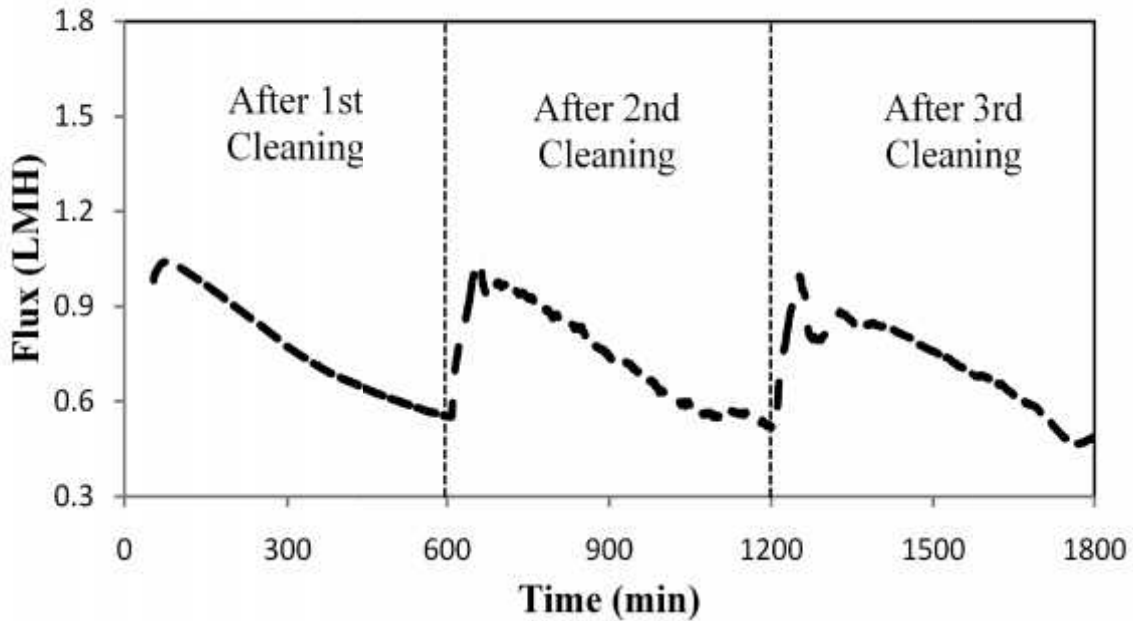


Figure 4-33: Hollow fiber membrane cleaning by reusing the same cleaning solution (0.0005M EDTA and 0.125 g/L NaOH for 30 minutes) for 3 times

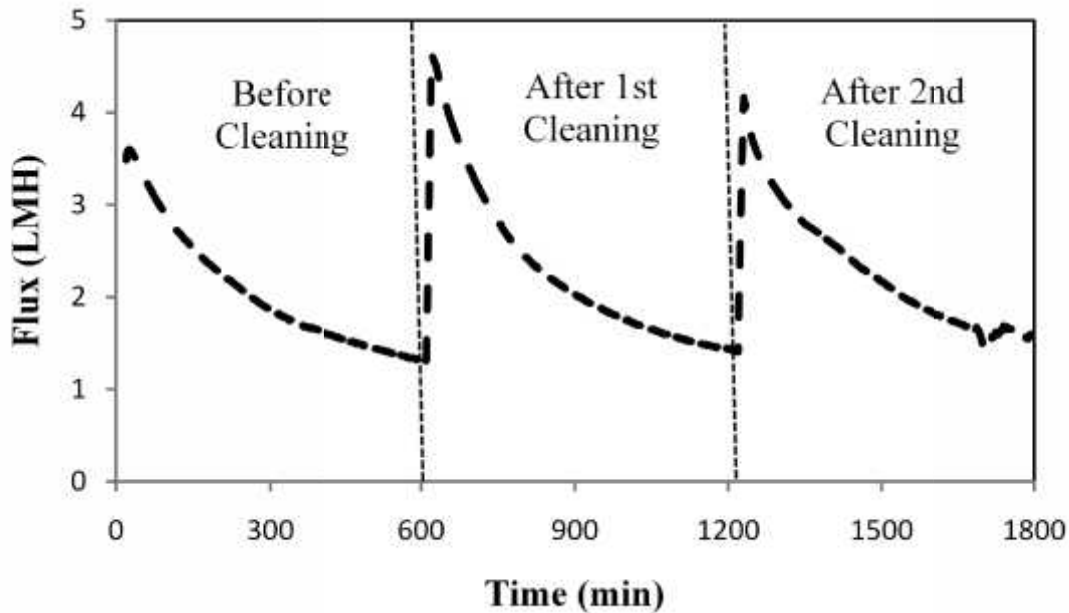


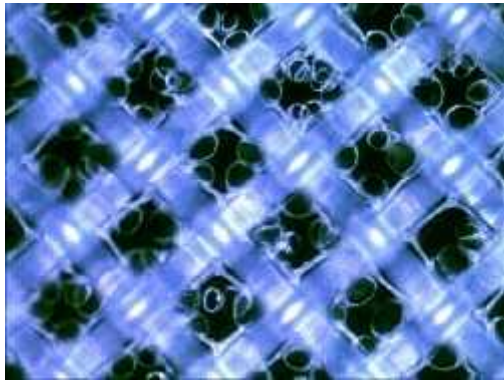
Figure 4-34: Cleaning of TEAB fouled membrane with 0.0005M EDTA and 0.125 g/L NaOH for 30 minutes

The optical microscopic images (top views), of the active layer, of cleaned and fouled flat sheet FO membranes are shown in **Figure 4-35**. The hollow fiber FO membrane was molded in a closed module so it was not technically possible to take images, however, similar experiments were performed on the flat sheet membranes at optimized cleaning conditions, and images were taken. **Figure 4-35a** demonstrates a nascent FO membrane in which the embedded polyester support and unclogged pores may easily be observed.

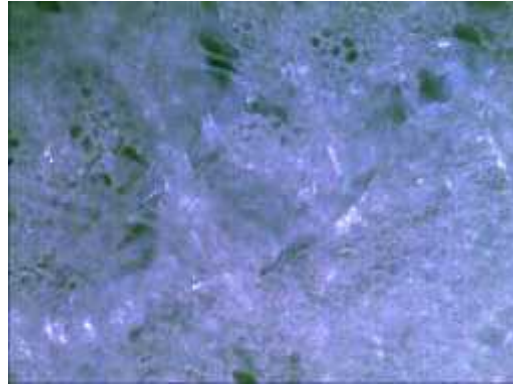
A severe SDS fouling over the membrane can be seen in **Figure 4-35b**. A thick white gel layer comprising of long chains of surfactants blocked the pores of the membrane. This proves our hypothesis that how surfactants can attach over the membrane surface and form a gel layer.

Table: 4-9: EDTA chemical cleaning for micellar fouled FO membranes

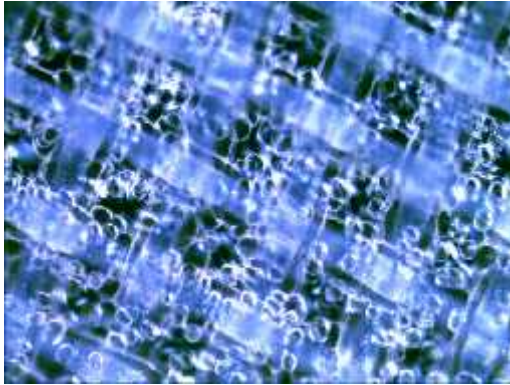
Experiment and membrane type	Average Flux of 10 hrs (LMH)			Inferences
	Before cleaning	After 1st cleaning	After 2nd cleaning	
Figure 4-28 Flat sheet	0.36	0.35 (97)	0.35 (97)	Cleaning in 1 hr was effective to recover the flux. The efficiency is better for hollow fiber than for flat sheet FO membranes
Figure 4-28 Hollow fiber	0.93	0.96 (103)	0.95 (102)	
Figure 4-29 Flat sheet	0.35	0.34 (97)	0.33 (94)	Similar to 1 hr cleaning efficiencies may be obtained by 30 minutes cleaning. Flux recovery was comparable in both types of membranes
Figure 4-29 Hollow fiber	1.08	1.10 (108)	1.11 (102)	
Figure 4-30 Hollow fiber	1.14	1.10 (96)	N/A	NaOH individually, cannot recover the flux completely. It is the combination of EDTA + NaOH that is effective
Figure 4-31 Hollow fiber	0.93	0.96 (103)	0.98 (105)	Since pH is not directly proportional to the NaOH concentration, so, 0.25 g/L and even 0.125 g/L NaOH with same EDTA concentration can give same cleaning efficiency as compared to 0.5 g/L NaOH
Figure 4-32 Hollow fiber	0.93	0.97 (104)	0.98 (105)	
Figure 4-33 Hollow fiber	0.76	0.73 (96)	0.70 (92)	Same cleaning solution cannot give same cleaning efficiency for repeated times. However, decline in cleaning efficiency is very little and it proves the usefulness of the cleaning solution
Figure 4-34 Hollow fiber	2.05	2.05 (100)	2.04 (99)	EDTA cleaning solution is not only good for SDS but, it is equally effective for cleaning the membrane fouled with cationic surfactant TEAB



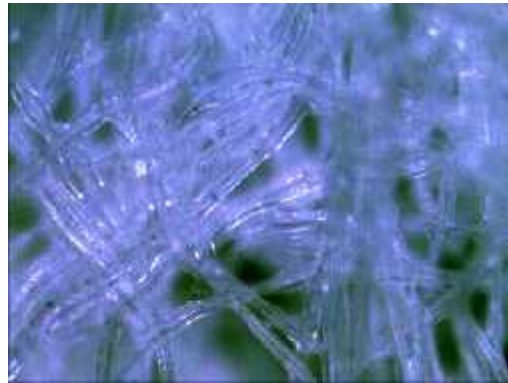
(a)



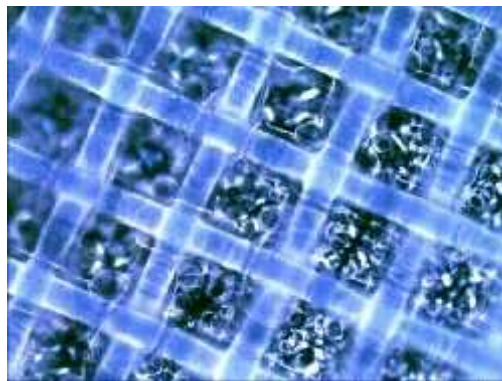
(b)



(c)



(d)



(e)

Figure 4-35: Optical microscopic images (200 times enlarged) of flat sheet FO membranes (a) nascent membrane, (b) fouled with SDS, (c) cleaned with EDTA solution after SDS fouling, (d) fouled with TEAB and (e) cleaned with EDTA solution after TEAB fouling

After cleaning with EDTA solution the membrane showed a reasonable recovery to its original form, as may be seen in **Figure 4-35c**. However, the pearl like micellar chains wrapped over the active layer may still be observed. It shows that although EDTA cleaning was effective to remove the gel layer but some micellar chains are still attached on the active layer, which may cause a flux decline when reusing the same membrane. This may be proved from the results in **Table 4-9**, where the average flux recovery (values in brackets) for flat sheet membranes was always below 100 %. Comparing **Figures 4-35 b** and **4-35 d**, it may be noted that TEAB fouling was less severe than the SDS fouling. Also, comparing **Figures 4-35 c** and **4-35 e** it may be noted that cleaned membrane surface after TEAB fouling resembled more to the nascent membrane compared to the cleaned membrane surface after SDS fouling. It may also be confirmed from the flux recovery results in **Table 4-9**, which show a greater flux recovery in case of cleaning after TEAB compared to the cleaning after SDS fouling.

4.2.3. Dynamics of FO Membrane Fouling

Table 4-10 summarizes the results when synthetic domestic wastewater was used as the feed solution and 2 M NaCl as draw solution, in batch mode, to identify the dynamics of hollow fiber FO membrane fouling. In all experiments the starting volumes of feed and draw were 2.5 L and 0.5 L, respectively. Characteristics of the synthetic wastewater are listed in **Table 3-2**. The actual values are the experimentally measured values and the calculated values are normalized with water volume added in the draw solution or water volume subtracted from the feed solution.

In first hour almost 34 mg/L TOC was transferred to the draw solution. The constant values of both feed and draw TOCs from 2nd to 6th hour shows that maximum TOC was transferred in the first hour and then the TOC did not pass through the FO membrane. It may be claimed that the

membrane initially allowed the organics to pass through it and then due to the combined effects of CP and pore clogging rest of the organics were trapped by the membrane. Almost 88 mg/L TOC was transferred from the feed solution to the draw solution during the whole experiment. There was, however, only an increase of 34 mg/L TOC of the draw solution and remaining 54 mg/L TOC might get trapped by the FO membrane and caused the fouling and concentration polarization. The passage of 3 mg/L of TOC to draw solution during FO-MBR operation was also observed in another study (Achilli et al., 2009 a). It draws to important conclusions, i) if we use FO-MBR instead of only FO filtration, the amount of TOC that leaks to the draw solution can be substantially reduced due to biodegradation by the sludge ii) passage of TOC towards the draw solution in the first hour is inevitable at this stage of FO and membrane manufacturers should seriously look into this issue.

The conductivity results in the **Table 4-10** discovered that almost 1.11 mS/cm conductivity was added in the feed solution during experiment, possibly due to the reverse transport. Again, the maximum reverse transport occurred in the first hour. In another study transfer of 10 mS/cm conductivity in first 12 days operation of a continuous FO-MBR; due to accumulation of feed solutes and reverse transported draw solutes is reported. After that conductivity was stabilized due to the sludge wastage (Zhang et al., 2012). It shows that the conductivity increase in FO-MBR may be controlled easily and it may not affect the processes on the feed side. The critical nature of the first hour in FO-MBR fouling and steady state achievement is also reported by other researchers (Qin et al., 2009), which supports this study of understanding the fouling behavior of FO membrane during first hour.

Table 4-10: Contaminant transfer through hollow fiber FO membrane

Time (hr)	Actual feed cond. (mS/cm)	Actual draw cond. (mS/cm)	Calculated draw cond. (mS/cm)	Calculated feed cond. (mS/cm)	Actual Feed TOC (mg/L)	Actual Draw TOC (mg/L)	Calculated draw TOC (mg/L)	Calculated feed TOC (mg/L)	Volume of water added in draw (mL)
0	0.38	139.9	139.9	0.38	240	0	0	240	0
1	0.98	105.6	106.9	0.40	214.2	34.56	0	255	154 (154)
2	1.13	94.8	93.1	0.42	220.1	22.05	0	266	251 (97)
3	1.22	88.9	83.3	0.43	221.5	18.46	0	277	339 (88)
4	1.40	80.5	76.4	0.45	220	14.48	0	287	415 (76)
5	1.51	75.9	71	0.47	220.5	10.51	0	297	485 (70)
6	1.59	74	66.9	0.48	218.4	12.08	0	306	545 (60)

4.2.4. Osmotic Backwashing Optimization

Table 4-11 summarizes the results of osmotic backwashing experiments; the methodology of the experiments is discussed in section 3.2.3. The osmotic backwash approach adopted in this study is more realistic and practicable compared to the studies that used DI water in replacement of draw solution and some weak brine solution in replacement of the feed solution (Achilli et al., 2009 a) or performed only with model foulants and not with the mixed sludge (Kim et al., 2012). In this study it was expected that during osmotic backwash the DI water will start flowing into the mixed sludge and it will displace the fouling layer, caused by the accumulation of sludge particles, from the membrane surface. Due to practical limitation of the hollow fiber membrane used, AL-DS configuration was used, which is more prone to ICP by mixed sludge as compared to AL-FS configuration.

The draw solution used in this study, 2 M NaCl, has an osmotic pressure of 96 bars and the feed solution, mixed sludge, around 12 bars as calculated with the Morse equation, 2-1. Looking at the sum of filtrate volumes extracted it may be discovered that the osmotic backwashing for 30 and 20 minutes was ineffective compared to the 60 minutes backwash because of negative water flux during back wash and adding more complexity to the system. This negative flux during the 30 and 20 minutes backwash may be attributed to the gradient inside the FO membrane established by 2 M NaCl (during filtration). This gradient was so strong that even rinsing it with DI water, before backwash, could not remove its effect completely. Also, the mixed sludge had not such a high osmotic pressure to establish its own gradient in the membrane. So, it may be inferred that the osmotic backwashing is not practical at least with hollow fiber FO-MBR.

Table 4-11: Osmotic backwashing in hollow fiber FO-MBR

Exp. No.	Condition	Cycles/day	Filtrate 1 (mL)	Filtrate 2 (mL)	Filtrate 3 (mL)	Sum of Filtrate volume (mL)	Backwash1 (mL)	Backwash 2 (mL)	Backwash 3 (mL)
1	420 min filtration + 60 min backwash	1	201	N/A	N/A	201	17	N/A	N/A
2	210 min filtration + 30 min backwash	2	108	73	N/A	181	-48	-19	N/A
3	140 min filtration + 20 min backwash	3	80	58	64	202	-33	-10	8

4.2.5. Cross-flow Velocity Optimization for FO-MBR

Cross-flow velocity is an important parameter to be optimized in the FO-MBR. It is generally believed that by increasing the cross-flow velocity, ECP may be reduced and hence flux increases. So, a straight line relationship exists between flux and cross-flow velocity upto certain limit, but after diminishing the ECP completely, increase in cross-flow is not effective to increase the net flux. In another study 0.5 M NaCl was used as draw solution and cross-flow velocity of the draw solution was varied from 0.1 to 0.7 m/s. A sharp increase in flux was observed with an increase in cross-flow velocity at low velocity (corresponding to the laminar flow pattern) and levels off when the flow pattern becomes turbulent. This could be attributed to a high salt concentration of the draw solution, resulting in a countable contribution of dilutive ECP to the flux (Qin et al., 2009). Positive effect of changing hydrodynamic conditions on fouling mitigation in FO is reported in other studies as well (Boo et al., 2013).

Table 4-12 demonstrates the effect of increasing cross-flow velocity of feed (DI water) and draw solution (1 M NaCl) on the net water flux through hollow fiber membrane. Since the hollow fiber FO module started vibrating over the 150 mL cross-flow velocity, so the velocity was not enhanced further.

Table 4-12: Effect of cross-flow velocity on flux through hollow fiber FO module

Cross flow velocity (mL/min)	50	100	150
Water Flux (LMH)	5.9	7.8	8.5

Figure 4-36 demonstrates that the concentrated draw solution addition maintained a constant conductivity of the draw solution to attain a constant osmotic pressure and flux. **Figure 4-37** illustrates a comparison of flux during the four runs of FO-MBR at four different cross-flow velocities of both the feed and draw solution. The detailed methodology is already discussed in section 3.2.4. The third run was done with 1000 mL/min cross-flow velocity and since its flux was less than 300 mL/min, so 700 mL/min cross-flow velocity was also studied in fourth run. It may be noticed that the flux with 300 mL/min was the highest during the course of the experiment. **Table 4-13** summarizes the EPS values before the start and after the end of each experiment. Since the experiments were conducted in AL-DS configuration, so it was believed that there would be a strong fouling due to the EPS. It was assumed that although increasing cross-flow velocity increases the flux by reducing ECP but, in FO-MBR higher cross-flow velocity will cause a shear stress on microbial flocs. This may support a higher EPS release, which ultimately may decrease the flux through severe ICP. Such inter dependent relation between ECP and ICP is modeled and reported in the literature (Suh and Lee, 2013).

Simultaneously looking at the **Tables 4-13** and **4-14** it may be discovered that the EPS always increased during the course of the experiment and particle size always decreased. However, no direct relationship may be established between these two as it is difficult to justify a bunch of living organisms (bacterial floc) as a particle. **Table 4-14** depicts that the flux is inversely proportional to the difference between the initial and final particle size and is directly proportional to the difference between initial and final MLSS.

Figure 4-38 shows AFM images of the support layer side of the all four membranes after the completion of experiment. It is important to note that the length and width of all images is same

but there is a difference in height values. Actually AFM gives the idea about the topography of a membrane surface. It can be observed clearly that the two cross-flow velocities that generated the higher flux have relatively smoother topography of the sludge layer compared to the other two velocities where sludge layer was uneven. Also, a thick yellowish sludge accumulation may be observed on membranes which produced less flux. Moreover, with less MLSS (4700 mg/L) the flux was higher compared to the higher MLSS. So, it is proved that both final EPS and particle size difference have strong influence on the flux through FO-MBR and 300 mL/min cross-flow velocity is the most suitable for attaining highest flux.

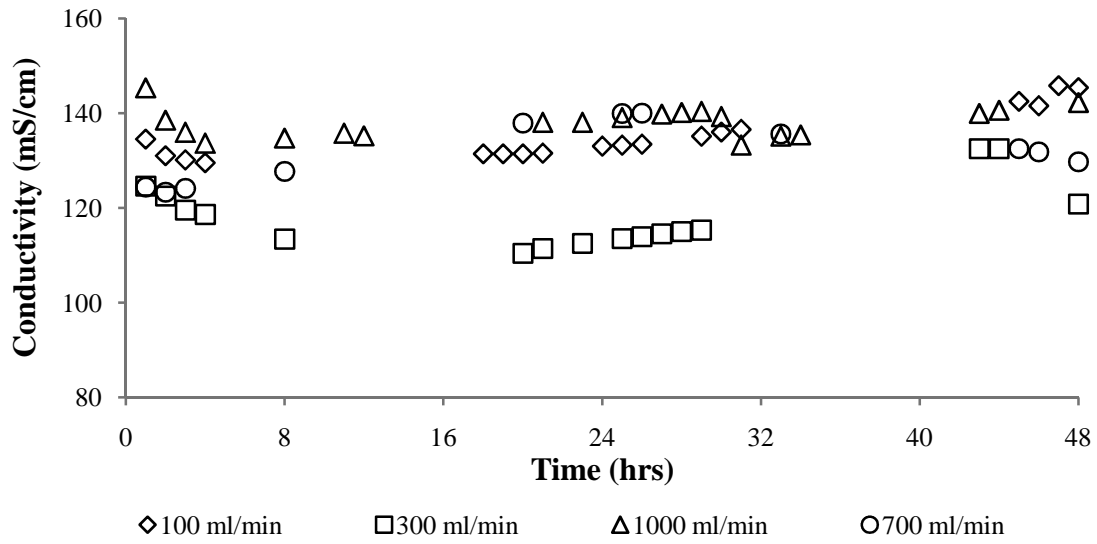


Figure 4-36: Conductivity of draw solution in flat sheet FO-MBR operation at different cross-flow velocities

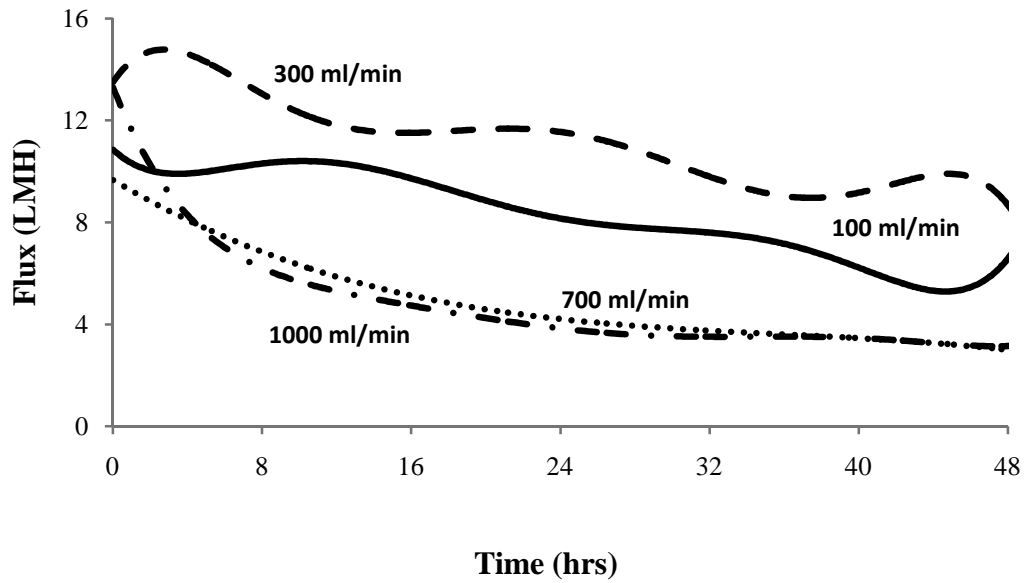


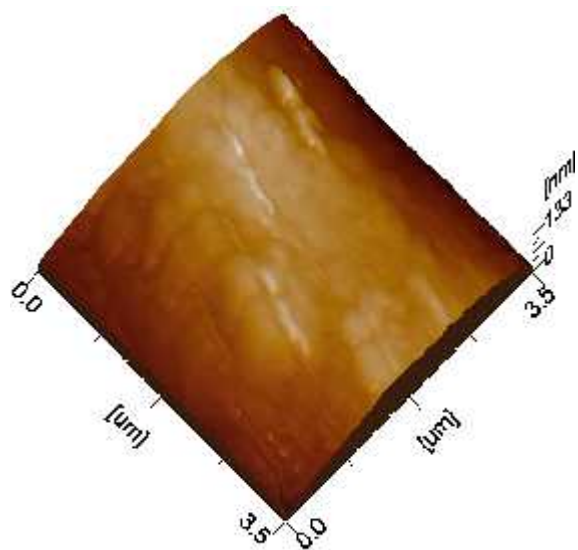
Figure 4-37: Flux generated during flat sheet FO-MBR operation at different cross-flow velocities

Table 4-13: Initial and final EPS during flat sheet FO-MBR four different runs

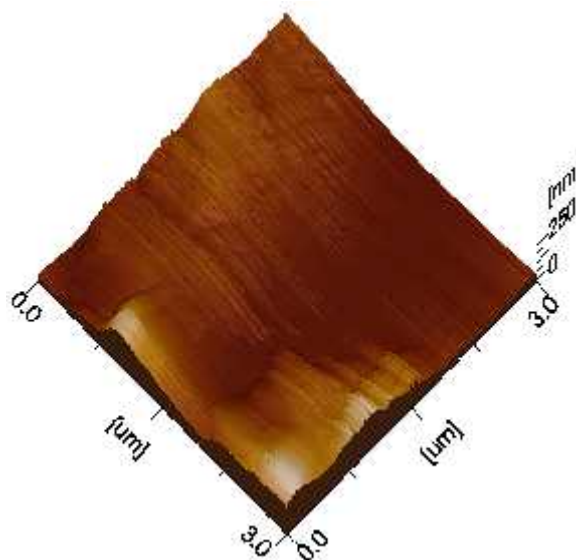
Cross-flow (mL/min)	Initial EPS (mg/L)					Final EPS (mg/L)					Difference between initial and final total EPS
	Protein (soluble)	Carbohy-drate (soluble)	Protein (Bound)	Carbohy-drate (Bound)	Total	Protein (soluble)	Carbohy-drate (soluble)	Protein (Bound)	Carbohy-drate (Bound)	Total	
100	108.4	36.8	92.9	70.4	308.5	271.5	73.7	224.9	75.7	645.8	337.3
300	221.1	54.9	52.7	18.3	347	186.6	72.6	63	64.6	386.8	39.8
1000	126.2	45.8	54.9	11.5	238.4	200.6	58.3	30.3	20.6	309.8	71.4
700	111.8	40.4	23.6	11.8	187.6	120.5	67.3	22.4	19.6	229.8	42.2

Table 4-14: Effect of cross-flow velocity on sludge particle size during flat sheet FO-MBR four different runs

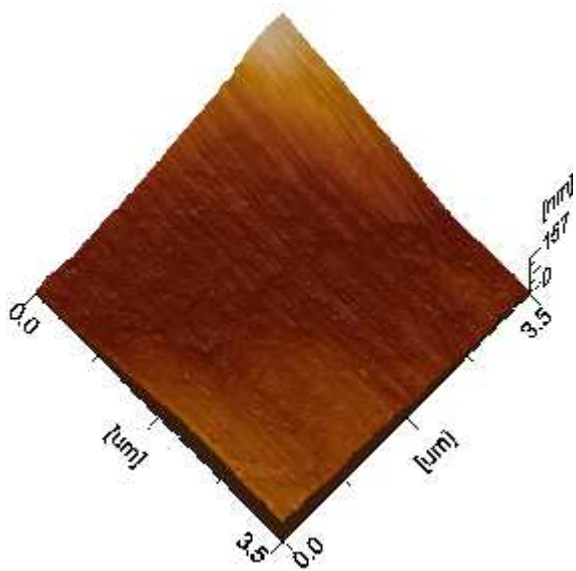
Cross-flow (mL/min)	Initial mean particle size (μm)	Final mean particle size (μm)	Difference (μm)	Initial MLSS (mg/L)	Final MLSS (mg/L)	Difference (mg/L)	Total volume extracted (mL)
100	16.19 \pm 14.7	14.83 \pm 9.0	-1.36	6000	4700	1300	1383
300	29.05 \pm 26.1	25.32 \pm 33.7	-3.73	6000	4700	1300	1847
1000	27.6 \pm 41.4	22.8 \pm 18.9	-4.8	6000	5100	900	1196
700	45.6 \pm 39.0	19.1 \pm 13.9	-26.5	6000	5600	400	1007



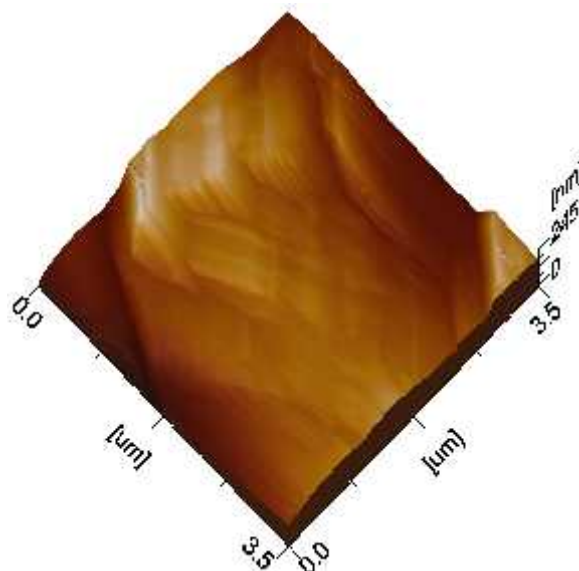
(a)



(b)



(c)



(d)

Figure 4-38: AFM image after (a) Run 1 (100 mL/min), (b) Run 2 (300 mL/min), (c) Run 3 (1000 mL/min) and (d) Run 4 (700 mL/min)

CONCLUSIONS AND RECOMMENDATIONS

The study had two distinctive objectives; i) to introduce micellar solutions as a potential draw solute for forward osmosis applications and ii) optimize processes for FO-MBR to increase water throughput. In context of the first objective micellar solutions were studied for stability of the flux generated, ECP and ICP to FO membranes, reverse transport, mass transfer, regeneration and microbial toxicity to the biomass. To achieve the second objective various processes were optimized to achieve maximum flux, like draw solution concentration, membrane cleaning protocol, osmotic backwashing and cross-flow velocity. The conclusions drawn from the study are mentioned below.

5.1. CONCLUSIONS

5.1.1. Development of Micellar Draw Solution

- The AL-DS configuration produced higher flux compared to AL-FS with same micellar solution concentration, due to less ICP. The ECP produced by the micellar draw solutions may be reduced by increasing the cross-flow velocity.
- Micellar solutions depicted fairly stable water fluxes, independent of the declining draw solution concentration, above their CMCs. However, micellar draw solutions behave like inorganics below CMCs.

- Flux generated through micellar draw solutions is not in a linear relationship with concentration. Micellar solutions depicted better fluxes than NaCl at lower operating concentrations (0.1 to 0.5 M).
- Mass transfer coefficient “k” of micellar draw solutions is of the same magnitude or 10 times lower than NaCl under similar operating conditions.
- Reverse transport of micellar solutions was 53-268 times lower as compared to the sodium chloride, at similar conditions.
- Micellar solutions can be recovered from the diluted draw solution upto 99 % with energy efficient methods like UF or Krafft temperature swing.
- The diluted micellar draw solution can be used directly for a applications like detergent, manufacturing of pesticides and contaminated site remediation.
- Chloride and sulfate containing inorganic draw solutions showed little or no toxicity to the *E.coli* and thus may be used in FO-MBR without any associated toxicity to the biomass; if reverse transported to the feed side.
- Reverse transported micellar draw solution of TEAB and SDS are biodegradable by *Pseudomonas* and mixed sludge and thus may be used in FO-MBR, however, TMOAB, MTAB and 1-OSA depicted toxicity and may not be recommended for FO-MBR.

5.1.2. Process Optimization of FO-MBR

- Draw solution concentration of 2 M was found most suitable for hollow fiber FO module since the higher concentrations caused extensive concentration polarization and net flux decline.
- Hollow fiber FO membrane fouled with inorganics showed upto 93 % flux recovery by NaOH and HNO₃ cleaning.

- Micellar fouled flat sheet and hollow fiber FO membranes showed 100 % flux recovery after cleaning with EDTA solution.
- Major transport of organic contaminants and draw solute across the FO membrane occurs in the first hour of operation of the FO-MBR.
- Osmotic backwashing was ineffective for flux recovery in hollow fiber FO-MBR.
- Cross-flow velocity of 300 mL/min was optimized to circulate the mixed activated sludge in FO-MBR, because lower velocities encouraged ECP and higher velocities encouraged ICP.

5.2. RECOMMENDATIONS

Although, many areas related to the introduction of micellar draw solutions and FO-MBR process optimization are covered in this study but there are some areas which were out of scope for this study and may be investigated in detail.

- The detailed mathematical modeling of the flux generated through micellar draw solutions keeping in view the constant osmotic pressure above CMC is very important to predict flux behaviors of different surfactants. Validation of the mathematical model through authentic experimental data is also very crucial.
- Different types of charged surfactants like Zwitterionic and Gemini surfactants and mixture of surfactants can be studied in detail to get high flux and minimum reverse transport.
- An experimental setup may be developed that can regenerate diluted micellar draw solution using both UF and Krafft temperature methods.
- Osmotic backwashing may be studied on flat sheet FO-MBR.

- There is also strong need to optimize the MLSS concentration for FO-MBR. Till now 6000 mg/L concentration is used because it is the minimum for MBR operations, but due to high associated ICP, higher MLSS concentrations may decrease the net flux in FO-MBR.
- Pilot scale FO setup for industrial single process wastewater treatment may be established, e.g. recovery of textile dyes from the dyeing wastewater.

REFERENCES

- Abboud, M. M., Khleifat, K.M., Batarseh, M., Tarawneh, K.A., Al-Mustafa A. and Al-Madadhah, M. (2007). Different optimization conditions required for enhancing the biodegradation of linear alkyl benzenesulfonate and sodium dodecyl sulfate surfactants by novel consortium of *Acinetobacter calcoaceticus* and *Pantoea agglomerans*. *Enzymes and Microbial Technology*. 41: 432-439.
- Abdulkarim, S.M., Fatimah, A.B. and Anderson, J.G. (2009). Effect of salt concentrations on the growth of heat-stressed and unstressed *Escherichia coli*. *Journal of Food Agriculture and Environment*. 7: 51-54.
- Achilli, A., Cath, T.Y., Marchand, E.A. and Childress, A.E. (2009 a). The forward osmosis membrane bioreactor: a low fouling alternative to MBR processes. *Desalination*. 239:10–21.
- Achilli, A., Cath, T.Y. and Childress, A.E. (2009 b). Power generation with pressure retarded osmosis: an experimental and theoretical investigation. *Journal of Membrane Sciences* 343: 42–52.
- Achilli, A., Cath, T.Y. and Childress, A.E. (2010). Selection of inorganic based draw solutions for forward osmosis application. *Journal of Membrane Science*. 364: 233-241.
- Alnaizy, R., Aidan, A. and Qasim, M. (2013). Copper sulfate as draw solute in forward osmosis desalination. *Journal of Environmental Chemical Engineering*. 1: 424-430.
- Alturki, A.A., Tadkaew, N., McDonald, J.A., Khan, S.J., Price, W.E. and Nghiem, L.D. (2010). Combining MBR and NF/RO membrane filtration for the removal of trace organics in indirect potable water reuse applications. *Journal of Membrane Science*. 365:206–215.

- Alturki, A., McDonald, J., Khan, S.J., Hai, F., Price, W.E. and Nghiem, L.D. (2012). Performance of a novel osmotic membrane bioreactor (OMBR) system: Flux stability and removal of trace organics. *Bioresource Technology*. 113: 201–206.
- APHA, AWWA and WEF.(2005). Standard methods for the examination of water and wastewater. American Public Health Association, 20th edition, Washington DC.
- Bellona, C., Marts, M. and Drewes, J. (2010).The effect of organic membrane fouling on the properties and rejection characteristics of nano filtration membranes.*Separation and Purification Technology*. 74: 44–54.
- Boo, C., Lee, S., Elimelech, M., Mengb, Z. and Hong, S. (2012). Colloidal fouling in forward osmosis: Role of reverse salt diffusion. *Journal of Membrane Science*. 390-391: 277-284.
- Boo, C., Elimelech, M. and Hong, S. (2013). Fouling control in a forward osmosis process integrating seawater desalination and wastewater reclamation.*Journal of Membrane Science*. 444: 148–156.
- Bowden, K.S., Achilli, A. and Childress, A.E. (2012). Organic ionic salt draw solutions for osmotic membrane bioreactors. *Bioresource Technology*.122: 207–216.
- Carmignani, G., Sitkiewitz, S and Webley, J.W. (2012).Recovery of retrograde soluble solute for forward osmosis water treatment.*Journal of Membrane Science*. 442:225-237.
- Cartinella, J.L., Cath, T.Y., Flynn, M.T., Miller, G.C., Hunter, K.W. and Childress, A.E. (2006). Removal of natural steroid hormones from wastewater using membrane contactor processes. *Environment Science and Technology*. 40: 7381–7386.

- Cath, T.Y., Childress, A.E. and Elimelech, M. (2006). Forward osmosis: Principles, applications, and recent developments. *Journal of Membrane Science*. 281:70–87.
- Cath, T.Y., Gormly, S., Beaudry, E., Flynn, M., Adams, V. and Childress, A. (2005). Membrane contactor processes for wastewater reclamation in space Part I. Direct osmotic concentration as pretreatment for reverse osmosis. *Journal of Membrane Science*. 257: 85–98.
- Chou, S., Shi, L., Wang, R., Tang, C. Y., Qiu, C., and Fane, A. G. (2010). Characteristics and potential applications of a novel forward osmosis hollow fiber membrane. *Desalination*. 261: 365–372.
- Cornelissen, E.R., Harmsen, D., Korte, K.F.D., Ruiken, C.J., Qin, J.J., Oo, H. and Wessels, L.P. (2008). Membrane fouling and process performance of forward osmosis membranes on activated sludge. *Journal of Membrane Science*. 319: 1–2.
- Dean-Raymond, D. and Alexander, M. (1977). Bacterial metabolism of quaternary ammonium compounds. *Applied and Environmental Microbiology*. 33: 1037-1041.
- Dubois, M., Gilles, K.A., Hamilton, J.K., Rebers, P.A. and Smith, F. (1956). Colorimetric method for determination of sugars and related substances. *Analytical Chemistry*. 28: 350–356.
- Ewa, L. and Marcin, B. (2006). Effect of selected anionic surfactants on activated sludge flocs. *Enzyme and Microbial Technology*. 39: 660–668.
- Ewa, L. and Marcin, B. (2007). The influence of the selected nonionic surfactants on the activated sludge morphology and kinetics of the organic matter removal in the flow system. *Enzyme and Microbial Technology*. 41: 26–34.
- Frank, B.S. (1972). Desalination of Sea Water, US Patent, 3670897.

- Frølund, B., Palmgren, R., Keiding, K. and Nielsen, P.H. (1996). Extraction of extracellularpolymer from activated sludge using a cation exchange resin. *Water Research*. 30:1749–1758
- Garcia-C, E.M. and McCutcheon, J.R. (2011). Dewatering press liquor derived from orange production by forward osmosis. *Journal of Membrane Science*. 372: 97–101.
- Ge, Q., Su, J.C., Chung, T.S. and Amy, G. (2011). Hydrophilic super paramagnetic nanoparticles: synthesis, characterization, and performance in forward osmosis processes. *Industrial Engineering Chemical Research*. 50: 382–388.
- Ge, Q., Su, J.C., Amy, G. and Chung, T.S. (2012). Exploration of polyelectrolytes as draw solutes in forward osmosis processes. *Water Research*. 46:1318–1326.
- Ge, Q., Ling, M. and Chung, T. (2013). Draw solutions for forward osmosis processes: Developments, challenges, and prospects for the future. *Journal of Membrane Science*. 442: 225–237.
- Hancock, N. T. and Cath, T. Y. (2009). Solute coupled diffusion in osmotically driven membrane Processes. *Environmental Science and Technology*. 43: 6769–6775.
- Herron, J.R., Beaudry, E.G., Jochums, C.E. and Medina, L.E. (1994).Osmotic concentration apparatus and method for direct osmotic concentration of fruit Juices, US Patent, 5281430.
- Herzberg, M., Kang, S. and Elimelech, M. (2009).Role of extracellular polymeric substances (EPS) in biofouling of reverse osmosis membranes.*Environment Science and Technology*. 43: 4393–4398.

- Holloway, R.W., Childress, A.E., Dennett, K.E. and Cath, T.Y. (2007). Forward osmosis for concentration of anaerobic digester concentrate. *Water Research*. 41: 4005–4014.
- Hough, W.T. (1970). Process for extracting solvent from a solution, US Patent, 3532621.
- Iyer, S. and Linda, Y. (2011). Systems and Methods for Forward Osmosis Fluid Purification Using Cloud Point Extraction, US Patent, 8021553.
- Jin, X., She, Q., Ang, X. and Tang, C.Y. (2012). Removal of boron and arsenic by forward osmosis membrane: Influence of membrane orientation and organic fouling. *Journal of Membrane Science*. 389: 182–187.
- Kang, S., Subramani, A., Hoek, E., Deshusses, M. and Matsumoto, M. (2004). Direct observation of biofouling in cross-flow microfiltration: mechanisms of deposition and release. *Journal of Membrane Science*. 244: 151–165.
- Kessler, J.O. and Moody, C.D. (1976). Drinking water from sea water by forward osmosis. *Desalination*. 18: 297–306.
- Kim, C., Lee, S. and Hong, S. (2012). Application of osmotic backwashing in forward osmosis: mechanisms and factors involved. *Desalination and Water Treatment*. 43: 314-322.
- Kravath, R. E. and Davis, J.A. (1975). Desalination of seawater by direct osmosis. *Desalination*. 16: 151–155.
- Lacoursiere, A., Thompson, B.G., Kole, M.M., Ward, D. and Gerson, D.F. (1986). Effects of carbon dioxide concentration on anaerobic fermentation of *Escherichia Coli*. *Applied Microbiology and Biotechnology*. 23: 404-406.

- Lay, W.C.L., Chong, T.H., Tang, C.Y.Y., Fane, A.G., Zhang, J.S. and Liu, Y. (2010). Fouling propensity of forward osmosis: investigation of the slower flux decline phenomenon. *Water Science and Technology*. 61:927–936.
- Lay, W.C.L., Zhang, J.S., Tang, C.Y., Wang, R., Liu, Y. and Fane, A.G. (2012). Factors affecting flux performance of forward osmosis systems. *Journal of Membrane Science*. 394–395: 151– 168.
- Lay, W.C.L., Zhang, Q., Zhang, J., McDougald, D., Tang, C.Y., Wang, R., Liu, Y. and Fane, A.G. (2011). Study of integration of forward osmosis and biological process: Membrane performance under elevated salt environment. *Desalination*. 283: 123–130.
- Lee, K.L; Baker, R. W. and Lonsdale, H.K. (1981). Membranes for power generation by pressure-retarded osmosis. *Journal of Membrane Science*. 8: 141–171.
- Lee, S., Boo, C., Elimelech, M. and Hong, S. (2010). Comparison of fouling behavior in forward osmosis (FO) and reverse osmosis (RO). *Journal of Membrane Science*. 365:34–39.
- Li, D., Zhang, X., Yao, J., Zeng, Y., Simon, G.P. and Wang, H. (2011 b). Composite polymer hydrogels as draw agents in forward osmosis and solar dewatering. *Soft Materials*. 7: 10048–10056.
- Li, Q. and Elimelech, M. (2004) Organic fouling and chemical cleaning of nanofiltration membranes: measurements and mechanisms. *Environmental Science and Technology*. 38:4683–4693.

- Li, D., Zhang, X., Yao, J., Simon, G. P. and Wang, J. (2011 a). Stimuli-responsive polymer hydrogels as a new class of draw agent for forward osmosis desalination. *Chemical Communication*. 47: 1710-1712.
- Ling, M. M., Wang, K. Y. and Chung, T. S. (2010). Highly water-soluble magnetic nano particles as novel draw solutes in forward osmosis for water reuse. *Industrial and Engineering Chemistry Research*. 49: 5869-5876.
- Ling, M.M. and Chung, T.S. (2011 a).Desalination process using super hydrophilic nanoparticles via forward osmosis integrated with ultra filtration regeneration. *Desalination*. 278: 194–202.
- Ling, M. M., Chung, T.S. and Lu, X.M. (2011 b). Facile synthesis of thermosensitive magnetic nanoparticles as smart draw solute in forward osmosis. *Chemical Communication*. 47: 10788–10790.
- Loeb, S., Titelman, L., Korngold, E. and Freiman, J. (1997).Effect of porous support fabric on osmosis through a Loeb-Sourirajan type asymmetric membrane. *Journal of Membrane Science* 129: 243–249.
- Loeb, S. and Bloch, M.R. (1973).Countercurrent flow osmotic processes for the production of solutions having a high osmotic pressure.*Desalination*. 13: 207–215.
- Lowry, O.H., Rosebrough, N.R., Farr, A.L. and Randall, R.J. (1951).Protein measurement with the folin phenol reagent.*Journal of Biological Chemistry*.193: 265.
- McCormick, P., Pellegrino, J., Mantovani, F. and Sarti, G. (2008). Water, salt, and ethanol diffusion through membranes for water recovery by forward (direct) osmosis processes. *Journal of Membrane Science*. 325:467–478.

- McCutcheon, J. R., McGinnis, R. L. and Elimelech, M. (2005). A novel ammonia–carbon dioxide forward (direct) osmosis desalination process. *Desalination*. 174: 1–11.
- McCutcheon, J.R. and Elimelech, M. (2006). Influence of concentrative and dilutive internal concentration polarization on flux behavior in forward osmosis. *Journal of Membrane Sciences*. 284: 237–247.
- McCutcheon, J.R. and Elimelech, M. (2008). Influence of membrane support layer hydrophobicity on water flux in osmotically driven membrane processes. *Journal of Membrane Science*. 318:458–466.
- McCutcheon, J.R.; McGinnis, R.L. and Elimelech, M. (2006). Desalination by a novel ammonia–carbon dioxide forward osmosis process: influence of draw and feed solution concentrations on process performance. *Journal of Membrane Science*. 278:114–123.
- McGinnis, R.L. (2002). Osmotic Desalination Process, US Patent, 6391205 B1.
- McGinnis, R. L. and Elimelech, M. (2008). Global Challenges in Energy and Water Supply: The Promise of Engineered Osmosis. *Environment Science and Technology*. 42:8625–8629.
- McGinnis, R.L. and Elimelech, M. (2007). Energy requirements of ammonia–carbon dioxide forward osmosis desalination. *Desalination*. 207: 370–382.
- Mi, B. and Elimelech, M. (2008). Chemical and physical aspects of organic fouling of forward osmosis membranes. *Journal of Membrane Science*. 320:292–302.
- Mi, B. and Elimelech, M. (2010a). Gypsum scaling and cleaning in forward osmosis: measurements and mechanisms. *Environment Science and Technology*. 44: 2022–2028.

- Mi, B. and Elimelech, M. (2010b). Organic fouling of forward osmosis membranes: fouling reversibility and cleaning without chemical reagents. *Journal of Membrane Science*. 348: 337–345.
- Myers, D. (2005). *Surfactant Science and Technology*. John Wiley and Sons, 3rd edition, NJ, USA.
- Naim, R., Levitsky, I. and Gitis, V. (2012). Surfactant cleaning of UF membranes fouled by proteins. *Separation and Purification Technology*. 94: 39.
- Nawaz, M.S., Gadelha, G., Khan, S.J. and Hankins, N.P. (2013). Microbial Toxicity Effects of Reverse Transported Draw Solute in the Forward Osmosis Membrane Bioreactor (FO-MBR). *Journal of Membrane Science*. (429): 323-329.
- Nayak, C.A., Rastogi, N.K. (2010). Forward osmosis for the concentration of anthocyanin from *Garcinia indica* Choisy. *Separation and Purification Technology*. 71:144–151.
- Neff, R.A. (1964). Solvent Extractor, US Patent, 3130156.
- Nguyen, N.C., Chen, S., Yang, H. and Hau, N.T. (2013). Application of forward osmosis on dewatering of high nutrient sludge. *Bioresource Technology*. 132: 224–229.
- Noh, M., Mok, Y., Lee, S., Kim, H., Lee, S.H., Jin, G.W., Seo, J.H., Koo, H., Parka, T.H. and Lee, Y. (2012). Novel lower critical solution temperature phase transition materials effectively control osmosis by mild temperature changes. *Chemical Communication*. 48: 3845–3847.
- Offen, H.W. and Turley, W.D. (1983). Pressure dependence of the critical micellar temperature. *Journal of Colloid and Interface Science*. 92: 575–579.

- Phillip, W.A., Yong, J. and Elimelech, M. (2010). Reverse draw solute permeation in forward osmosis: modeling and experiments. *Environmental Science and Technology*. 44 :5170–5176.
- Phuntsho, S., Shon, H.K., Hong, S.K., Lee, S.Y. and Vigneswaran, S. (2011). A novel low energy fertilizer driven forward osmosis desalination for direct fertigation: evaluating the performance of fertilizer draw solutions. *Journal of Membrane Science*. 375:172–181.
- Proksova, M., Vrbanova, A., Sladckova, D., Gregorova, D. and Augustin, J. (1999). Dialkylsulphosuccinate toxicity towards commonasterrigena NH₃. *Journal of Trace and Microbial Techniques*. 16:475–80.
- Qin, J., Oo, M.H., Tao, G., Cornelissen, E.R., Ruiken, C.J., De-Korte, K.F., Wessels, I.P. and Kekre, K.A. (2009). Optimization of operating conditions in forward osmosis for osmotic membrane bioreactor. *The Open Chemical Engineering Journal*. 3: 27-32.
- Schramm, L. L., Stasiuk, E. N. and Marangoni, D. G. (2003). Surfactants and their applications. *Annual Reports on the Progress of Chemistry Section "C"*. 99: 3-48.
- Sekowska, A., Kung, H. and Danchin, A. (2000). Sulfur Metabolism in *Escherichia coli* and Related Bacteria: Facts and Fiction. *Journal of Molecular Microbiology and Biotechnology*. 2:145-177.
- Shcherbakova, V.A., Laurinavichius, K.S. and Akimenko, V.K. (1999). Toxic effect of surfactants and probable products of their biodegradation on methanogenesis in an anaerobic microbial community. *Chemosphere*. 29:1861–90.

- Singh, K.L., Kumar, A. and Kumar, A. (1998). *Bacillus cereus* capable of degrading SDS shows growth with a variety of detergents. *World Journal of Microbiology and Biotechnology*. 14: 777-779.
- Stache, K. (1989). Apparatus for Transforming Sea Water, Brackish Water, Polluted Water or the Like into a Nutritious Drink by Means of Osmosis, US Patent, 4879030.
- Stone, M.L., Wilson, A.D., Harrup, M.K. and Stewart, F.F. (2013). An initial study of hexavalent phosphazene salts as draw solutes in forward osmosis. *Desalination*. 312: 130-136.
- Su, J.C., Chung, T.S., Helmer, B.J. and Dewit, J.S. (2012). Enhanced double-skinned FO membranes with inner dense layer for wastewater treatment and macro- molecule recycle using sucrose as draw solute. *Journal of Membrane Science*. 396: 92–100.
- Suh, C. and Lee, S. (2013). Modeling reverse draw solute flux in forward osmosis with external concentration polarization in both sides of the draw and feed solution. *Journal of Membrane Science*. 427: 365–374.
- Takenaka, S., Takashi, T., Taira, K., Murakami, S. and Aoki, K. (2007). Adaptation of *Pseudomonas* sp. Strain 7-6 to Quaternary Ammonium Compounds and Their Degradation via Dual Pathways. *Applied and Environmental Microbiology*. 73: 1797-1802.
- Tang, C., She, Q., Lay, W., Wang, R., Fane, A.G. (2010). Coupled effects of internal concentration polarization and fouling on flux behavior of forward osmosis membranes during humic acid filtration. *Journal of Membrane Sciences*. 354: 123–133.
- Us'yarov, O.G. (2004). Critical micellization concentration of ionic surfactants: Comparison of theoretical and experimental results. *Colloid Journal* 66: 612–616.

- Vrijenhoek, E., Hong, S., Elimelech, M. (2001). Influence of membrane surface properties on initial rate of colloidal fouling of reverse osmosis and nanofiltration membranes. *Journal of Membrane Sciences*. 188: 115–128.
- Wallace, M., Cui, Z. and Hankins, N.P. (2008). A thermodynamic benchmark for assessing an emergency drinking water device based on forward osmosis. *Desalination* 227: 34–45.
- Wang, K.Y., Ong, R. C. and Chung, T.S. (2010). Double-skinned forward osmosis membranes for reducing internal concentration polarization. *Industrial and Engineering Chemistry Research*.49 :4824–4831.
- Wang, K.Y., Yang, Q., Chung, T.S. and Rajagopalan, R. (2009). Enhanced forward osmosis from chemically modified polybenzimidazole (PBI) nanofiltration hollow fiber membranes with a thin wall. *Chemical Engineering Science*.64 :1577–1584.
- Wang, R., Shi, L., Tang, C.Y., Chou, S., Qiu, C. and Fane, A.G. (2010a). Characterization of novel forward osmosis hollow fiber membranes. *Journal of Membrane Science*. 355:158-167.
- Wang, Y., Wicaksana, F., Tang, C.Y. and Fane, A.G. (2010b). Direct microscopic observation of forward osmosis membrane fouling. *Environmental Science and Technology*. 44: 7102–7109.
- William, Phillip, A., Jui, S.Y. and Menachem, E. (2010). Reverse Draw Solute Permeation in Forward Osmosis: Modeling and Experiments. *Environment Science and Technology* 44: 5170–5176.
- Williams, M.D. and Pirbazari, M. (2007). Membrane bioreactor process for removing biodegradable organic matter from water. *Water Research*. 41: 3880–3893.

- Xiao, J. and Li, W. (2008). Study on osmotic pressure on non-ionic and ionic surfactant solutions in the micellar and micro emulsion regions. *Fluid Phase Equilibria*. 263:231-235.
- Xiao, D., Tang, C.Y.Y., Zhang, J.S., Lay, W.C.L., Wang, R. and Fane, A.G. (2011). Modelingsalt accumulation in osmotic membrane bioreactors: implications for FOmembraneselection and system operation. *Journal of Membrane Science*. 366: 314–324.
- Yaeli, J. (1992). Method and Apparatus for Processing Liquid Solutions of Suspensions Particularly Useful in the Desalination of Saline Water, US Patent, 5098575.
- Yang, Q., Wang, K.Y. and Chung, T.S. (2009). Dual-layer hollow fibers with enhanced flux as novel forward osmosis membranes for water production. *Environment Science and Technology*. 43: 2800–2805.
- Yong, J.S; Phillip, W.A. and Elimelech, M. (2012). Coupled reverse draw solute permeation and water flux in forward osmosis with neutral draw solutes. *Journal of Membrane Science*. 392-393: 9–17.
- Zhao, S. and Zou, L. (2011). Effects of working temperature on separation performance, membrane scaling and cleaning in forward osmosis desalination. *Desalination*. 278: 157–164.
- Zhao, S., Zou, L. and Mulcahy, D. (2011). Effects of membrane orientation on process performance in forward osmosis applications. *Journal of Membrane Science*. 382: 308-315.
- Zhang, J., Loong, W.L.C., Chou, S., Tang, C., Wang, R. and Fane, A.G. (2012). Membrane biofouling and scaling in forward osmosis membrane bioreactor. 403-404: 8-14.

Zhu, X. and Elimelech, M. (1997). Colloidal fouling of reverse osmosis membranes: measurements and fouling mechanisms. *Environment Science and Technology*. 31: 3654–3662.

ANNEXURES

Annexure... A

PUBLICATIONS AND CONFERENCE PRESENTATIONS

The outcomes of the study were presented at some international conferences as well as were published or are under review in some prestigious journals, as listed below.

1. **Nawaz, M.S.**, Gadelha, G., Khan, S.J. and Hankins, N.P. (2013). Microbial Toxicity Effects of Reverse Transported Draw Solute in the Forward Osmosis Membrane Bioreactor (FO-MBR). **Journal of Membrane Science**. (429): 323-329.
2. Khan, S.J., Ahmed, A., **Nawaz, M.S.** and Hankins, N.P. (2014). Membrane Fouling and Performance Evaluation of Conventional MBR, moving biofilm MBR and oxic/anoxic MBR. **Water Science and Technology**. (69): 1403-1409.
3. Gadelha, G., **Nawaz, M.S.**, Hankins, N.P., Khan, S.J. Wang, R. and Tang, C.Y. (2014). Assessment of Micellar Solutions as Draw Solution for Forward Osmosis. **Desalination**. (354): 97-106.
4. **Nawaz, M.S.**, Khan, S.J., Gadelha, G., Hankins, N.P., Wang, R. and Tang, C.Y. Micellar Solutions as Novel Draw Solutes in Forward Osmosis Systems. Presented at the 1st **International Conference on Desalination using Membrane Technology**, Sitges, Spain, April 7th -10th, 2013.
5. **Nawaz, M.S.**, Parveen, F., Khan, S.J., Gadelha, G., Hankins, N.P., Wang, R. and Tang, C.Y. Membrane Fouling and Microbial Toxicity in the FO-MBR Using a Micellar Draw Solution. Presented at “**Engineering with Membranes (EWM) Towards a Sustainable Future** Saint-Pierre d’Oléron, France” 3-7 September 2013.

6. **Nawaz, M.S., Khan, S.J., Hankins, N.P., Qazi, I. A., Khan, Z. Evaluation of Micellar Solution as Draw Solutes in Forward Osmosis Applications.** Presented at 5th World Engineering Congress (WEC), NUST, Pakistan, 23-25 September 2013.